hESC- and iPSC-Derived Fibroblasts for Skin Engineering and Repair

A dissertation submitted by

Yulia Shamis

In partial fulfillment of the requirements
for the degree of

Doctor of Philosophy

in

Cell, Molecular and Developmental Biology

TUFTS UNIVERSITY

Sackler School of Graduate Biomedical Sciences

August, 2012

ADVISER: Dr. Jonathan A. Garlick

Abstract

The unlimited biological potential of pluripotent stem cells, such as human embryonic stem cells (hESCs) and induced pluripotent stem cells (iPSCs), as seen by their ability to differentiate into any cell type in the human body, makes them promising candidates for regenerative medicine applications. Novel differentiation approaches are continuously being developed to generate therapeutically-relevant cell types from hESCs and iPSCs. However, before these pluripotent stem cell-derivatives can be implemented in regenerative medicine, thorough testing of their phenotypic stability and functional abilities are required.

I hypothesized that pluripotent stem cells could be directed to differentiate to mesenchymal lineage fates, and that these cells would recapitulate the essential functional features of dermal fibroblasts within three-dimensional (3D) *in vitro* tissue models. Generation of mesenchymal cells from hESCs was first explored using two distinct differentiation protocols. The first protocol was based on spontaneous differentiation of hESCs followed by selective isolation of CD73-positive mesenchymal cells. The second protocol was based on a directed differentiation approach by culturing hESCs under defined substrate and media condition and exposure to bone morphogenic protein 4 (BMP4). I further studied the therapeutic potential of these cells using a spectrum of phenotypic assays and 3D tissue models to assess their contribution to wound re-epithelialization, production and assembly of extracellular matrix, and regulation of angiogenesis.

While both differentiation approaches generated mesenchymal cells with similar morphology, surface marker, and gene expression profiles, there were marked differences

in functional properties. Cells that were generated using the directed differentiation approach demonstrated functionality of dermal fibroblasts as seen by their capacity to support development of stratified squamous epithelia and re-epithelialization of wounds generated in bioengineered 3D skin tissues that was mediated by production of soluble growth factors. In addition, hESC- and iPSC-derived fibroblasts generated using the directed differentiation approach produced and assembled thick extracellular matrices reminiscent of skin stromal tissue, induced vascular sprouting, and promoted the formation and stabilization of vascular networks *in vitro* in 3D models of dermal regeneration and angiogenesis. Furthermore, the administration of hESC-derived fibroblasts into severe mouse hindlimb ischemia model, prevented autoamputation of ischemic limbs, attenuated tissue necrosis, and improved blood perfusion, thus demonstrating the repair-competent phenotype of these cells *in vivo.*

These findings highlight the robust therapeutic potential of hESC- and iPSC-derived fibroblasts, and demonstrate our ability to characterize the functional properties of these cells following differentiation in unique 3D assays *in vitro* and *in vivo.*

Acknowledgments

Graduate school has been an outstanding academic experience, and this dissertation would not have been possible without the guidance and support of many colleagues, friends, and family. First and foremost I offer my sincerest gratitude to my thesis advisor and mentor, Dr. Jonathan A. Garlick, who has supported me throughout my thesis research with his patience and knowledge while allowing me the room to work in my own way. One simply could not wish for a better or friendlier supervisor. I would also like to thank my thesis committee, Drs. James E. Schwob, David Kaplan, John J. Castellot, and David J. Mooney for their helpful criticism, advice, and insight throughout the evolution of this project.

In my daily work I have been blessed with a friendly and cheerful group of fellow students. I would like to thank the current and former members of the Garlick laboratory, whom I consider both friends and colleagues. Drs. Mark W. Carlson and Kyle J. Hewitt, the stem cell team, have helped establish the human embryonic stem cell cultures and differentiation protocols and provided an experienced ear for my doubts about experimental designs, data analysis, and the way my thesis work is going. Dr. Addy Alt-Holland has never failed to impress me with her enthusiasm, creativity, and willingness to work long hours, and in many ways I have learned a lot from her. Dr. Christophe Egles has kept me entertained with his huge repertoire of anecdotes and stories but has also given me useful insights on scientific theories and the meaning of life. Teresa DesRocher, Hiba Qary, Mariam Margvelashvili, Cathy Zhao, Shumin Dong, Anna Maione, Avi Smith, Elana Knight, Jennifer Landmann, and Judith Edwards have all provided me with

insight and guidance, and offered something much greater in all the years I have known them: a friendly smile and a happy work environment.

I would also like to thank great collaborators, Drs. Laurence Daheron, Aristidis Veves, Donald Phinney, Eduardo A. Silva, Yevgeny Brudno, and Adam G. Sowalsky, for providing exciting leads and technical assistance. I would like to show my gratitude to fellow graduate students of the Cell, Molecular and Developmental Biology program for our shared experiences and for stimulating and welcoming social environment. In addition, I would like to acknowledge the academic and technical support of the Tufts University Sackler School of Graduate Biomedical Sciences, its faculty and staff.

Finally, I thank my family for supporting me throughout all my studies. My parents, Dolores and Nikolay Shamis, and my brothers, Konstantin and Valery, have provided great confidence and motivation. And of course I could not have done this without my husband, Neetzan Zimmerman, who was always there to comfort me and provide me with encouragement when all hope seemed to be lost. Thank you.

Table of Contents

List of Figures

List of Tables

Abbreviations

2D Two-dimensional
3D Three-dimensional
AA L-ascorbic acid-2-phosphate
ALCAM Activated leukocyte cell adhesion molecule
ANOVA One-way analysis of variance
ANG-1 Angiopoetin-1
αSMA Alpha smooth muscle actin
BMDC Bone marrow-derived cell
COL1 Type I Collagen
COL3 Type III Collagen
HDF Human dermal fibroblasts
NHK Normal human keratinocytes
BMP4 Bone morpogenetic protein4
CALLA Common leucocyte lymphocytic leukaemia antigen
DMEM Dulbecco's minimum essential media
DMSO Dimethyl sulfoxide
EB Embryoid body

ECM	Extracellular matrix
EDK	ES-derived keratin-expressing cell
EDTA	Ethylenediaminetetraacetic acid
EGF	Epidermal growth factor
ELISA	Enzyme-linked immunosorbent assay
EpSC	Epidermal stem cell
FACS	Fluorescence-activated cell sorting
GFP	Green fluorescent protein
FN	Fibronectin
H9-MSC	(H9) hESC-derived mesenchymal cells
H&E	Hematoxylin and eosin
HCAM	Lymphocyte homing-associated cell adhesion molecule
HGF	Hepatocyte growth factor
HEPES	4-(2-hydroxyethyl)-1-piperazineethanesulfonic acid
hESC	Embryonic stem cell
HLA	Human leukocyte antigen
HMVEC	Human blood microvascular endothelial cell
HSE	Human skin equivalent
HUVEC	Human umbilical vein endothelial cell
iPDK	iPS-derived keratin-expressing cell
iPSC	Induced pluripotent stem cell
K14	Cytokertin 14
K18	Cytokeratin 18
LCA	Leukocyte Common Antigen
LDPI	Laser Dopler perfusion image
MACS	Magnetic-activated cell separation
MCAM	Melanoma cell adhesion molecule
MEF	Mouse embryonic fibroblast
MSC	Mesenchymal stem cell
NEAA	Non-essential amino acids
PD	Population doubling
PDGF	Platelet-derived growth factor
PDGFRβ	PDGF-receptor beta
PECAM	Platelet endothelial cell adhesion molecule
RFP	Red fluorescent protein
RGD	Arginyl-glycyl-aspartic acid
RNA	Ribonucleic acid
RT-PCR	Reverse-transcriptase polymerase chain reaction
SCES	Serum-containing embryonic stem cell (media)
SCID	Severe combined immunodeficiency
SFM	Serum free medium
SKP	Skin-derived precursor
Thy-1	Thy-1 cell surface antigen
TF	Coagulation factor III
TGF	Transforming growth factor
TSP-1	Thrombospondin-1

VEGF Vascular endothelial growth factor
VCAM-1 Vascular cell adhesion protein-1
Vim Vimentin
vSMC Vascular smooth muscle cell

Chapter 1: Background and Introduction

1.1 – Cutaneous Wound Healing

Cutaneous wound healing is a complex process of skin repair after injury that involves a highly coordinated interplay among cells, soluble factors, and extracellular matrix. The wound healing process is set in motion immediately after injury by activating various intercellular and intracellular pathways, including blood coagulation cascade, inflammatory pathways, chemotaxis, angiogenesis, deposition and degradation of extracellular matrix (ECM), and re-epithelialization (Werner and Grose 2003). Because of high complexity, many local and systemic factors can contribute to the deregulation of wound healing process, including advanced age, malnutrition, infection, immobility, skin-related diseases, vascular diseases, and diabetes, causing the development of chronic wounds (Sen, Gordillo et al. 2009). Development of chronic wounds frequently results in long-term disability, which has significant implications on a health-related quality of life and economic burden (Sen, Gordillo et al. 2009).

In adults, the normal wound repair process results in the partial restoration of skin architecture and function by forming fibrotic scar tissue. In contrast, during prenatal development, injured fetal tissues can be completely restored without fibrosis through the poorly understood process of regeneration (Larson, Longaker et al. 2010). Human pluripotent stem cells, such as human embryonic stem cells (hESC) and induced pluripotent stem cells (iPSC), can provide a research model to study human development, including the morphogenesis of skin. Knowledge gained from studying the differentiation of pluripotent stem cells into skin precursor cells might help to discover the pathways that need to be reactivated to allow regeneration. In addition, iPSC may be used to generate unlimited number of autologous cells for cell-based therapies and skin tissue engineering.

Engineering complex tissues *in vitro* from hESC and iPSC derivatives may provide an important tool for studying organogenesis and mechanisms of early human development. In this chapter I will review the process of cutaneous wound healing, focused on major events that distinguish skin repair and regeneration.

Classic Stages of Wound Repair

Cutaneous wound healing is a dynamic process that involves interaction between epidermal and dermal cells, deposition and remodeling of ECM, and controlled angiogenesis, all coordinated by an array of cytokines and growth factors. This process is classically divided into three overlapping phases – inflammation, proliferation, and remodeling (Werner and Grose 2003; Gurtner, Werner et al. 2008) (Figure 1.1).

The first phase, inflammation, is initiated immediately after the formation of the blood clot, which aside from providing a barrier against invading microorganisms also serves as a scaffold for infiltrating cells and as a reservoir of growth factors required for the latter stages of the wound healing. Neutrophils are first recruited to the wound site, followed by monocytes and lymphocytes. These inflammatory cells cleanse the wound through phagocytosis and by producing a wide variety of proteinases and reactive oxygen species as a defense against contaminating organisms. These inflammatory cells are also an important source of growth factors and cytokines, which initiate the next phase of wound healing, proliferation (Martin and Leibovich 2005).

The proliferative stage begins with the migration and proliferation of dermal fibroblasts from the tissue surrounding the wound. Fibroblasts subsequently deposit large amounts of ECM, which is known as provisional matrix, consisting predominantly of

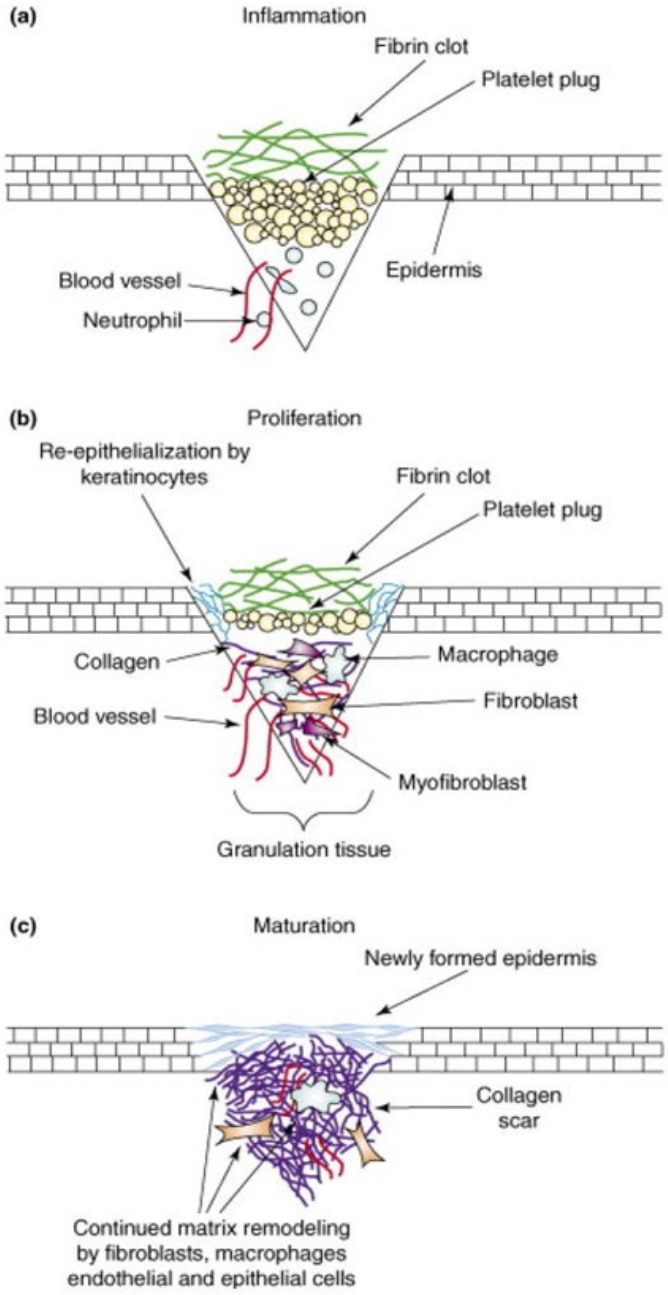

Figure 1.1. Schematic representation of different stages of cutaneous wound repair.
A. 12–24 h after injury, inflammatory phase. The wounded area is filled with a blood clot. Neutrophils have invaded into the clot. ***B.*** 3–7 d after injury, proliferation phase. Macrophages are abundant in the wound, endothelial cells migrate into the clot and form new blood vessels, fibroblasts migrate into the wound tissue and deposit extracellular matrix, the new tissue is called granulation tissue, keratinocytes proliferate at the wound edge and migrate above the granulation tissue ***C.*** 1–2 wk after injury, remodeling phase. Fibroblasts have transformed into myofibroblasts, leading to wound contraction and collagen remodeling. This figure was adapted from (Chen, Przyborowski et al. 2009)

type III collagen and fibronectin. Furthermore, wound fibroblasts acquire a contractile phenotype and transform into myofibroblasts, a cell type which plays an important role in wound contraction (Sarrazy, Billet et al. 2011). Massive angiogenesis occurs concurrently with fibroblast proliferation leading to the migration of endothelial cells into the wound and formation of new blood vessels. The resulting wound connective tissue is

known as granulation tissue. The formation of granulation tissue allows the re-epithelialization to take place, as epithelial cells migrate across the granulation tissue to form a barrier between the wound and the environment (Werner and Grose 2003; Gurtner, Werner et al. 2008).

Finally, in the remodeling phase, a transition from granulation tissue to mature scar occurs, characterized by gradual degradation of type III collagen and deposition of stronger type I collagen. The scar tissue is mechanically insufficient and lacks appendages, including hair follicles, sebaceous glands, and sweat glands (Widgerow 2011). In contrast, embryonic wound healing results in essentially perfect repair, suggesting fundamental differences in the regenerative process of human adult and embryonic tissues (Larson, Longaker et al. 2010).

Wound Repair vs. Regeneration

The process of tissue repair is distinct from the process of tissues regeneration. Wound repair is an adaptation of the organ that leads to the restoration of its continuity by synthesis of scar tissue without restoration of the normal tissue function. In contrast, wound regeneration restores the normal structure and function of the organ (Gurtner, Werner et al. 2008; Larson, Longaker et al. 2010). For example, in response to skin injury, the fetal dermis has the ability to restore the original collagen matrix (Longaker, Whitby et al. 1990) and regenerate missing dermal structures, such as sebaceous glands and hair follicles (Beanes, Hu et al. 2002). The capacity for scarless fetal wound repair was initially attributed to the intrauterine environment, which is enriched with hyaluronic acid and growth factors (Larson, Longaker et al. 2010). However, multiple studies have

demonstrated that scarless repair is intrinsic to fetal tissues and the intrauterine environment is neither necessary nor sufficient for scarless repair (Larson, Longaker et al. 2010). For example, adult sheep skin transplanted onto the backs of fetal sheep healed incisional wounds with scar (Longaker, Whitby et al. 1994) while human fetal skin healed without scar when it was transplanted into the subcutaneous tissue of adult mice (Lorenz, Longaker et al. 1992). Thus, understanding the mechanism of fetal scarless healing may lead to new therapeutic strategies for improving adult wound healing.

Although the exact mechanisms for scarless fetal regeneration are mostly unknown, they are thought to be due to differences between inflammatory response, cytokines and growth factors, ECM modulators, differential gene expression, and stem cell function in fetal and postnatal wounds (Table 1.1) (Larson, Longaker et al. 2010). It has been shown that scraless wounds are characterized by relative lack of inflammation, and introduction of inflammation into fetal wounds results in an increased number of

	Adult Wound Healing	Fetal Wound Healing
Collagen content	Predominance of type I collagen provides strength and rigidity, but impedes cellular migration and regeneration	Predominance of type III collagen is optimal for cellular migration and proliferation
Hyaluronic acid	Low levels of hyaluronic acid inhibit cellular movement	High levels of hyaluronic acid facilitates cellular movement and traps water
Extracellular matrix modulators	Low matrix metalloproteinase to tissue-derived inhibitor ratio favors accumulation of collagen	High matrix metalloproteinase to tissue-derived inhibitor ratio favors extracellular matrix modulators turnover and remodeling
Adhesion proteins	Diminished up-regulation of adhesion proteins results in slower fibroblast migration	Rapid up-regulation stimulates cell attachment and migration
Platelets	Release platelet-derived growth factor, TGF-β1, and TGF-β2	Decreased degranulation and aggregation
Inflammatory cells	Many	Few
Interleukins	Rapid increase in proinflammatory cytokines, such as interleukin-6 and interleukin-8	Increased expression of the anti-inflammatory cytokine interleukin-10, which decreases production of interleukin-6 and interleukin-8
TGF-β	High levels of TGF-β1 and TGF-β2	Low levels of TGF-β1 and TGF-β2; increased TGF-β3
Gene expression	Delayed up-regulation of genes involved in cell growth and proliferation	Rapid up-regulation of genes involved in cell growth and proliferation
Progenitor cells	Skin progenitor cells found at inadequate numbers to mediate scarless repair	Skin progenitor cells migrate to sites of injury and mediate scarless repair

TGF, transforming growth factor.

Table 1.1 – Adult vs. Fetal Wound Healing. Table summarizes the differences between fetal and postnatal wounds. Adapted from (Larson, Longaker et al. 2010).

inflammatory cells, such as neutrophils and microphages, followed by an increase collagen deposition and scarring (Frantz, Bettinger et al. 1993) demonstrating an important role of inflammation in formation of scar tissue. Some studies suggest that ECM of fetal wounds is optimized to facilitate cellular migration and proliferation due to abundance of adhesion proteins, such as tenascin and fibronectin, and higher ratio of matrix metalloproteinases to matrix metalloproteinase inhibitors, which might favors remodeling over accumulation of collagen (Whitby, Longaker et al. 1991; Cass, Bullard et al. 1998; Dang, Beanes et al. 2003). It has also been shown that fetal fibroblasts display increased expression of hyaluronic acid receptors and synthesize more type III and type IV collagens than their adult counterparts (Alaish, Yager et al. 1994; Beanes, Hu et al. 2002), thus reducing the formation of scar tissue enriched in type I collagen. In addition, the number of contractile fibroblasts, the myofibroblasts, is significantly lower in fetal wounds (Estes, Vande Berg et al. 1994; McCluskey and Martin 1995). It has been shown that fetal fibroblasts produce decreased levels of inflammatory cytokines, including interleukin-6 and interleukin-8 (Liechty, Crombleholme et al. 1998; Liechty, Adzick et al. 2000), and display elevated levels of growth factors when compared to adult fibroblasts (Hsu, Peled et al. 2001). Furthermore, genomic microarray analysis has shown the upregulation of groups of genes involved in cell growth and proliferation in fetal wound tissues, which likely contributes to accelerated wound closure in fetus vs. adult tissues (Colwell, Longaker et al. 2008).

The tissue regeneration may have important links to tissue development where undifferentiated stem cells are the source from which differentiated cell types arise in order to recreate functionally organized adult tissues. In this case, the optimal solution to

both chronic wounds and scar formation is likely to be the administration of stem cells. Stem cells and their derivatives administrated into the wound by themselves or as part of a tissue-engineered construct may provide the cues necessary for the regeneration of fully functional skin.

Stem Cells in Action

Although the extent of stem cell involvement in cutaneous wound healing is complex and not fully understood, these cells are known to play a significant role in promoting wound vascularization, attenuating scar formation, and inducing re-epithelialization, and thus in better skin healing. Both resident skin stem cells resigning in the epidermis and the dermis and circulating bone-marrow derived stem cells have been shown to promote wound repair and tissue regeneration through proliferation and differentiation and through paracrine communication with other resident cells (Taylor, Lehrer et al. 2000; Abe, Donnelly et al. 2001; Ito, Liu et al. 2005; Hocking and Gibran 2010; Feng, Mantesso et al. 2011). Following injury, stem cells become activated and re-enter the cell cycle, in addition, they release multiple paracrine signals that regulate the local cellular responses to injury. For example, during wound re-epithelialization, epidermal stem cells proliferate and differentiate to provide keratinocytes, which then migrate and cover the healing wound. This epidermal proliferation is controlled, at least in part, by a double paracrine mechanism in which epithelial cells produce IL-1α, which stimulates production of growth factors, such as KGF and GM-CSF, by dermal fibroblasts, which in turn induces epithelial proliferation and differentiation and further production of IL-1α. This double paracrine loop ultimately leads to an activation of

epidermal stem cells at the wound edge, which is critical for wound re-epithelialization (Szabowski, Maas-Szabowski et al. 2000; Angel and Szabowski 2002). HGF represents another example of stromal-derived signaling which is particularly important for wound healing (Matsumoto and Nakamura 1997; Chmielowiec, Borowiak et al. 2007; Schnickmann, Camacho-Trullio et al. 2009; Suga, Eto et al. 2009; Rosova, Link et al. 2010) . In response to tissue injury, the production of HGF is activated around the blood clot in the dermis and in hair follicles. In response to upregulation of HGF in the dermis, epidermal cells at the wound edge upregulate the expression of HGF receptor c-Met, proliferate, and migrate to close the wound. Mice with conditional knockout of c-Met from keratinocytes showed strongly delayed re-epithelialization in response to skin wounds, and the cells that eventually covered the wounds in these mice were found to have escaped the recombination event in which c-Met was deleted (Chmielowiec, Borowiak et al. 2007). Although it has been known that many other growth factors are involved in the re-epithelialization process, these factors cannot compensate for the lack of HGF (Chmielowiec, Borowiak et al. 2007; Schnickmann, Camacho-Trullio et al. 2009) indicating the importance of HGF signaling pathway in cutaneous wound healing.

It has been long argued whether the epidermis is renewed by epidermal stem cells or by stem cells generated in the hair follicle (Taylor, Lehrer et al. 2000). Undoubtedly, multipotent epidermal stem cells from the hair follicles can contribute to epidermal repair, but this occurs only when a wound cannot repair itself through the migration of epidermal cells from the neighboring unwounded epidermis (Blanpain, Lowry et al. 2004; Ito, Liu et al. 2005; Levy, Lindon et al. 2005; Watt, Lo Celso et al. 2006). With respect to dermal regeneration, increasing evidence suggests that mesenchymal stem cells

are responsible for enhancing wound regeneration (Hocking and Gibran 2010; Smith, Willis et al. 2010; Feng, Mantesso et al. 2011). Dermal papilla cells can express markers of adipogenic, chondrogenic and osteogenic differentiation and can even form neurospheres *in vitro*, which express markers of neural crest stem cells (Gharzi, Reynolds et al. 2003; Fernandes, McKenzie et al. 2004; Bajpai, Mistriotis et al. 2012). Therefore, dermal papilla cells seem to be functionally related to mesenchymal stem cells isolated from other tissues, such as bone marrow-derived and adipose tissue-derived mesenchymal stem cells, and may contribute to dermal regeneration (Hocking and Gibran 2010). The regeneration of epidermal appendages after wounding, specifically hair follicles, has been reported in mice (Ito, Yang et al. 2007). This study showed that stem cells from the bulge regions outside the wound, but also other populations of dermal cells that have not been yet fully characterized can contribute to the regeneration of hair follicles. Whether this process is exactly similar in humans remains to be studied.

In addition, it has been proposed that extensive skin injury stimulates the recruitment of circulating bone marrow-derived cells (BMDCs), which include fibrocytes that originate the population of myofibroblast, essential to the wound contraction (Abe, Donnelly et al. 2001; Yang, Scott et al. 2005). Studies in mice showed that regenerated skin contains BMDCs in the hair follicle, the sebaceous glands, and the epidermis (Badiavas, Abedi et al. 2003), and their engraftment is significantly up-regulated in wounded epidermis (Brittan, Braun et al. 2005) . It has been suggested that in the wound environment, BMDCs secrete paracrine factors that suppress inflammation, inhibit fibrosis, enhance angiogenesis, and stimulate mitosis and differentiation of tissue-intrinsic stem cells (Javazon, Keswani et al. 2007; Meirelles Lda, Fontes et al. 2009). It

has been also shown that after engrafting into the wound BMDCs showed stem cell-like properties by differentiating into keratinocytes and various cells in the dermis, indicating that BMDCs may be able to replenish epidermal and mesenchymal stem cell populations in the skin (Brittan, Braun et al. 2005).

In conclusion, skin contains multiple stem cell populations: the epidermal stem cells in the basal layer, the epidermal stem cells in the hair follicle, different populations of mesenchymal stem cells in the dermis and hair follicle, and recruited mesenchymal stem cells from the bone marrow. The stem cells in the basal layer of the epidermis contribute only to epidermal turnover and regeneration, whereas the hair follicle stem cells also contribute to hair follicle and sebaceous gland turnover. Upon injury, stem cells from the bone marrow are also recruited. Together, these stem cell populations are able to regenerate the epidermis and the dermis after injury. Thus, the understanding the molecular mechanisms and environmental cues that control the fate of epidermal and mesenchymal stem cells during wound healing will allow the design of new strategies for tissue regeneration, the strategies that enhance proliferation and migration of stem cells, decrease scarring, promote wound vascularization, and, ultimately, induce formation of epidermal appendages.

1.2 – Stem Cell Sources for Skin Regeneration

There are many types of stem cells, and all share the characteristics of being able to self-renew and give rise to differentiated progeny. Different sources of stem cells serve independent functions in development, tissue homeostasis and tissue repair. Totipotent stem cells are the most primitive embryonic cells that can develop into a complete embryo including extraembryonic tissues. With subsequent divisions totipotent stem cells become restricted to pluripotent stem cells that give rise only to cells of three embryonic germ layers, namely ectoderm, mesoderm, and endoderm. With further development, pluripotent stem cells become restricted to multipotent stem cells that give rise only to cells of specific organ or tissue. Multipotent stem cells, also known as adult stem cells, are important for tissue homeostasis and repair since they are capable of self-renewal and differentiation during the lifetime of the organism. For this reason, adult stem cells can be found in a metabolically quiescent state in most of the tissues, including skin. These cells are relatively rare and difficult to isolate without the contamination of unipotent progenitors that can divide only a limited number of times and differentiate only into a specific type of cell.

Both adult and embryonic stem cell sources have the potential to meet the challenges of skin regeneration, mainly due to their self-renewal capabilities along with the ability to give rise to skin relevant lineages, such as mesenchymal, epidermal, and endothelial lineage cells. In fact, improved vascularization is required to ensure successful implantation of tissue-engineered skin substitutes and to promote healing of chronic wounds (Supp and Boyce 2005; O'Ceallaigh, Herrick et al. 2006). Moreover,

tissue-engineered skin substitutes prepared with epidermal and mesenchymal precursors differentiated from stem cells may be available in a shorter time due to their high proliferative capacity and in earlier differentiation stages, which can contribute to an advanced quality healing and to skin regeneration rather than repair. Numerous studies have begun to reveal the potential of stem cells from different sources for skin regeneration, where rebuilding of fully functional skin is the main concern, including skin appendages and blood supply. In this chapter I will review the available sources of stem cells highlighting their potential for therapeutic use in skin regeneration.

Adult Stem Cells (MSCs, EpSCs, and SKPs)

Mesenchymal stem cells (MSCs) are prototypical stem cells with a broad tissue distribution and ability to differentiate into mesodermal as well as non-mesodermal lineages. The endogenous role for MSCs is maintenance of stem cell niches, such as hematipoietic, and organ homeostasis, and therefore MSCs are expected to contribute to the wound repair process. Although MSCs have been isolated from a variety of human tissues, including bone marrow, adipose tissue, liver, spleen, heart, dental tissues, and dermis (Bartsch, Yoo et al. 2005; Hoogduijn, Crop et al. 2007; Jo, Lee et al. 2007; Riekstina, Cakstina et al. 2009; Pan, Fouraschen et al. 2011), the nature of these cells is not fully understood. The MSC phenotype is defined based on morphologic, phenotypic, and functional criteria, which is a fibroblastic morphology in culture, a surface antigen profile of CD105+, CD73+, CD90+, and CD34-, and CD45-, and a differentiation potential that includes adipogenesis, chondrogenesis, and osteogenesis (Dominici, Le Blanc et al. 2006). Adult MSCs may be closely associated with perivascular niches since

they express characteristics in common with pericytes, the mesenchymal cells supporting capillary networks (Caplan 2008). However, it remains a possibility that MSCs also exist in other cell subsets of nonpericyte origin (Gharzi, Reynolds et al. 2003; Fernandes, McKenzie et al. 2004; Feng, Mantesso et al. 2011; Bajpai, Mistriotis et al. 2012) .

Several studies have shown that adult MSCs have the potential to regenerate skin in cutaneous wounds through differentiation into specialized cell types and paracrine signaling (Brzoska, Geiger et al. 2005; Vojtassak, Danisovic et al. 2006; Chun-mao, Su-yi et al. 2007; Paunescu, Deak et al. 2007; Wu, Chen et al. 2007; Yoshikawa, Mitsuno et al. 2008; Bey, Prat et al. 2010). It has been shown that MSCs are able to differentiate *in vitro* into epithelial-like cells expressing early epithelial markers, including p63, cytokeratin 18 and 19, and β1-integrin (Brzoska, Geiger et al. 2005; Chun-mao, Su-yi et al. 2007; Paunescu, Deak et al. 2007), suggesting the potential for these cells to contribute to epidermal regeneration and reconstruction of skin appendages. MSCs have been examined in skin repair and regeneration after various acute and chronic skin injuries, such as acute incisional and excisional wounds, diabetic skin ulcers, radiation burns, and thermal burns (Vojtassak, Danisovic et al. 2006; Wu, Chen et al. 2007; Yoshikawa, Mitsuno et al. 2008; Bey, Prat et al. 2010). These *in vivo* studies have shown that transplantation of autologous and allogeneic MSCs on the surface of cutaneous wounds decreases inflammation and accelerates neovascularization, formation of granulation tissue, and wound re-epithelialization. Increasing evidence suggests that one mechanism of action by which MSCs improve wound healing may involve paracrine signaling (Caplan and Dennis 2006; Meirelles Lda, Fontes et al. 2009; Giuliani, Fleury et al. 2011). In wound environment, MSC release cytokines and growth factors that

suppress the local immune system, inhibit fibrosis, enhance angiogenesis, and stimulate mitosis and differentiation of tissue-intrinsic stem cells. In light of this, understanding the paracrine signaling mediated by MSCs may help develop novel therapies for impaired wound healing.

Epidermal stem cells (EpSCs) are another example of skin resident stem cells that represent a valuable therapeutic option in skin tissue engineering and wound repair. Self-renewing EpSCs reside in the basal layer of the epidermis and in the hair follicle (Blanpain, Lowry et al. 2004; Watt, Lo Celso et al. 2006). While EpSCs residing in the basal epidermal layer are thought to be unipotent, EpSCs from the hair follicle can contribute to the regeneration of new hair follicles and sebaceous glands, and to epidermal re-epithelialization during wound repair (Taylor, Lehrer et al. 2000; Blanpain, Lowry et al. 2004). EpSCs share the epidermal niche with their daughter cells, the transient amplifying cells, that have limited proliferation potential before differentiating (Jones and Watt 1993). Despite the effort undertaken to characterize EpSCs from both the epidermis and the hair follicle, specific markers of EpSCs are still in question (Watt 1998; Kaur and Li 2000; Li, Miao et al. 2008). It has been suggested that integrin β_1 is a marker for EpSCs since the β_1-enriched fractions of keratinocytes adhere more rapidly to some ECM proteins and have a higher colony-forming efficiency than unfractionated cells (Jones and Watt 1993; Watt 1998). To this day *in vitro* clonal potential of epidermal cells is used as a criteria for isolating epidermal cells with enriched stem cell population (Watt, Lo Celso et al. 2006). Although EpSCs can benefit from the improvement of the isolation technique, these cells are critically important for skin regenerative therapies.

EpSCs are used for generating large numbers of keratinocytes for allografts and xenografts and for constructing tissue-engineered skin substitutes.

In addition, the population of skin-derived precursors (SKPs) has been isolated from the dermal papilla (Toma, McKenzie et al. 2005) and other follicular and extrafollicular sites (Wong, Paratore et al. 2006). SKPs share many characteristics of neural crest stem cells and can differentiate into both neural and mesodermal lineages, including neurons, glia, and smooth muscle cells. Similar to neural crest stem cells, SKPs grow in suspension as spheres and characterized by expression of nestin, vimentin, fibronectin, and neural crest stem cell markers p75 and Sox10. The discovery that SKPs can easily propagate in culture and generate functional neuronal and glial cells raises a number of exciting biotechnological prospects. In relation to skin regeneration, SKPs might be explored to promote the regeneration of skin nervous appendages. However, before SKPs can become a clinically relevant stem cell source, optimization of isolation protocols as well as understanding of their origin and endogenous function is required (Hunt, Jahoda et al. 2009).

Embryonic Stem Cells (hESC and iPSC)

Human embryonic stem cells (hESCs) are pluripotent stem cells that have been derived from the inner cell mass of day 5–7 blastocysts (Thomson, Itskovitz-Eldor et al. 1998) (Figure 1.2A). Pluripotency of hESCs distinguishes them from adult stem cells capable of producing only limited variety of differentiated cell types. (Klimanskaya, Chung et al. 2005). Following the initial isolation and characterization of hESC lines, these cells have attracted interest for their potential to differentiate into a wide range of cell lineages for

therapeutic applications as well as studying the mechanisms of human development and disease. Human ESC are typically cultured in media containing animal products on feeder layers of irradiated murine embryonic fibroblasts, which are necessary to maintain their undifferentiated state but compromise their clinical applications (Martin, Muotri et al. 2005) (Figure 1.2A). In order to improve clinical relevancy of hESCs, animal product

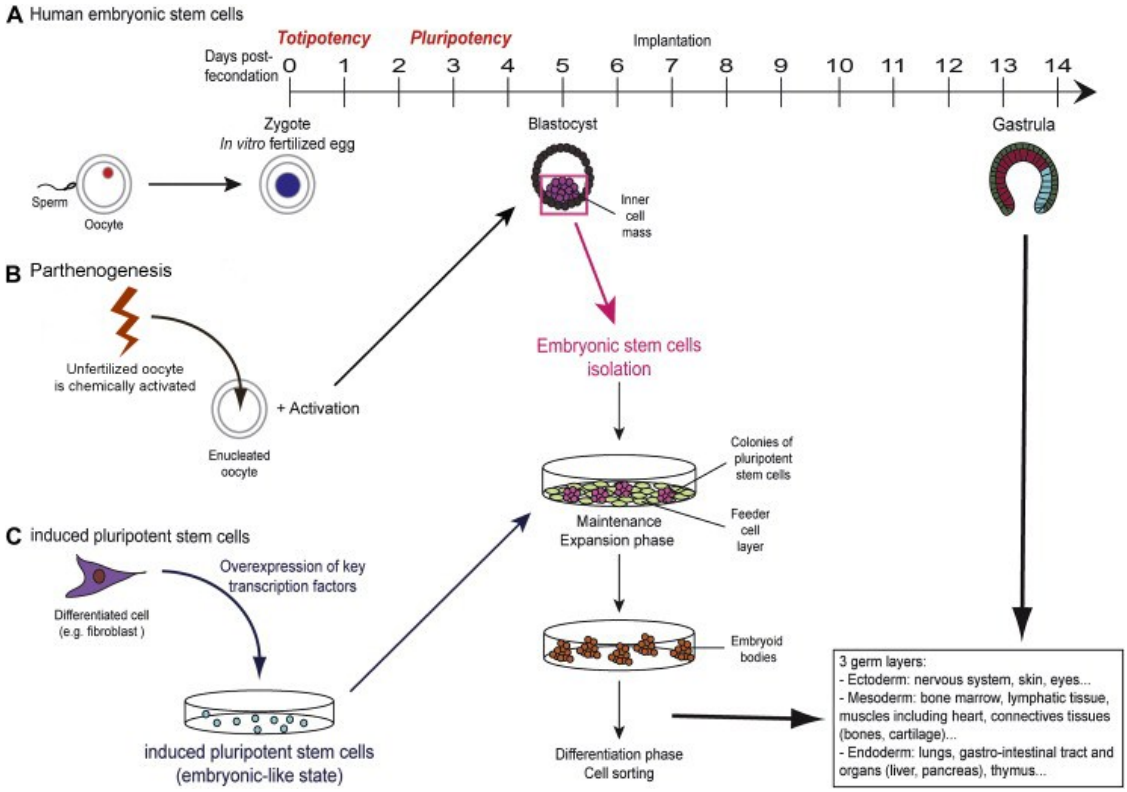

Figure 1-2. Isolation, generation, and culture of pluripotent stem cells. A. Human embryonic stem cells (hESCs) are isolated from the inner cell mass of the blastocyst and grown on feeder cell layers of irradiated murine embryonic fibroblasts. When removed from feeder layers and transferred to suspension, hESCs form embryoid bodies. **B.** An unfertilized oocyte is activated and starts to cleave as a normal embryo Parthenogenetic pluripotent cells are isolated from the inner cell mass of the blastocyst and grow in culture like hESCs. **C.** iPSCs are generated from somatic cells that have been reprogrammed to acquire a pluripotent state through overexpression of embryonic-associated genes. Once they are reprogrammed, they can be grown in culture like hESCs. This figure was adapted and modified from (Brignier and Gewirtz 2010)

- free culture systems have been developed (Xu, Inokuma et al. 2001; Xu, Jiang et al. 2004; Vallier 2011) followed by derivation of new hESC lines under completely cell- and serum-free conditions. When grown in suspension, hESCs form three-dimensional

aggregates of undifferentiated and differentiated cells from varies developmental stages, the embryoid bodies (EBs) (Figure 1.2A). Theoretically, early progenitor cells from EBs can be sorted according to their specific markers and further differentiated into desired cell types by adding growth factors. However, being based on spontaneous differentiation, this technique does not allow robust differentiation of specific cell types, which is limiting for regenerative medicine applications. Directed differentiation of hESCs in defined media and substrate conditions mimicking developmental stages of human embryo has been proven to be of more practical use.

The most basic objection to hESC research is that it deprives embryos of any further potential to develop into a complete human being. In order to minimize these ethical concerns, the technique allowing isolation of a single blastomere without human embryo destruction has been successfully established (Chung, Klimanskaya et al. 2008). In addition, human embryo destruction can be avoided by using parthenogenesis of an unfertilized oocyte or by inducing pluripotency in somatic cells. The last two techniques are particularly exciting because they allow the production of immune-compatible hESCs. In parthenogenesis, an unfertilized oocyte is activated and starts to cleave as a normal embryo, and then hESC culture is established from a blastocyst (Revazova, Turovets et al. 2007) (Figure 1.2B). The absence of the paternal contribution greatly diminishes the human leukocyte antigen (HLA) variability (Revazova, Turovets et al. 2007). This technique can be used to create cell banks of different HLA-type pluripotent stem cells for therapeutic applications. To induce pluripotency in somatic cells, a somatic cell is being reprogrammed by reactivating of embryonic-associated genes to acquire a pluripotent state (Figure 1.2C). Induced pluripotent stem cells (iPSCs) generated using

this reprogramming technique are immunologically identical to their somatic donor cell and can be used to generate patient-specific cells for therapeutic applications. Initially, induction of pluripotent stem cells from mouse embryonic and adult fibroblasts was accomplished by retroviral-transduction of Oct4, Sox2, Klf4 and cMyc (Takahashi and Yamanaka 2006). The iPSCs generated by this method demonstrated the morphology, growth characteristics, and gene expression associated with embryonic stem cells and produced viable, fertile mice through tetraploid complementation (Takahashi and Yamanaka 2006; Zhao, Li et al. 2009). Human iPSC have also been generated using the combination of Oct4, Sox2, Klf4 and cMyc with retroviral system (Takahashi, Tanabe et al. 2007) and using the combination of Oct4, Sox2, Lin28 and Nanog with lentiviral system (Yu, Vodyanik et al. 2007). Human iPSCs displayed the same properties as hESCs including generation of viable, fertile mice through tetraploid complementation (Zhao, Li et al. 2010).

Although the iPSC technology can provide patient-specific cells and sidestep many ethical issues surrounding hESCs, there are still many challenges to overcome before iPSC can be used in clinic, including low reprogramming efficiency, risk of mutation associated with viral transfections, and incomplete reprogramming. In addition, it would be necessary to understand whether the developmental potential of iPSCs is equivalent to that of hESCs. Some studies have suggested that iPSCs have more fragile genomes and so they are more prone to DNA abnormalities than hESCs, which could make them unsafe to use therapeutically (Sheridan, Theriault et al. 2011). However, the field is developing very quickly and many techniques ensuring the safety of iPSCs have been already introduced, including the use of small-molecule compounds (Huangfu,

Maehr et al. 2008) and recombinant proteins (Lin, Ambasudhan et al. 2009) that mimic the action of reprogramming transcription factors, and alternative non-integrating adenoviral vectors (Maherali, Ahfeldt et al. 2008; Maherali and Hochedlinger 2008) that reduce the risk of insertional mutagenesis caused by viral integration into the genome.

In conclusion, among all stem cell sources available for skin regenerative therapies, pluripotent stem cells represent a very promising one. Although adult stem cells, such as MSCs and EpSCs, have shown great promise in skin therapeutic applications (Mansilla, Marin et al. 2005; Caplan and Dennis 2006; Vojtassak, Danisovic et al. 2006; Wu, Chen et al. 2007; Yoshikawa, Mitsuno et al. 2008; Bey, Prat et al. 2010; Carlson, Faria et al. 2011), isolation of these cells is limited by donor tissue availability and requires invasive procedures. Despite many efforts undertaken to assemble techniques that allow better population purification, definitive stem cell markers are not yet available and the isolation of stem cells of sufficient purity and quantity remains difficult. As an example, the markers for isolation of MSCs are shared with dermal fibroblasts (Haniffa, Wang et al. 2007; Covas, Panepucci et al. 2008; Lorenz, Sicker et al. 2008) and the markers for isolation of EpSC are share with transient amplifying cells (Watt 1998; Kaur and Li 2000; Li, Miao et al. 2008) making the purification of these cell populations difficult. In addition, when isolated from their resident tissues and expanded *in vitro*, adult stem cells have limited proliferative capacity, quickly lose their differentiation potential, and reduce production of bioactive factors including growth factors and cytokines (Siddappa, Licht et al. 2007; Kretlow, Jin et al. 2008; Roobrouck, Ulloa-Montoya et al. 2008; Wagner, Bork et al. 2009). Furthermore, stem cells obtained from different donors are not uniform and show significant differences with respect to

their gene expression profiles and functional properties (Siddappa, Licht et al. 2007; Zhukareva, Obrocka et al. 2010). Beyond this, aging and aging related disorders have been shown to impair significantly the survival and function of adult stem cells, thus limiting their therapeutic potential (Kretlow, Jin et al. 2008; Roobrouck, Ulloa-Montoya et al. 2008). In light of this, pluripotent stem cells represent a valuable alternative source for therapeutic applications due to their unique characteristics of unlimited self-renewal and ability to differentiate into all cell lineages, which might promote the use of these cells over adult stem cells.

1.3 – Differentiation of hESCs and iPSCs for Skin Tissue Regeneration

To achieve skin regeneration complete with functional dermis, epidermis, and skin appendages, it is thought to be essential to regenerate the various skin-specific stem cells and their niches (Chuong, Wu et al. 2006; Chuong, Cotsarelis et al. 2007). Pluripotent stem cells, such as hESCs and iPSCs, have the unique potential to generate any type of stem and progenitor cell required for skin tissue regeneration. However, the full realization of this potential relies on establishment of reproducible and efficient differentiation protocols for deriving specific cell types from hESCs and iPSCs. Given that skin regeneration is more efficient in fetal tissues (Gurtner, Werner et al. 2008; Larson, Longaker et al. 2010), generating of fetal-like progenitors from hESCs and iPSCs rather than more mature cell types may be necessary for efficient reconstitution of fully

functioning skin complete with dermal and epidermal layers, skin appendages, and blood supply.

There are two main strategies that have been used to commit pluripotent stem cells into specific lineage: the formation of EBs and directed differentiation. Formation of EBs is based on spontaneous differentiation of pluripotent stem cells in suspension culture into three primary germ layers, the ectoderm, the endoderm, and the mesoderm, mimicking early embryonic development. The growth factors and the media conditions can be further manipulated to enrich for specific cell types, which then can be isolated from the total cell mixture by magnetic-activated cell separation (MACS) or fluorescent-activated cell sorting (FACS). However, being based on spontaneous differentiation, this technique does not allow robust differentiation of specific cell types and contaminant cell lineages are naturally present, which is limiting for regenerative medicine applications. An alternative directed differentiation strategy is based on the recapitulating of the sequential stages of embryonic development in monolayer culture of hESCs and iPSCs (Irion, Nostro et al. 2008; Murry and Keller 2008).

As in embryonic development where lineage specification is guided by morphogen gradients, the directed differentiation of hESCs and iPSCs relies on the application of similar signaling gradients to induce differentiation into specific lineages. However, the lineage commitment that occurs during embryonic development involves complex signaling pathways and multiple stimuli that have not been fully understood. Thus, the directed differentiation protocols are usually designed to induce differentiation of pluripotent stem cells along specific pathways using different cocktails of morphogens and growth factors and then enrich for desired cell type using various selective

conditions. Such ESC- and iPSC-based differentiation strategies can help to examine the impact of specific signaling pathways and substrates on lineage commitment, and better understand the molecular events that occur during human development. Cells differentiated from pluripotent stem cells are characterized based on marker expression and functional properties. Since these *in vitro* differentiation systems do not support three-dimensional tissue formation, the functional interaction between different cell types derived from pluripotent stem cells should be further examined using tissue-engineering techniques. Development of such methods and protocols for differentiation of therapeutically-relevant skin cells, such as mesenchymal, epidermal, and endothelial progenitor cells, have already begun and will be reviewed in this chapter.

Differentiation of Epidermal Cells

Epidermis is derived from the cells covering the embryo after neurulation, and are therefore of ectodermal origin (Aberdam, Gambaro et al. 2007). During skin development, the epidermal commitment of the ectoderm is coordinated by signaling cues provided by the mesoderm (Aberdam, Gambaro et al. 2007). The strategy of recapitulating epidermal development *in vitro* was first introduced by Coraux et al., who described the differentiation of epidermal precursors along with mesenchymal precursors within the same culture of mouse ESCs grown in the presence of bone morphogenic protein 4 (BMP4) (Coraux, Hilmi et al. 2003). This study demonstrated that ESC culture is capable to recapitulate coordinated development of ectodermal and mesodermal layers during skin morphogenesis. The BMP4 signaling plays an important role in the early choice between neural and epidermal commitment of the embryonic ectoderm. Thus, the

administration of BMP4 allowed epidermal lineage commitment of mouse ESCs by inducing Smad-dependent apoptosis of Sox1-positive neural precursors (Gambaro, Aberdam et al. 2006).

The importance of BMP4 for epidermal lineage differentiation was further confirmed in human ESCs by obtaining a fairly pure population of keratinocytes following exposure to retinoic acid in conjunction with BMP4 signaling (Metallo, Ji et al. 2008). Furthermore, fully functional basal keratinocytes with the ability to form a stratified epithelium that resembles normal human epidermis both *in vitro* and *in vivo* were generated by Guenou et al. from hESCs (Guenou, Nissan et al. 2009). The investigators derived the keratinocyte lineage by growing hESCs in the presence of ascorbic acid and BMP4 for 40 days. This study showed the progressive loss of the pluripotency gene markers Oct4 and Nanog, the transient expression of keratins 8 and keratin 18, followed by the induction and maintenance of keratin 5, keratin 14, integrin α5, and integrin β4 expression in culture. The obtained keratinocytes were able to able to form stratified squamous epithelia in 3D skin equivalent tissues and following grafting *in vivo* in immunedeficient mice. Importantly, these keratinocytes could be passaged up to nine times without loss of proliferative potential and epidermal differentiation properties. As expected, hESC-derived keratinocytes showed low expression of HLA antigens indicating that keratinocyte allografts derived from hESCs could be transplanted onto patients awaiting autologous grafts with a reduced risk of rejection.

Most recent study indicated that autologous iPSCs have the potential to provide a source of keratinocytes for regenerative therapies for specific skin diseases, such as epidermolysis bullosa (Itoh, Kiuru et al. 2011). In this study iPSC were generated from

normal human fibroblasts and from fibroblasts isolated from patients with recessive dystrophic epidermolysis bullosa carrying a genetic defect in COL7A1 gene. The keratinocytes generated from these iPSCs using a differentiation protocol based on the combination of retinoic acid with BMP4 were able to form stratified squamous epithelia in 3D skin equivalent tissues. This technology offers the possibility to restore the expression of COL7A1 in patient-derived iPSCs. Patient-derived iPSCs are more suitable than keratinocytes for homologous recombination-based gene targeting because of their unlimited proliferation capability. The patient-specific keratinocytes can be then isolated from corrected iPSCs and used for autologous transplantation to restore skin function.

In conclusion, despite the different approaches that have been employed to drive pluripotent stem cells towards the epithelial lineage, no standardized protocols exist for generating epidermal stem cells. Additional research is required to increase yield and insure purity of generated epidermal stem cells. Without reliable protocols to obtain epidermal stem cells functional tissue engineering strategies would be difficult to implement. Besides that, there is still a long way to be explored in order to generate significant knowledge regarding the mechanisms and molecular cues governing specification of epidermal lineage. Meanwhile, the studies described above provide important proof-of-principle for using pluripotent stem cell sources for regenerative skin therapies.

Differentiation of Mesenchymal Cells

The regeneration of dermal tissue, which is frequently lost in patients with full-thickness skin defects, is very important and needs to be studied in more detail. Whereas

the barrier function of the skin can be restored by grafting split-skin grafts or epithelial sheets composed of fully confluent keratinocytes, the lack of dermis or generation of scar tissue means that patients cannot regulate body temperature and maintain skin elasticity (Gallico, O'Connor et al. 1984; Compton 1992). Moreover, in the absence of mesenchymal cells, the split-skin grafts or keratinocyte grafts often fail to regenerate dermal-epidermal junctions, which leads to ulceration or graft rejection (Woodley, Peterson et al. 1988; Lamme, Van Leeuwen et al. 2000). In addition, the optimal wound healing of chronic wounds, such as venous and arterial ulcers depends on successful formation of granulation tissue, which also is mediated by mesenchymal cells. It is now generally accepted that a stromal component is needed to promote skin regeneration and ensure wound healing. The derivation of mesenchymal cell populations from pluripotent sources, such as hESCs and iPSCs, would provide an important source of homogenous, reliable, and well-defined populations of mesenchymal cells for regenerative medicine.

Several methods have been developed for isolating MSC-like cells from hESCs and iPSCs. The initial attempt to generate MSCs from hESCs was based on combining two strategies, the induction of mesenchymal differentiation of hESCs by co-culture with mouse OP9 stromal cells followed by sorting of CD73-positive cells using FACS. (Barberi, Willis et al. 2005). The obtained mesenchymal cells have satisfied the criteria commonly used to identify adult MSCs, including fibroblastic morphology, the expression of multiple MSC-specific markers, and the ability to differentiate into osteoblasts, adipocytes and chondrocytes (Dominici, Le Blanc et al. 2006). An alternative method for the derivation of MSCs from both hESCs that circumvented the use of mouse cell cultures has also been reported (Lian, Lye et al. 2007). In feeder layer-free

conditions, hESCs were cultured in a medium supplemented with bFGF and PDGF to encourage proliferation of putative MSCs, and then sorted by FACS for CD105+/CD24- cell population. The same technique has also been applied to isolate MSCs from human iPSCs (Lian, Zhang et al. 2010). In this study iPSC-derived MSCs have been transplanted into mouse limb ischemia model showing their active contribution to vascular and muscle tissue regeneration. In addition, two recent studies reported the isolation of vasculogenic pericytes using EBs generated from iPSCs (Dar, Domev et al. 2012), and the isolation of nestin-positive SKP-like population using monolayer cultures of hESCs (Wu, Gu et al. 2011). Similar to the population of iPSC-derived MSCs (Lian, Zhang et al. 2010), the administration of iPSC-derived pericytes promoted significant vascular and muscle regeneration in mouse limb ischemia model (Dar, Domev et al. 2012). Compared with previously reported hESC-derived MSCs, hESC-derived SKP-like progenitors were more plastic, and could differentiate into representative derivatives of all three primary germ layers, including mature smooth muscle cells, cardiomyocytes, functional hepatocytes, and neural cells (Wu, Gu et al. 2011).

So far only one study has reported the regeneration of dermal tissue using mouse ESC-derivatives (Coraux, Hilmi et al. 2003). In this study, ESCs generated both epithelial and mesenchymal lineage cells, which self-organized into epidermal and dermal compartments within 3D organotypic culture. After initial induction of ESCs with BMP4, the cells were harvested and then cultivated in transwells at the air-liquid interface. Under these conditions ESC-derived cells differentiated into keratinocytes that formed a stratified squamous epithelium in the top compartment, but also differentiated into fibroblasts that self-organized into dermal compartment underneath. This experiment

demonstrated that ESC can recapitulate many aspects of embryonic skin formation, including the dynamic reciprocal induction of both ectodermal and mesodermal commitments to form a 3D functional skin (Coraux, Hilmi et al. 2003).

The ability to derive fibroblasts from pluripotent stem cell sources is important for designing effective strategies for cutaneous tissue regeneration and wound healing. As stromal constituents of many tissues, fibroblasts play an essential role in regulating normal tissue homeostasis and wound healing through their synthesis of ECM and secretion of growth factors (Schultz and Wysocki 2009). Incorporation of primary stromal fibroblasts into tissue-engineered biomaterials has already shown great promise for their application in regenerative medicine (Wong, McGrath et al. 2007). However, the therapeutic potential of stromal fibroblasts has been limited by our incomplete understanding of the precursor cells that give rise to them and by their phenotypic heterogeneity (Koumas, King et al. 2001; Chang, Chi et al. 2002; Sorrell and Caplan 2004). In light of this, next-generation treatment strategies in engineering and repair will require the use of novel sources of fibroblasts that can offer well-defined progenitor populations and more predictable tissue outcomes upon their therapeutic use. Human pluripotent stem cells offer an alternative source of fibroblasts for therapeutic use that should be explored in more details.

Differentiation of Vascular Cells

Angiogenesis and vasculogenesis, the formation of new blood vessel, are crucial for tissue growth, development, and wound healing. Together with pericytes, vascular

cells are responsible for vascularization of the healing tissue and the deregulation of these processes can lead to formation of ischemic chronic wounds. (Werner and Grose 2003; Gurtner, Werner et al. 2008). Besides wound healing, tissue engineering represent an additional filed that can benefit from increased accessibility of endothelial cells from pluripotent stem cell sources. Vascularization of bioengineered tissues is fundamental for survival, structural organization, and engraftment of bioengineered tissues after *in vivo* transplantation (Levenberg, Ferreira et al. 2010).

Vascular cells at various stages of development are typically isolated from EBs grown in suspension for 10 to 15 days. The ideal time for isolation was chosen by the period in which vascular markers, such as CD34, CD31, and vascular endothelial cadherin (VE-cad), are most highly expressed during differentiation (Gerecht-Nir, Dazard et al. 2005). Differentiated cells are then dissociated, labeled with anti-CD34, -CD31, or -CD144 (VE-cad) antibodies and separated from the cell mixture by MACS or FACS. Isolated vascular cells are then cultured in media conditions that support specific differentiation and expansion pathways (Levenberg, Golub et al. 2002; Gerecht-Nir, Dazard et al. 2005; Levenberg, Ferreira et al. 2010). Isolation of mature endothelial cells is performed from 13 to 15 days old EBs based on co-expression of CD31/CD144 and expanded in endothelial growth media supplemented with VEGF. The functionality of these cells can be evaluated in immunedeficient mice upon subcutaneous implantation within varies scaffolds. The retrieved implants demonstrated human CD31-positive human microvessels, which contain mouse blood cells (Levenberg, Golub et al. 2002; Wang, Au et al. 2007).

Precursors of endothelial cells, the vascular progenitors that give rise to both endothelial and perivascular mesenchymal cells, can be isolated at earlier stages of EB differentiation, at day 10, where CD34 serves as a specific marker (Ferreira, Gerecht et al. 2007; Wang, Au et al. 2007). CD34-positive cells can be subsequently cultured in endothelial growth medium supplemented either with VEGF to give rise to mature endothelial cells, or with PDGF-BB to give rise to smooth muscle cells and pericytes. However, in terms of clinical applications, this technique is not optimal because of the low differentiation efficiency of endothelial and vascular progenitor cells, which make up only ~2% of the EBs from which they are purified, difficulties in *in vitro* expansion, and requirement for cell-sorting procedures (Wang, Au et al. 2007; Levenberg, Ferreira et al. 2010).

So far, one study has reported directed differentiation of rhesus monkey ESCs to endothelial cells in the monolayer culture by culturing ESCs in endothelial growth medium supplemented with VEGF followed by subculture on Collagen IV (Kaufman, Lewis et al. 2004). Although these cells could form capillary-like structures characteristic of endothelial cells both *in vitro* and *in vivo*, they completely lacked the expression of the major markers of vascular progenitors, VE-cad and CD31 (Kaufman, Lewis et al. 2004). Recently, an alternative approach for derivation of fairly pure population of endothelial cells from hESCs without cell-sorting was reported (Nakahara, Nakamura et al. 2009). This method involves culturing EBs in differentiation medium with VEGF, BMP4, SCF, IL3, IL6, and FMS-related tyrosine kinase-3 ligand. Importantly, the obtained endothelial cells could be passaged up to ten times without loss of proliferative potential and functional properties as demonstrated by effective recruitment into neovascularity *in vivo.*

As for the specification of vascular lineage fates, some research has been done to explore the mechanisms that control the initial specification of endothelial cells in hESCs. These studies confirmed the existence of hemangioblast cells, the common progenitors of hematopoietic and endothelial cells (Wang, Li et al. 2004; Woll, Morris et al. 2008). These cells were identified as CD34(bright)CD31(+)Flk1(+) and could differentiate into both endothelial cells and hemathopoetic cells *in vitro*. Development of the hemangioblast cell population was largely dependent on canonical Wnt signaling, specifically Wnt1, as inhibition of this signaling pathway resulted in a reduced generation of these cells (Woll, Morris et al. 2008).

In conclusion, despite the different approaches that have been employed to drive pluripotent stem cells towards the vascular lineage fates, no standardized protocols exist for generating vascular progenitor cells. The isolation of hemangioblasts or vascular progenitor cells from iPSC has not been shown yet. Overall, the derivation of endothelial cells from hESCs relies on formation of EBs and administration of variable concentrations of VEGF. However, the administration of hematopoietic cytokines has also been promising considering that hematopoiesis and angiogenesis are intimately associated. *In vivo* functionality assessment of hESC-derived endothelial cells has only been demonstrated for some of the differentiation strategies, possibly due to low cell numbers, as most strategies have not accomplished the homogenous differentiation. Additional research is required to overcome these issues and to allow robust generation of endothelial cells for regenerative medicine.

1.4 – Tissue-engineered Skin for Therapeutic and Research Applications

Understanding the mechanisms of embryonic development, stem cell biology, and biomaterial engineering are the key to achieving next generation tissue-engineered skin substitutes. Such skin substitutes would offer the complete regeneration of functional skin, including epidermis, dermis, all the skin appendages, and blood vessels for rapid vascularization and integration with the surrounding host tissue. As discussed earlier (see Chapter 1.2 – Stem Cells Sources for Skin Regeneration), the available cell sources for skin tissue engineering and cell replacement therapy constitute autologous adult stem cells and iPSCs, and allogeneic hESCs. While patient-specific stem cells possess many potential advantages (Mansilla, Marin et al. 2005; Caplan and Dennis 2006; Vojtassak, Danisovic et al. 2006; Wu, Chen et al. 2007; Yoshikawa, Mitsuno et al. 2008; Bey, Prat et al. 2010; Carlson, Faria et al. 2011), they are not easily available, and therefore, cannot be easily adapted for the large scale production of skin tissue-engineered products. Despite many efforts undertaken to isolate various adult stem cell populations, the stem cell markers are not definitive and do not allow the isolation of pure populations of stem cells (Watt 1998; Kaur and Li 2000; Haniffa, Wang et al. 2007; Covas, Panepucci et al. 2008; Li, Miao et al. 2008; Lorenz, Sicker et al. 2008). In addition, when expanded *in vitro*, adult stem cells have shown limited proliferative capacity, quickly lose their differentiation potential, and reduce production of bioactive factors including growth factors and cytokines (Siddappa, Licht et al. 2007; Kretlow, Jin et al. 2008; Roobrouck, Ulloa-Montoya et al. 2008; Wagner, Bork et al. 2009). Furthermore, stem cells obtained from different donors are not uniform and demonstrate significant functional differences,

making the preparation of large scale standardized therapeutic products rather difficult (Siddappa, Licht et al. 2007; Zhukareva, Obrocka et al. 2010). In light of this, immunologically privileged pluripotent stem cells, which are genetically stable to prevent tumor formation, would appear to be a promising alternative for an off-the-shelf widely available skin therapy. Significant advances have already been made in the field of tissue engineering by generating various skin substitutes. Currently available skin substitute products and their clinical and research applications will be discussed in this chapter.

Tissue-engineered Skin Substitutes

The development of tissue-engineered skin substitutes, such as epidermal, dermal, and composite skin substitutes, represents a significant advance in the field of wound healing. These tissue-engineered skin replacements have been finding widespread application, especially in the case of burns and chronic wounds. The early studies carried out by (Rheinwald and Green 1975; Bell, Ivarsson et al. 1979; Yannas and Burke 1980) formed the basis for the development of modern tissue-engineered skin substitutes that combine living cells with natural or synthetic biomaterials. At present, a variety of tissue-engineered skin substitutes are available for clinical use (Table 1-2), none of which, however, can replace all of the functions of intact human skin (Supp and Boyce 2005; Metcalfe and Ferguson 2007; Groeber, Holeiter et al. 2011). When applied to skin wounds, these bioengineered products can offer protection from fluid loss and contamination, while delivering extracellular matrix components, cytokines, and growth

Brand name/manufacturer	Graft type			Cell source	Biomaterial	Life-span
	Cell-free	Cell-based	Cell-seeded			
A. Epidermal constructs						
CellSpray Clinical Cell Culture (C3), Perth, Australia		x		Autologous keratinocytes	–	Permanent
Epicel Genzyme Biosurgery, Cambridge, MA, USA		x, cell sheet		Autologous keratinocytes	–	Permanent
EpiDex Modex Therapeutiques, Lausanne, Switzerland		x, cell sheet		Autologous keratinocytes	–	Permanent
EPIBASE Laboratoires Genevrier, Sophia-Antipolis, Nice, France		x, cell sheet		Autologous keratinocytes	–	Permanent
MySkin CellTran Ltd, Sheffield, UK			x	Autologous keratinocytes	Synthetic, silicone support layer with a specially formulated surface coating	Permanent
Laserskin or Vivoderm Fidia Advanced Biopolymers, Padua, Italy			x	Autologous keratinocytes	Recombinant, (HAM)	Permanent
Bioseed-S BioTissue TechnologiesGmbH, Freiburg, Germany			x	Autologous keratinocytes	Allogeneic, fibrin sealant	Permanent
B. Dermal constructs						
AlloDerm LifeCell Corporation, Branchburg, NJ, USA	x			–	Allogeneic human acellular lyophilized dermis	Permanent
Karoderm Karocell Tissue Engineering AB, Karolinska University Hospital, Stockholm, Sweden	x			–	Allogeneic human acellular dermis	Permanent
SureDerm HANS BIOMED Corporation, Seoul, Korea	x			–	Allogeneic human acellular lyophilized dermis	Permanent
GraftJacket Wright Medical Technology, Inc., Arlington, TN, USA	x			–	Allogeneic human acellular pre-meshed dermis	Permanent
Matriderm Dr Suwelack Skin and HealthCare AG, Billerbeck, Germany	x			–	Xenogeneic bovine non-cross-linked lyophilized dermis, coated with α-elastin hydrolysate	Permanent
Permacol Surgical Implant Tissue Science Laboratories plc, Aldershot, UK	x			–	Xenogeneic porcine acellular diisocyanite cross-linked dermis	Permanent
OASIS Wound Matrix Cook Biotech Inc, West Lafayette, IN, USA	x			–	Xenogeneic porcine acellular lyophilized small intestine submucosa	Permanent
EZ Derm Brennen Medical, Inc., MN, USA	x			–	Xenogeneic porcine aldehyde cross-linked reconstituted dermal collagen	Temporary
Integra Dermal Regeneration Template Integra NeuroSciences, Plainsboro, NJ, USA	x			–	Xenogeneic and synthetic: polysiloxane, bovine cross-linked reconstituted	Semi-permanent
Terudermis Olympus Terumo Biomaterial Corp., Tokyo, Japan	x			–	Xenogeneic and synthetic: silicone, bovine lyophilized cross-linked collagen sponge made of heat-denatured collagen	Semi-permanent
Pelnac Standard/Pelnac Fortified Gunze Ltd, Medical Materials Center, Kyoto, Japan	x			–	Xenogeneic and synthetic: silicone/silicone fortified with silicone gauze TREX, atelocollagen derived from pig tendon	Semi-permanent
Biobrane/Biobrane-L UDL Laboratories, Inc., Rockford, IL, USA	x			–	Xenogeneic and synthetic: silicone film, nylon fabric, porcine collagen	Temporary
Hyalomatrix PA Fidia Advanced Biopolymers, Abano Terme, Italy	x			–	Allogeneic and synthetic: HYAFF layered on silicone membrane	Semi-permanent
TransCyte (DermagraftTC) Advanced BioHealing, Inc., New York, NY and La Jolla, CA, USA			x	Neonatal allogeneic fibroblasts	Xenogeneic and synthetic: silicone film, nylon mesh, porcine dermal collagen	Temporary
Dermagraft Advanced BioHealing, Inc., New York, NY and La Jolla, CA, USA			x	Neonatal allogeneic fibroblasts	Allogeneic and synthetic: PGA/PLA, ECM	Temporary
Hyalograft 3D Fidia Advanced Biopolymers, Abano Terme, Italy			x	Autologous fibroblasts	Allogeneic: HAM	Permanent
C. Composite epidermal/dermal constructs						
Apligraf Organogenesis Inc., Canton,Massachusetts, CA, USA			x	Allogeneic keratinocytes and fibroblasts	Bovine collagen	Temporary
OrCel Ortec International, Inc., New York, NY, USA			x	Allogeneic keratinocytes and fibroblasts	Bovine collagen sponge	Temporary
PolyActive HC Implants BV, Leiden,The Netherlands			x	Autologous keratinocytes and fibroblasts	Synthetic PEO/PBT	Temporary
TissueTech Autograft System (Laserskin and Hyalograft 3D) Fidia Advanced Biopolymers, Abano Terme, Italy			x	Autologous keratinocytes and fibroblasts	Recombinant, HAM	Temporary

PEO: polyethylene oxide terephthalate.
PBT: polybutylene terephthalate.
PGA: polyglycolic acid (Dexon).
PLA: polylactic acid (Vicryl).
ECM: extracellular matrix.
HAM: hyaluronic acid membrane (microperforated).

Table 1-2. Commercially available skin constructs. Adapted from (Groeber, Holeiter et al. 2011)

factors, enhancing significantly natural host wound healing responses. Acellular dermal substitutes can also be used in combination with autografts to ensure their survival and engraftment.

Epidermal constructs are prepared from cultured autologous keratinocyte sheets transplanted alone or in combination with supportive biomaterials, such as silicon support layer or fibrin sealant (Table 1-2A). Allogeneic cryopreserved epidermal cultures like Celaderm™ also available but require further clinical studies (Alvarez-Diaz, Cuenca-Pardo et al. 2000; Khachemoune, Bello et al. 2002). Dermal constructs are used for the treatment of full-thickness burns prior to the application of epidermal cells. There is a wide variety of commercially available dermal constructs (Table 1-2B), which can be grafted permanently or temporarily depending on the conditions of the wound. Some of these substitutes like Dermagraft® consist of living allogeneic fibroblasts cultured on biodegradable mesh. The therapeutic action of the dermal substitutes consist of living fibroblasts depends on fibroblast-mediated secretion of ECM proteins and growth factors into the wound that facilitate formation of wound granulation tissue and promote wound re-epithelialization (Supp and Boyce 2005). Composite skin constructs consist of epidermal and dermal layers are the most advanced skin substitutes currently available for the clinical use (Table 1-2C). These constructs, such as Apligraf®, consist of living allogeneic fibroblasts and keratinocytes incorporated into a scaffold. These type of skin substitutes has been shown to provide ECM proteins and growth factors, facilitate wound closure, and reduce pain (Supp and Boyce 2005). While some research shows that allogeneic fibroblasts can be tolerated by the host (Kolokol'chikova, Budkevich et al. 2001), allogeneic keratinocytes are usually rejected (Strande, Foley et al. 1997; Clark,

Ghosh et al. 2007); therefore, composite substitute can only be used temporarily as a biological wound dressing.

In conclusion, so far, no manufactured skin substitute has provided an outcome consistently comparable to an autograft. Tissue-engineered skin substitutes are relatively simple single layer or bilayer constructs that lack the complexity of full-thickness functional skin. In order to enhance existing skin replacement therapy, development of new strategies to incorporate or induce formation of differentiated structures into a skin construct is necessary. However, cellular and biomaterial components of skin substitutes are continually being developed and improved and the next generation of tissue-engineered products will likely benefit from the novel pluripotent stem cell sources, such as hESCs and iPSC, to create cost-effective bioengineered skin replacement products with improved function and higher resemblance to native skin.

Vascularized Tissue Constructs

Tissue-engineered skin grafts require rapid vascularization for stable perfusion and integration with the host tissue. Rapid vascularization is important not only for the sufficient nutrient supply of the tissue but also for regulating normal wound healing by transporting signaling molecules and cells, such as microphages and circulating progenitor cells (Lammert, Cleaver et al. 2001; Badiavas, Abedi et al. 2003; Hausman and Rinker 2004; Brittan, Braun et al. 2005; Beaudry, Hida et al. 2007). There are two main strategies used to grow capillaries in an implanted tissue: (i) by promoting effective invasion of host blood vessels into the implant, and, (ii) by engineering pre-vascularized tissues *in vitro* (Kannan, Salacinski et al. 2005; Lokmic and Mitchell 2008). The first

strategy of promoting host angiogenesis relies on the release of pro-angiogenic growth factors by the implanted construct. The second strategy of engineering pre-vascularized tissue is achieved by recapitulating some developmental processes typical of vasculogenesis *in vitro* by incorporating relevant cell types, such as vascular progenitor cells, endothelial cells, and perivascular mesenchymal cells into the tissue engineering construct. This strategy is specifically important because it allows engineering tissues of clinically relevant size and complexity (Hausman and Rinker 2004; Kannan, Salacinski et al. 2005; Lokmic and Mitchell 2008).

It has been recently shown that successful vascularization and survival of full-thickness autologous skin grafts depends on early anastomoses between graft and bed vessels, mainly within the central area of the graft (O'Ceallaigh, Herrick et al. 2006). This study has indicated the importance of engineering blood vessels within skin constructs in order to facilitate rapid integration of a tissue-engineered skin graft. The formation of vascular-like network inside tissue-engineered skin in order to improve graft vascularization was first reported by Black et al. In this study, the skin equivalent construct was fabricated by incorporating dermal fibroblasts and umbilical vein endothelial cells into collagen scaffold with keratinocytes grown on the top of the scaffold. In this construct, a capillary-like network formed by self-organization of endothelial cells in cooperation with fibroblasts. This vessel-like network demonstrated formation of the lumen with typical intercellular junctions and a basement membrane of laminin and collagen IV (Black, Berthod et al. 1998). The improved graft vascularization following transplantation was later demonstrated using similar pre-vascularized skin constructs (Tremblay, Hudon et al. 2005). Significantly, the perfusion of tissue-

engineering transplant was as fast as for the full-thickness human skin transplant, indicating the functionality of the engineering vasculature and its successful anastomosis into the host vasculature. In addition, the contribution of mesenchymal cells to the maturation of engineered capillary-like networks was investigated *in vivo* after transplantation of pre-vascularized skin constructs (Benjamin, Golijanin et al. 1999; Schechner, Nath et al. 2000; Shepherd, Enis et al. 2006). These studies indicated the important role of vascular smooth muscle cell-mediated remodeling and stabilization of tissue engineered vascular networks.

In conclusion, among the major challenges facing tissue-engineering is to develop pre-vascularized tissue-engineered skin substitutes that would be able to integrate rapidly into the host tissue. Further research is necessary to explore alternative cell sources, such as hESC- and iPSC-derived endothelial cells and pericytes, and to better understand the contribution of mesenchymal cells to the maturation and stabilization of the engineered vasculature both *in vitro* and *in vivo*. In addition, pre-vascularized tissues can also provide an effective *in vitro* model to study physiology and physiopathology of the vasculature in a more complex tissue context.

Tissue-engineered Skin as In Vitro Model System

The tissue-engineered human skin has been developed to reproduce the key structural and functional aspects of natural skin. Thus, besides their use *in vivo* as skin replacements, skin constructs can be used as an *in vitro* model system to investigate skin morphogenesis and wound repair. The key advantages of the tissue-engineered skin

constructs for basic research include the following: (i) the organization of a 3D architecture of the reconstructed epidermis and dermis, (ii) the establishment of an epithelial-mesenchymal crosstalk, which can be manipulated and studied, (iii) the possibility to generate split-thickness or full-thickness wounds allowing to study the process regulating skin regeneration, (iv) the option to prepare skin constructs from any species and genetic backgrounds allowing to generate disease models or study the contribution of different cell populations, including those differentiated from hESCs and iPSCs. Single-layered epidermal tissue constructs have been extensively used in pharmacological as well as in molecular and stem cell biology research to test various compounds (Fentem and Botham 2002; de Jager, Groenink et al. 2006; Kandarova, Liebsch et al. 2006; Gabbanini, Lucchi et al. 2009) and to investigate the nature of the epithelial hierarchy at both molecular and cellular levels (Watt, Lo Celso et al. 2006). Although epidermal tissue constructs have proven to be very useful, they can be further improved by the addition of the dermal layer.

Stromal fibroblasts have only recently begun to receive more attention in the context of complex cell-cell interactions. It has been shown that this cell population is far from being homogeneous (Sorrell and Caplan 2004; Nolte, Xu et al. 2008), and it has been speculated that some chronic wounds are due to the changes in the composition of fibroblast population (Ongenae, Phillips et al. 2000; Kim, Kim et al. 2003; Harding, Moore et al. 2005). Experiments conducted using composite skin constructs containing both keratinocytes and fibroblasts layers have demonstrated the contribution of epithelial-mesenchymal cross-talk to epithelial morphogenesis by establishing that double-paracrine mechanism regulates the growth of both keratinocytes and fibroblasts (Szabowski, Maas-

Szabowski et al. 2000; Angel and Szabowski 2002) . Composite skin constructs have also served as a model for the formation of basement membrane (Breitkreutz, Mirancea et al. 2004; Segal, Andriani et al. 2008), and contributed to the understanding of the mechanism controlling wound re-epithelialization (Ponec, Weerheim et al. 1997; Egles, Shamis et al. 2008; Egles, Huet et al. 2010). In addition, composite skin substitute can potentially be used as *in vitro* model to study functionality of hESC- and iPSC-derived keratinocytes, fibroblasts, and endothelial cells and their behavior during wound healing process.

Furthermore, stromal fibroblasts produce and assemble ECM, the process essential for the formation of granulation tissue and the remodeling following injury, as well as for maintaining normal tissue homeostasis. This process can be studied *in vitro* using 3D model of dermal regeneration. 3D dermal-like tissue can be assembled *in vitro* by growing stromal fibroblasts on a transwell membrane in the presence of ascorbic acid over the course of 3-5 weeks. Ascorbic acid is known to increase collagen synthesis by stimulating transcription of collagen genes and by acting as co-factor in post-translational pro-collagen hydroxylation that is essential for the stabilization of collagen triple helical structure (Peterkofsky 1972; Murad, Grove et al. 1981; Chojkier, Houglum et al. 1989) Stromal tissues formed under these conditions bear striking biochemical and physical resemblance to the normal human dermis composed of multilayers of fibroblasts surrounded by dense accumulations of mature collagen fibrils in the extracellular space (Hata and Senoo 1989; Pouyani, Ronfard et al. 2009; Throm, Liu et al. 2010). Such dermal constructs have been defined in the previous studies as cell-derived "self-assembled" ECM (Pouyani, Ronfard et al. 2009; Throm, Liu et al. 2010). This system

allows to compare different populations of fibroblasts, including hESC- and iPSC-derived fibroblasts, for their matrix-production properties, and to establish their potential contribution to the formation of granulation tissue and matrix remodeling.

1.5 – Conclusions and Future Prospects

Understanding the biology of stem cells and their role in tissue development and wound repair is essential for tissue engineering and regenerative medicine. Stem cells are found in most tissues from the early stages of human development to the adulthood. All stem cells may prove useful for regenerative medicine applications, but each of the different types has both promise and limitations. Multipotent stem cells, which are found in certain adult tissues, such as MSCs, EpSC, and SKPs, may be limited to producing only certain types of specialized cells. In contrast, pluripotent stem cells, such as hESCs, which are derived from a very early stage in human development, have the potential to give raise to any cell type from any developmental stage. Additionally, recent advances in generating iPSCs have provided the opportunity to establish patient-specific pluripotent stem cells, which can be used to generate autologous cells. The unlimited expansion potential of hESCs and iPSCs and their ability to generate therapeutically relevant cell types makes them promising candidates for regenerative medicine applications.

Specifically in skin regeneration, the use of pluripotent stem cell sources can help to overcome some of the limitations of the current approaches. For achieving the complete regeneration of fully functional skin including epidermis, dermis, skin

appendages, and blood supply, it is essential to be able to regenerate the various skin-specific stem cells and their niches (Chuong, Wu et al. 2006; Chuong, Cotsarelis et al. 2007). Human ESCs and iPSCs have the unique potential to generate any type of stem cell or progenitor cell required for skin tissue regeneration. However, the full realization of this potential relies on the establishment of reproducible and efficient differentiation protocols. Development of such protocols for differentiation of therapeutically-relevant skin cells has already begun. Numerous protocols for derivation of mesenchymal, epidermal and endothelial progenitor cells from pluripotent stem cell sources are being continuously developed and improved. However, before these pluripotent stem cell-derivatives can be implemented in regenerative medicine, rigorous analysis of their safety and thorough testing of their functional abilities is required.

There are many issues that need to be addressed before moving hESCs and iPSCs to clinical applications. Although the development of iPSC technologies have helped to sidestep many ethical issues surrounding hESCs, there are still many challenges to overcome before iPSC can be used in clinic, including low reprogramming efficiency, risk of mutation associated with viral transfections, and incomplete reprogramming. Before iPSCs are being considered for clinical use, it is important to develop and test new techniques ensuring the safety of iPSCs, such as use of small-molecule compounds (Huangfu, Maehr et al. 2008), recombinant proteins (Lin, Ambasudhan et al. 2009), and non-integrating adenoviral vectors (Maherali, Ahfeldt et al. 2008; Maherali and Hochedlinger 2008) that reduce the risk of insertional mutagenesis caused by viral integration into the genome. Additionally, iPSCs have been shown to have more fragile genomes than hESCs and so to be prone to DNA abnormalities (Sheridan, Theriault et al.

2011). Beyond genetic abnormalities, epigenetic alterations have also been identified in iPSC lines (Lister, Pelizzola et al. 2009). These aberrant DNA methylation found in iPSCs are also maintained in cells differentiated from iPSC, which may affect their ability to differentiate into specific lineages (Lister, Pelizzola et al. 2011). Thus, more research is necessary to understand whether the developmental potential of iPSCs is equivalent to that of hESCs. In addition, genetic and epigenetic screens may be necessary to ensure the safety of iPSC lines prior to clinical use. Another concern is tumorigenicity of iPSCs due to incomplete differentiation. It has been shown that small number of residual undifferentiated iPSCs could be isolated and expanded after long-term differentiation of cells *in vitro* or *in vivo* (Fu, Wang et al. 2012). The obvious implication of these findings is to developing of efficient differentiation protocols that insure reconsider the strategies for solving the tumorigenic problem of iPSCs. Besides improving the reprogramming process, it is essential to develop better differentiation protocols and purification techniques.

Although the regenerative medicine applications for hESCs and iPSCs are not yet available, significant advances have been made in our understanding of pluripotent stem cells and their differentiation potential. Future research is focusing on improving differentiation protocols and developing screening techniques to ensure efficiency and safety of hESC- and iPSC-derivatives. Therefore, in this thesis I have explore the utility of 3D *in vitro* tissue models to predict the therapeutic potential and *in vivo* tissue outcomes of pluripotent stem cell-derivatives.

Chapter 2: Fibroblasts Derived from Human Embryonic Stem Cells Direct Development and Repair of 3D Human Skin Equivalents

Publications:

The findings of this project have been published in *Stem Cell Research & Therapy, 2(1):10-19, 2011.* "Fibroblasts derived from human embryonic stem cells direct development and repair of 3D human skin equivalents". Shamis Y, Hewitt KJ, Carlson MW, Margvelashvilli M, Dong S, Kuo CK, Daheron L, Egles C, Garlick JA.

Author Contributions:

Yulia Shamis: designed and performed all the experiments, analyzed data, and wrote the manuscript

Kyle J. Hewitt: developed protocol for directed differentiation of hESC to EDK fibroblasts (see Apendix I, and Figure 2-1 A and 2-1B), discussed the results, and commented on the manuscript

Mark W. Carlson: provided technical assistance for the maintenance of hESCs, discussed the results, and commented on the manuscript

Margvelashvilli M: performed RT-PCR analysis of EDK cells (see Figure 2-1D), discussed the results, and commented on the manuscript

Shumin Dong: provided technical assistance for the tissue processing and histology, discussed the results, and commented on the manuscript

Laurence Daheron: derived H9-MSCs (see Figure 2-1F), discussed the results and commented on the manuscript

Kuo CK: discussed the results and commented on the manuscript

Christophe Egles: discussed the results and commented on the manuscript

Jonathan A. Garlick: supervised the project, discussed the results, and assisted in the writing of the manuscript

Abstract

Pluripotent human stem cells hold great promise as a source of progenitor and terminally differentiated cells for application in future regenerative therapies. However, such therapies will be dependent upon the development of novel approaches that can best assess tissue outcomes of pluripotent stem cell-derived cells and will be essential to better predict their safety and stability following *in vivo* transplantation.

In this study we demonstrated that engineered, human skin equivalents (HSEs) can be used as a platform to characterize fibroblasts that have been derived from human embryonic stem cells (hESCs). We characterized the phenotype and the secretion profile of two distinct hESC-derived cell lines with properties of mesenchymal cells (EDK and H9-MSC) and compared their biological potential upon induction of differentiation to bone and fat and following their incorporation into the stromal compartment of engineered, HSEs.

While both EDK and H9-MSC cell lines exhibited similar morphology and mesenchymal cell marker expression, they demonstrated distinct functional properties when incorporated into the stromal compartment of HSEs. EDK cells displayed characteristics of dermal fibroblasts that could support epithelial tissue development and enable re-epithelialization of wounds generated using a three-dimensional (3D) tissue model of cutaneous wound healing, which was linked to elevated production of hepatocyte growth factor (HGF). Lentiviral shRNA-mediated knockdown of HGF resulted in a dramatic decrease of HGF secretion from EDK cells that led a marked reduction of their ability to promote keratinocyte proliferation and re-epithelialization of cutaneous wounds. In contrast, H9-MSCs demonstrated features of mesenchymal stem

cells (MSCs) but not those of dermal fibroblasts, as they underwent multilineage differentiation in monolayer culture, but were unable to support epithelial tissue development and repair or to produce elevated levels of HGF.

Our findings demonstrate that hESCs could be directed to specified and alternative mesenchymal cell fates whose function could be distinguished in engineered HSEs. Characterization of hESC-derived mesenchymal cells in 3D, engineered HSEs demonstrates the utility of this tissue platform to predict the functional properties of hESC-derived fibroblasts before their therapeutic transplantation.

Introduction

The use of pluripotent human stem cells, including embryonic stem cells (hESCs) and induce pluripotent stem cells (hiPSCs), for future therapies provides advantages over more traditional sources of progenitor cells, such as adult stem cells, due to their ability to give rise to a variety of differentiated cell types and to their unlimited expansion potential (Cedar, Cooke et al. 2007; Klimanskaya, Rosenthal et al. 2008). However, such therapies will be dependent upon the development of novel approaches that can best assess tissue outcomes of hESC- and hiPSC-derived cells and will be essential to better predict their safety and stability following *in vivo* transplantation. One possible approach would be to use three-dimensional (3D) engineered tissues to monitor the functional outcomes of hESCs and hiPSC-derivatives. By providing an *in vivo*-like microenvironment that enables progenitor cells to manifest their *in vivo* characteristics in 3D tissue context, tissue engineering can play an important role in determining the

function, stability, and safety of hESC- and hiPSC -derived cells before their future application.

Stromal fibroblasts play a critical role in regulating tissue homeostasis and wound repair through the synthesis of extracellular matrix proteins and by secreting paracrine-acting growth factors and cytokines that have a direct effect on the proliferation and differentiation of adjacent epithelial tissues (Smola, Thiekotter et al. 1993; Matsumoto and Nakamura 1997; Szabowski, Maas-Szabowski et al. 2000; Andriani, Margulis et al. 2003; Chmielowiec, Borowiak et al. 2007). Despite the critical impact of this reciprocal cross-talk between stromal fibroblasts and epithelial cells on tissue homeostasis, little is known about the identity and maturational development of the precursor cells that give rise to these fibroblasts. This incomplete understanding of fibroblast lineage development is in large part due to the lack of definitive markers and to their cellular heterogeneity *in vivo* that has complicated their isolation, characterization, and potential therapeutic applications (Sorrell and Caplan 2004; Sorrell, Baber et al. 2007; Phan 2008; Sorrell, Baber et al. 2008).

In light of this, pluripotent human stem cells may serve as an alternative to adult tissues of more uniform fibroblasts that may provide more predictable tissue outcomes upon their therapeutic use. Several previous studies have demonstrated the derivation of mesenchymal stem cell (MSC)-like cells from hESCs that can differentiate to bone, fat, and cartilage (Barberi, Willis et al. 2005; Olivier, Rybicki et al. 2006; Lian, Lye et al. 2007; Boyd, Robbins et al. 2009), and fibroblast-like cells that have been used as autogeneic feeders to support the culture of undifferentiated hESCs (Xu, Jiang et al. 2004; Yoo, Yoon et al. 2005; Choo, Ngo et al. 2008; Chen, Chuang et al. 2009). In our

previous work we have demonstrated that hESCs give rise to mesenchymal cells (Hewitt, Shamis et al. 2009), however, we have not determined if hESCs-derived mesenchymal cells can manifest the functional properties of dermal fibroblasts that can support the organization and development of 3D skin-like tissues also known as human skin equivalents (HSEs) through epithelial-mesenchymal cross-talk. Since the morphogenesis, homoeostasis, and repair of many tissues depends on interactions between epithelial cells and their adjacent stromal fibroblasts (Smola, Thiekotter et al. 1993; Matsumoto and Nakamura 1997; Szabowski, Maas-Szabowski et al. 2000; Andriani, Margulis et al. 2003; Chmielowiec, Borowiak et al. 2007)], the functional analysis of hESC-derived fibroblasts could best be accomplished in such engineered HSEs that demonstrate many features of their *in vivo* counterparts.

In this study, we have characterized two cell lines with features of mesenchymal cell lineages (EDK and H9-MSC) that differ from each other in their production of HGF, a growth factor known to be secreted by dermal fibroblasts that support epithelial development and repair. In monolayer cultures, we found that EDK and H9-MSCs exhibited considerable overlap as seen by their mesenchymal morphology and expression of surface markers characteristic of both MSCs and dermal fibroblasts**.** However, EDK cells could not undergo differentiation to bone and fat and demonstrated properties similar to stromal fibroblasts that could support epithelial tissue development and enable re-epithelialization HSEs that was linked to the elevated expression and secretion of HGF. In contrast, H9-MSCs displayed multipotent differentiation capacity typical of an MSC phenotype (Dominici, Le Blanc et al. 2006), but did not support epithelial tissue development or repair, possible due to low level of HGF production. When HGF

secretion from EDK cells was suppressed by shRNA, epithelial repair was significantly decreased, suggesting that the regenerative phenotype of EDK cells is mediated, at least in part, by HGF secretion. HSEs used in our studies provided a complex tissue microenvironment that enabled characterization of the functional properties of hESC-derived fibroblasts and provide an important platform to further establish their stability, safety, and efficacy for future therapeutic transplantation.

Materials and Methods

Cell Culture

Human ESC (H9) line was maintained in culture as previously described (Thomson, Itskovitz-Eldor et al. 1998), on irradiated feeder layers of mouse embryonic fibroblasts (MEF). EDK cells were prepared using our previously described protocol (Hewitt, Shamis et al. 2009). Briefly, we derived multiple, independent EDK cell lines by first growing H9-hESCs on MEFs fixed in 4% formaldehyde in keratinocyte (NHK) medium supplemented with 0.5nM human BMP-4 (R&D Systems, Minneapolis, MN) from day 4-7 of differentiation. These EDK cell lines were then propagated first on tissue culture plastic and then expanded on Type I collagen-coated plates (BD Biosciences, San Jose, CA) in NHK medium. This protocol is summarized in Figure 2-1A. For a step-by-step protocol and media formulations, see Appendix I. H9-MSCs were provided by Dr. Laurence Daheron. H9-MSCs were generated from H9-hESCs as previously described (Seda Tigli, Ghosh et al. 2009). Briefly, H9-hESC were grown on irradiated feeder layers of MEFs in in IMDM (Invitrogen, Carlsbad, CA) supplemented with 1% FBS for 10 days and then switched to MSCGM (Lonza, Basel, CH) for 4 extra days to enrich for MSC

population. Differentiating cells were then FACS-sorted for CD73-positive cells and expanded in MSCGM (Lonza, Basel, CH), first on tissue culture plastic and then passaged on Type I collagen-coated plates (BD Bioscience, San Jose, CA). This protocol is summarized in Figure 2-2. Control human dermal fibroblasts (HDF) were derived from newborn foreskin and grown in DMEM (Invitrogen, Carlsbad, CA) supplemented with 10% FBS (Hyclone, Logan, UT). For all experiments, HDF, EDK and H9-MSC were expanded in specific cell culture media and then maintained in NHK media consisting of 3:1 DMEM:F12 (Invitrogen, Carlsbad, CA), 5% FCII (Hyclone, Logan, UT), 0.18mM adenine, 8mM HEPES, 0.5 µg/mL hydrocortisone, 10^{-10} M cholera toxin, 10ng/mL EGF, 5µg/mL insulin (all from Sigma, St. Louis, MO). All cell lines were routinely checked for mycoplasma contamination using MycoAlert® Mycoplasma detection kit (Lonza, Rockland, ME).

Preparation of 3D Tissue Constructs

Engineered, 3D human skin equivalents (HSEs) were constructed as previously described (Garlick, Parks et al. 1996). Briefly, HDF, EDK, or H9-MSCs were added into Type I Collagen gels (Organogenesis, Canton, MA) to a final concentration of 2.5×10^4 cells/ml. Type I Collagen gels prepared without fibroblasts were used as controls. $5x10^5$ human keratinocytes (NHK) were seeded onto the collagen matrix, and tissues were then maintained submerged in low calcium epidermal growth media for 2 days, for additional 2 days in normal calcium media, and then raised to the air–liquid interface. For the preparation of 3D tissue models of cutaneous wound healing, HSEs constructed using HDF were wounded with a 4mm punch and placed on the surface of a contracted collagen gel populated with either HDF, EDK, H9-MSCs, or without cells as previously

described (Garlick, Parks et al. 1996; Egles, Shamis et al. 2008). The method is summarized in (Figure 2-3). For a step-by-step protocol, see Appendix II. Wounded cultures were maintained at the air–liquid interface for 72 or 96 hours at 37 °C in 7.5% CO_2 to monitor re-epithelialization. For quantitative analysis of wound re-epithelialization, tissue samples were fixed in 4% neutral-buffered formalin, embedded in paraffin, and serially sectioned at 8 μm. Histological sections were stained with hematoxylin and eosin (H&E), images were captured using a Nikon Eclipse 80i microscope (Nikon Instruments Inc., Melville, NY, USA) equipped with a SPOT RT camera (Diagnostic Instruments, Sterling Heights, MI, USA) and analyzed using Spot Advanced software (Diagnostic Instruments, Sterling Heights, MI, USA).

Real-time RT-PCR

Total RNA was extracted from confluent cultures of EDK, H9-MSC, or HDF cells using RNeasy kit (Qiagen, Valencia, CA) and cDNA was transcribed with 1μg RNA using the Quantiscript Reverse Transcriptase (Qiagen, Valencia, CA). The relative level of gene expression was assessed using 20 ng of cDNA, 200 nM of each primer, and 2X SYBRgreen (Applied Biosystems, Foster City, CA) at a total sample volume of 12.5 μL and samples were run in triplicates on the Bio-Rad CFX96 Real-Time PCR Detection System according to manufacturer's instructions (Applied Biosystems, Foster City, CA) . The relative level of gene expression was assessed using the $2^{-\Delta\Delta Ct}$ method and results are presented as an average of two experiments and three technical replicates. The following oligonucleotide primer sequences were used: GAPDH-F1: 5'-tcgacagtcagccgcatcttcttt-3', GAPDH-R1: 5'-accaaatccgttgacctt-3', HGF-F1: 5'-aggggcactgtcaataccatt-3', HGF-R1: 5'-cgtgaggatactgagaatcccag-3'; p75NTR-F: 5'-

ggcttcggacccccggtctc-3', p75NTR-R: 5'-tcgtctactcgagctggccaa-3'; HNK1-F: 5'-tgtgagtggtaatgaggagcc-3', HNK1-R: 5'-gcagagtccagggcagcacg-3'; Sox10-F: 5'-atacgacactgtcccggccctaaa-3', Sox10-R: 5'-ttctcctctgtccagcctgttctc-3'; T-F: 5'-tattggcaactttggcacacca-3' T-R: 5'-ggcttcactaataactggacgaatcac -3'; Gata4-F: 5'-ggaggcgagatgggacgggt-3' GATA4-R: 5'-tggggaccccgtggagctt-3'; MSGN1-F: 5'-tcttcttctccctgtccagc-3', MSGN1-R: 5'-gtctgtgagttccccgatgt-3'; TBX4-F: 5'-cagcactaccagcacgagaa-3', TBX-4R: 5'-ctcagcatttgctggtcgta-3' ; RUNX1-F: 5'-gtcagcccacaccacccagc-3', RUNX1-R: 5'- gtcaggtcgggtgccgttga -3'.

Proliferation Kinetics

HDF, EDK, and H9-MSC of the same passage (p7) underwent additional passaging every 7 days upon reaching 70-80% confluence. Cell numbers were determined by counting trypsinized cells using a hemocytometer, and data were recorded as an average of three measurements for each passage. As cell numbers were first determined at p8, the number of population doublings (PD) was first calculated for p8 using the following formula: $X=[\log10(N_H)-\log10(N_1)]/\log10(2)$. The N_H is the harvested cell number and the N_1 is the plated cell number. The PD for each passage was calculated and added to the PD of the previous passages to calculate the cumulative population doublings.

shRNA Knockdown

The pLKO.1-puro non-target shRNA control vector and the pLKO.1-puro vector containing shRNA against HGF (TRCN clone 3310) were purchased from Sigma (Sigma, MISSION shRNA, St. Louis, MO, USA). Lentiviral particles were generated in 293FT cells using ViraPower™ Lentiviral Expression System (Invitrogen, Carlsbad, CA)

according to manufacturer's protocol. Knockdown viruses were tittered using an end-point dilution assay and cell lines were infected with lentiviruses at a multiplicity of infection (MOI) of 1. Stable cell lines were selected with puromycin (2μg/ml) (Sigma, St. Louis, MO).

ELISA

Tissue culture supernatants were harvested after 24h incubation and processed using DuoSet HGF ELISA kit (R&D Systems, Minneapolis, MN) according to manufacturer's protocol. Media was assayed in triplicates from at least three independent samples. For monolayer cultures, the values were normalized according to cell numbers counted in the respective cultures at the time of supernatant harvesting and expressed in pg/ml per 10^4 cells.

Antibody-based Cytokine Array

HDF, EDK, or H9-MSCs 10^6 cells were plated onto 100mm tissue culture plates and grown to 80-90% confluence in tissue culture medium. Then tissue culture media was replaced with 5ml of DMEM (Invitrogen, Carlsbad, CA) supplemented with 1% FBS (Hyclone, Logan, UT) for additional 24 hours incubation. Tissue culture supernatants were harvested, and the supernatants from the plates containing equal cell numbers were processed using Proteome Profiler Human Angiogenesis Antibody Array (R&D Systems, Minneapolis, MN) according to manufacturer's protocol. Histogram profiles were generated by quantifying the mean spot pixel densities from the array membrane using ImageJ software (U. S. National Institutes of Health, Bethesda, Maryland, USA).

Histology, Immunohistochemistry, and Immunofluorescence

HDF, EDK, or H9-MSCs were grown to 80-90% confluence on Type I Collagen-coated coverslips, fixed in 4% paraformaldehyde and permeabilized using 0.1% triton X-100. Cells were stained using primary monoclonal antibodies directed against vimentin (Abcam, Cambridge, MA), α-SMA (Chemicon, Temecula, CA), Thy-1 (Calbiochem, San Diego, CA) followed by Alexa 488-conjugated goat anti-mouse secondary antibodies (Invitrogen, Carlsbad, CA) for 1 hour. 3D tissue constructs tissues were fixed in 4% paraformaldehyde and frozen in O.C.T. compound (Sakura Finetek USA, Torrance, CA), sectioned at 8µm, and immunostained using primary antibodies directed against K1/10 (Abcam, Cambridge, CA), Involucrin (Abcam, Cambridge, CA) followed by either Alexa Fluor 594 or Alexa Fluor488-conjugated goat anti-mouse secondary antibodies (Invitrogen, Carlsbad, CA). For morphologic analysis, hemotoxylin and eosin staining (H&E) was performed on paraffin-embedded tissues sectioned at 8µm thickness. For proliferation analysis, 3D tissue constructs were labeled with a 6 hour pulse of BrdU (Sigma, St. Louis, MO) at a final concentration of 10µM. Immunohistochemical staining was performed on paraffin-embedded tissues sectioned at 8µm thickness using monoclonal antibodies against BrdU (Roche, Indianapolis, IN) and Vectastain ABC (peroxidase) kit (Vector Labs, Burlingame, CA). The number of BrdU-positive cells was determined and expressed as a percentage of total cells in the basal layer. Two independent experiments with a minimum of three observations for each condition were analysed.

Flow Cytometry

HDF, EDK, or H9-MSCs were grown to 80-90% confluence, trypsinized, pelleted, and resuspended in 2% FBS in PBS solution. Cell suspensions were mixed with 15µl of PE-conjugated anti-CD73, -CD10, -CD13, -CD105, -CD106, -CD166, -CD44, -CD90, -CD140b, -CD117, -CD34, -CD45, -CD31 or Isotype control-IgG1k (BD Pharmingen, San Jose, CA), and flow cytometric analysis was performed using a FACSCalibur (Becton Dickinson, San Jose, CA) and analyzed using CellQuest (Becton Dickinson, San Jose, CA) and Summit V4.3 software (Dako, Carpentaria, CA).

Osteogenic and Adipogenic Differentiation Assays

To induce osteogenesis HDF, EDK, or H9-MSCs were grown to confluence in the presence of 100 nM dexamethasone, 0.05mM ascorbic acid, and 10 mM -glycerophosphate (all from Sigma, St. Louis, MO) in DMEM (Invitrogen, Carlsbad, CA) supplemented with 1% of non-essential amino-acids (Invitrogen, Carlsbad, CA), and 10% FBS (Hyclone, Logan, UT). After 28 days, cultures were fixed in 1% formaldehyde, and stained for 10 minutes with Alizarin red solution (Sigma, St. Louis, MO) to determine calcium deposition, and staining was quantified spectrophotometrically (A_{550}) after solubilization with 10% CPC (Sigma, St. Louis, MO). To induce adipogenesis HDF, EDK, or H9-MSCs were grown to confluence in 24-well plates in the presence of 1µM dexamethasone, 50 µM indomethacin, 5 µg/ml insulin, and 0.5 mM 3-isobutyl-1-methyl-xanthine (all from Sigma, St. Louis, MO) in DMEM (Invitrogen, Carlsbad, CA) supplemented with 1% of non-essential amino-acids (Invitrogen, Carlsbad, CA), and 10% FBS (Hyclone, Logan, UT). After 28 days, cultures were fixed in 4% formalin and stained with Oil Red O solution (Sigma, St. Louis, MO) for 30 minutes to visualize oil

droplets, and staining was quantified spectrophotometrically (A_{500}) after solubilisation with isopropanol. All results are presented as mean ± standard deviation of three independent experiments and three technical replicates.

Statistical Analysis

Statistical analyses were carried out using IBM SPSS Statistics 19 software (IBM, Armonk, NY). All results are reported as mean ± standard deviation of at least three independent samples. Statistical comparison between two groups was performed using Student's t-test. When comparing more than two groups One-Way Analysis of Variance (ANOVA) test was used followed by the post hoc Tukey's multiple comparison tests. Results were considered significant for $p \leq 0.05$.

Results

Differentiation of EDK and H9-MSC from hESCs

So far only one study by Coraux et al. has reported dermal regeneration by use of ESCs. In this study, mouse ESCs generated both epithelial and mesenchymal lineage cells, which self-organized into epidermal and dermal compartments within 3D tissue construct (Coraux, Hilmi et al. 2003). These experiments demonstrated that ESCs can recapitulate some of the aspects of embryonic skin formation, including the dynamic reciprocal induction of both ectodermal and mesodermal lineage commitment. Using similar methodology described by Coraux et al., we demonstrated the directed differentiation of human ESCs to derive cell populations with properties of both mesenchymal and epithelial cell types, named EDK (Hewitt, Shamis et al. 2009). The

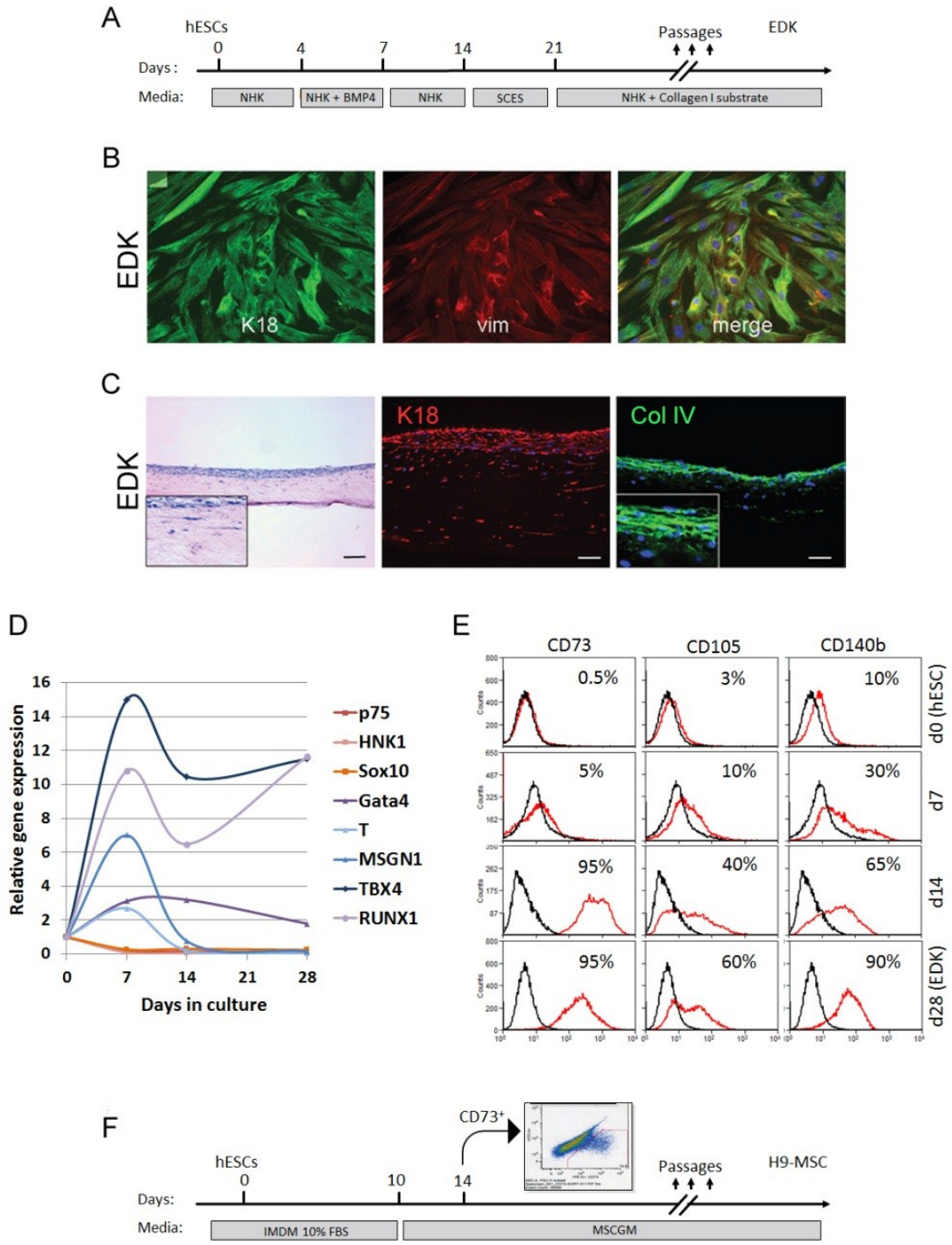

Figure 2-1. Differentiation of EDK and H9-MSC from hESCs. A. Schematic of the protocol for differentiating EDK from hESCs. **B.** EDK cells co-express epithelial marker cytokeratin 18 (K18, green) and mesenchymal marker vimentin (Vim, red) by immunofluorescence. **C.** Morphology of HSEs formed with EDK cells incorporated into epidermal and dermal compartments. Bars,100µm. **D.** RT-PCR analysis of mesenchymal precursor markers during different differentiation stages of EDK. Data are presented as fold increase in the level of gene expression compared to d0 (hESCs). **E.** Flow cytometry analysis of MSC markers during different differentiation stages of EDK. The percentages of cells positive for the surface markers (red profile) are shown. Each experiment is normalized to isotype control (black profile) **F.** Schematic of the protocol for differentiating H9-MSC from hESCs.

differentiation protocol is shown schematically in Figure 2-1A. For a detailed protocol and media formulations, see Appendix I. As demonstrated by Hewitt et al., the resulting EDK cells co-express early epithelial marker cytokeratin 18 (K18) and mesenchymal marker vimentin (Vim) (Figure 2-1B). When incorporated into 3D tissue construct, EDK cells failed to form stratified squamous epithelium, but instead formed disorganized layers of K18 expressing cells (Figure 2-1C). EDK cells also expressed Type IV collagen (Coll IV) that was retained in the cell cytoplasm and not deposited in the basement membrane zone (Figure 2-1C, inset).

To characterize the mesenchymal lineage specification of EDK cells, we differentiated hESCs towards EDKs and analyzed the expression of markers associated with mesenchymal phenotype at intermediate stages of hESC differentiation using quantitative RT-PCR and flow cytometry analysis. Markers were selected to monitor the expression of neural crest precursors of mesenchymal cells (HNK1, p75NTR, and Sox10), mesodermal precursors of mesenchymal cells (GATA4, T brachyury homolog, TBX4, RUNX1 and MSGN1), and mesenchymal stem cell markers (CD73, CD105/Endoglin, and CD140b/PDGFRβ). Data analysis revealed a gradual decrease in the expression level of neural crest markers (HNK1, p75NTR, and Sox10), transient induction of mesodermal markers following BMP4 treatment at day 7 (GATA4, T brachyury homolog, and MSGN1), and steady induction of TBX4 and RUNX1, and MSC markers (CD73, CD105/Endoglin, and CD140b/PDGFRβ) throughout the time course of hESC differentiation to EDK cells (Figure 2-1D and 2-1E). Together, this temporal gene and protein expression data suggest that the tested culture conditions are conductive to differentiation of hESCs towards mesodermal precursors at the expense of neural crest

and may be producing mesenchymal stem cells. H9-MSCs were generated using an alternative differentiation protocol that has previously been described to derive MSC from hESCs based on FACS-isolation of CD73-positive cell subpopulations (Seda Tigli, Ghosh et al. 2009). The differentiation protocol is shown schematically in Figure 2-1F.

Comparative characterization of EDK, H9-MSC, and primary dermal fibroblasts

EDK and H9-MSC populations showed similar fibroblast morphology *in vitro* and expression of Thy-1 and Vim by immunofluorescence that were similar to that seen in primary human dermal fibroblasts (HDF), while α-SMA-positive cells were observed more frequently in EDK cultures than in either H9-MSC or HDF (Figure 2-2A and 2-2B). Surface marker profiling of EDK and H9-MSCs was performed by flow cytometry and compared to the profile generated for HDFs. EDK and H9-MSC lines presented a similar profile of surface antigen expression characteristic of mesenchymal cells. All cell lines expressed CD73, CD105, CD90, CD166, CD44, CD13, and CD146 and lacked expression of hematopoietic and endothelial lineage markers CD45, CD34, and CD31 (Table 2-1). HDF showed low expression of CD117, and CD106 when compared to hESC-derived mesenchymal cells. The intensity of fluorescent labeling and the distribution of labeled cells were similar for CD73, CD105, CD106, CD44, CD166, and CD13 when EDK and H9-MSC were compared. However, expression of CD10 was significantly higher, while CD146 was lower in the EDK cell line when compared to H9-MSCs. This elevated expression of CD10 and reduced expression of CD146 was also seen in HDFs, suggesting a fibroblast-like phenotype for EDK cells. These findings indicated that while both hESC-derived cell populations exhibited characteristic

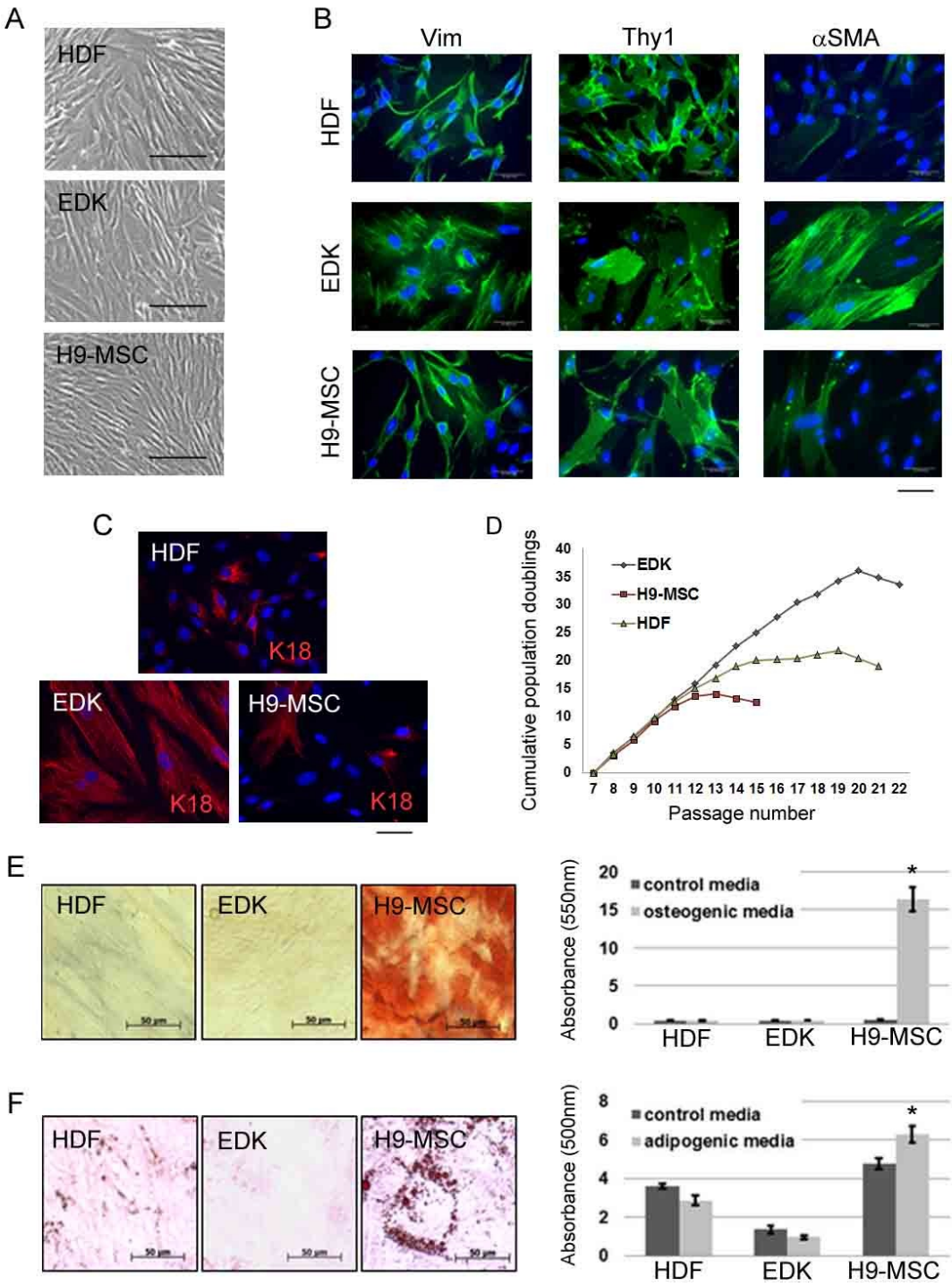

Figure 2-2. Comparative characterization of EDK, H9-MSC, and HDF. A. Cellular morphology of HDF, EDK, and H9-MSC using phase contrast. Bars, 50µm. **B.** Expression of mesenchymal markers Vim, Thy1, and α-SMA by immunofluorescence. Bar, 50µm. **C.** Expression of early epithelial marker K18 by immunofluorescence. Bar, 50µm. **D.** Growth capacity of HDF, EDK, and H9-MSC was assessed by calculating cumulative population doublings during serial subculture. **E.** Osteogenic differentiation was induced using the β-glycerophosphate method, calcium deposition was stained with Alzarin Red. Bars, 50µm. Quantification of Alizarin Red staining (t-test: *p< 0.05). **F.** Adipogenic differentiation was induced using the 3-isobutyl-1-methylxanthine method, lipid vesicles were stained with Oil Red O. Bars, 50µm. Quantification of Oil Red O staining (t-test: *p< 0.05).

mesenchymal surface markers, differences in their CD profile suggested differences in their biological potential.

In vitro expansion potential of EDK, H9-MSC, and HDF was assessed by calculating population doublings (PDs) during serial subculture. All three cell lines were thawed at passage 7 and subcultured weekly over a period of 3 months. The cultures were considered to have lost their growth potential when cells underwent less than one PD per passage. As demonstrated by their cumulative growth curves, EDK, H9-MSC, and HDF showed significant differences in their growth kinetics (Figure 2-2C). All tested cell lines demonstrated very similar PDs until passage 11 (mean PD of 3.3 ± 0.3). The decline in PDs was first seen in H9-MSC that occurred at passage 11 (PD = 1.8 ± 0.3) followed by loss of growth potential at passage 15. The decline in PDs of HDF fibroblasts first occurred at passage 13 (PD = 1.8 ± 0.6) followed by loss of growth potential at passage

Surface marker	Antigen	HDF	EDK	H9-MSC
CD73	SH3, ecto-5'-nucteotidase	99	99	99
CD105	SH2, endoglin	99	60	95
CD90	Thy-1	99	99	99
CD117	c-Kit	5	10	10
CD13	Aminopeptidase N	99	98	97
CD10	CALLA	99	99	30
CD146	MCAM	60	60	90
CD106	VCAM-1	5	60	60
CD166	ALCAM	99	95	95
CD44	Hyaluronate, HCAM	99	99	99
CD45	LCA	1.5	1.5	1.5
CD31	PECAM	1.5	1.5	1.5
CD34	surface glycoprotein	5	1.5	5

The percentage of cells positive for the cell surface markers are shown, each experiment is normalized to isotype control and has been repeated at least two times.

Table 2-1. Comparison of surface antigen expression on HDF, EDK, and H9-MSC by flow cytometry. EDK and H9-MSCs express markers associated with MSC phenotype (positive for expression CD73, CD105, CD90, CD10, CD13, CD44, CD106, CD146, CD117, CD166; negative for expression of hematopoietic and endothelial markers CD45, CD34, and CD31). HDF show low expression of CD106 and CD117. EDK and H9-MSCs show significant differences in expression of CD146 and CD10 antigens.

19. The decline in PDs of EDK cells was seen after passages 20 (PD = 1.8 ± 0.6) followed by loss of growth potential at passage 22. These results demonstrated that the growth of EDK and HDF was markedly prolonged when compared to H9-MSC.

To assess the multilineage differentiation potential of EDK, H9-MSC, and HDF, we performed osteogenic and adipogenic differentiation assays. After 4 weeks under differentiation conditions, H9-MSCs cultures contained calcium deposits as detected by Alizarin red (Figure 2-2D), Oil Red-O-positive lipid droplets (Figure 2-2E). In contrast, EDK and HDF did not show this differentiation potential as cells did not form osteoblasts or adipocytes (Figure 2-2C and 2-2D). These findings demonstrated that EDK and H9-MSC cell lines had divergent cell fates, as seen by their potential to form osteoblasts and adipocytes. While H9-MSCs manifested properties of MSC-like progenitors, absence of multilineage differentiation potential in EDK cells suggested that these cells may underwent developmental restriction to fibroblast lineage fate (Sudo, Kanno et al. 2007).

EDK cells function as dermal fibroblasts in 3D human skin equivalents

Since the paracrine cross-talk between fibroblasts and epithelial cells is required for the development of stratified epithelial tissue, we next incorporated EDK or H9-MSC into human skin equivalents (HSEs) as a functional assay for their capacity to support normal skin development (Figure 2-3A). For a detailed protocol of HSEs preparation, see Appendix II. EDK or H9-MSC were embedded into collagen gels and allowed to contract the gel for 7 days, normal human keratinocytes (NHK) were then seeded onto the surface of collagen gels, and tissues were grown at an air-liquid interface for an additional 7days to compare their capacity to support the formation of stratified squamous epithelium.

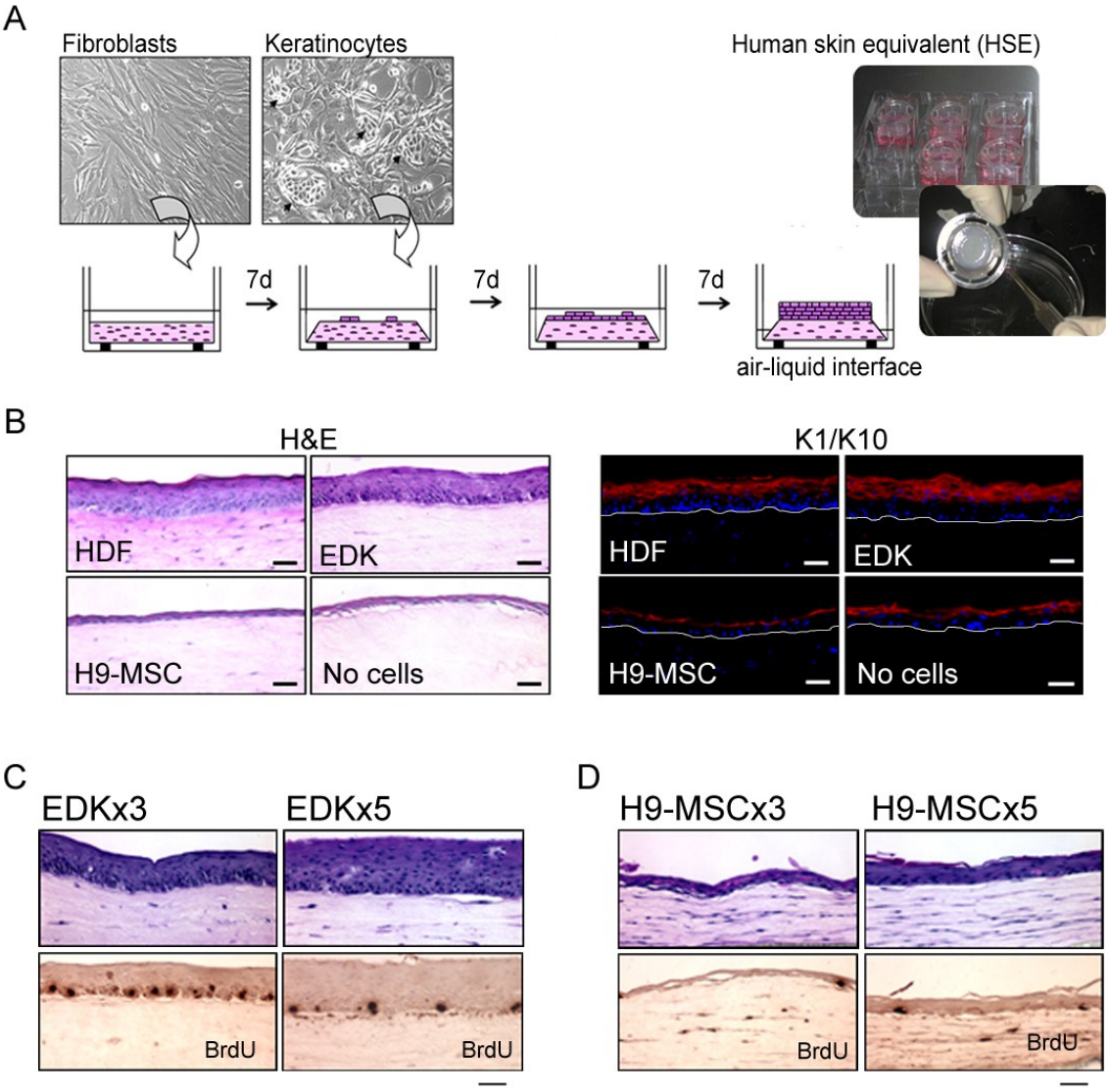

Figure 2-3. EDK cells but not H9-MSC, promote epidermal morphogenesis in human skin-equivalent (HSE) tissues. A. Schematic of the protocol for preparation of HSEs. The assembly of HSE requires preparation of cellular collagen layer, which serve as a dermal equivalent containing fibroblasts. After 7 days, keratinocytes are seeded on top of the contracted cellular layer. The co-cultures are maintained submerged for 7days and then lifted to an air-liquid interface to form cornified layers. **B.** Tissue morphology of HSEs constructed using HDF, EDK, H9-MSC, or without cells as analyzed by H&E staining (H&E). The expression pattern of the epidermal differentiation marker keratin 1/10 was analyzed by immunofluorescence (red). H9-MSCs generated a thin and poorly-developed epithelium that was similar to tissues generated in the absence of any fibroblast support. Bars, 50μm. **C.** The thickness of epithelia correlates with the number of EDK cells. Collagen gels prepared with the higher number of 5 times but not 3 times EDK cells caused enhanced epithelial stratification. Bar, 50μm. **D.** Higher density of H9-MSCs showed no significant effect on epithelial stratification. Proliferation was determined by staining with BrdU, which demonstrated that proliferation in EDK tissues (panel C) was higher than in H9-MSC tissues (panel D).

HSEs constructed with HDFs or no cells embedded into collagen gels served as positive and negative controls, respectively. Morphological analysis revealed that EDK cells promoted epithelial tissue development in a manner similar to HDFs, while tissues grown in the presence of H9-MSC did not support normalization of the overlying epithelium (Figure 2-3B). HSEs constructed with EDK cells developed a fully-stratified, multi-layered epithelium that was well-differentiated and demonstrated tissue architecture similar to epithelial tissues generated with control HDF cells. In contrast, tissues populated with H9-MSCs generated a thin and poorly-developed epithelium that was similar to tissues generated in the absence of any fibroblast support. The characteristic supra-basal distribution of keratin 1/10, a marker of differentiated keratinocytes, in both EDK and HDF containing tissues confirmed the capacity of EDK cells to promote normal epithelial morphogenesis and differentiation (Figure 2-3B). In addition, when higher number of 3 and 5 times EDK and H9-MSCs were incorporated into collagen gels, higher densities of EDK but not H9-MSCs. caused enhanced epithelial stratification. Proliferation of basal keratinocytes was determined by BrdU incorporation assay, which demonstrated that proliferation in EDK tissues was higher than in H9-MSC tissues (Figure 2-3C and 2-3D).

Since efficient development of HSEs is dependent on paracrine support from connective tissue fibroblasts, as has been previously shown for mature fibroblasts (Smola, Thiekotter et al. 1993; Matsumoto and Nakamura 1997; Andriani, Margulis et al. 2003; Chmielowiec, Borowiak et al. 2007), we compared the secretory profile of EDK, H9-MSC, and HDF cells. Supernatants from EDK, H9-MSC, and control HDF cultures containing equal cell numbers were harvested and assayed using an antibody-based

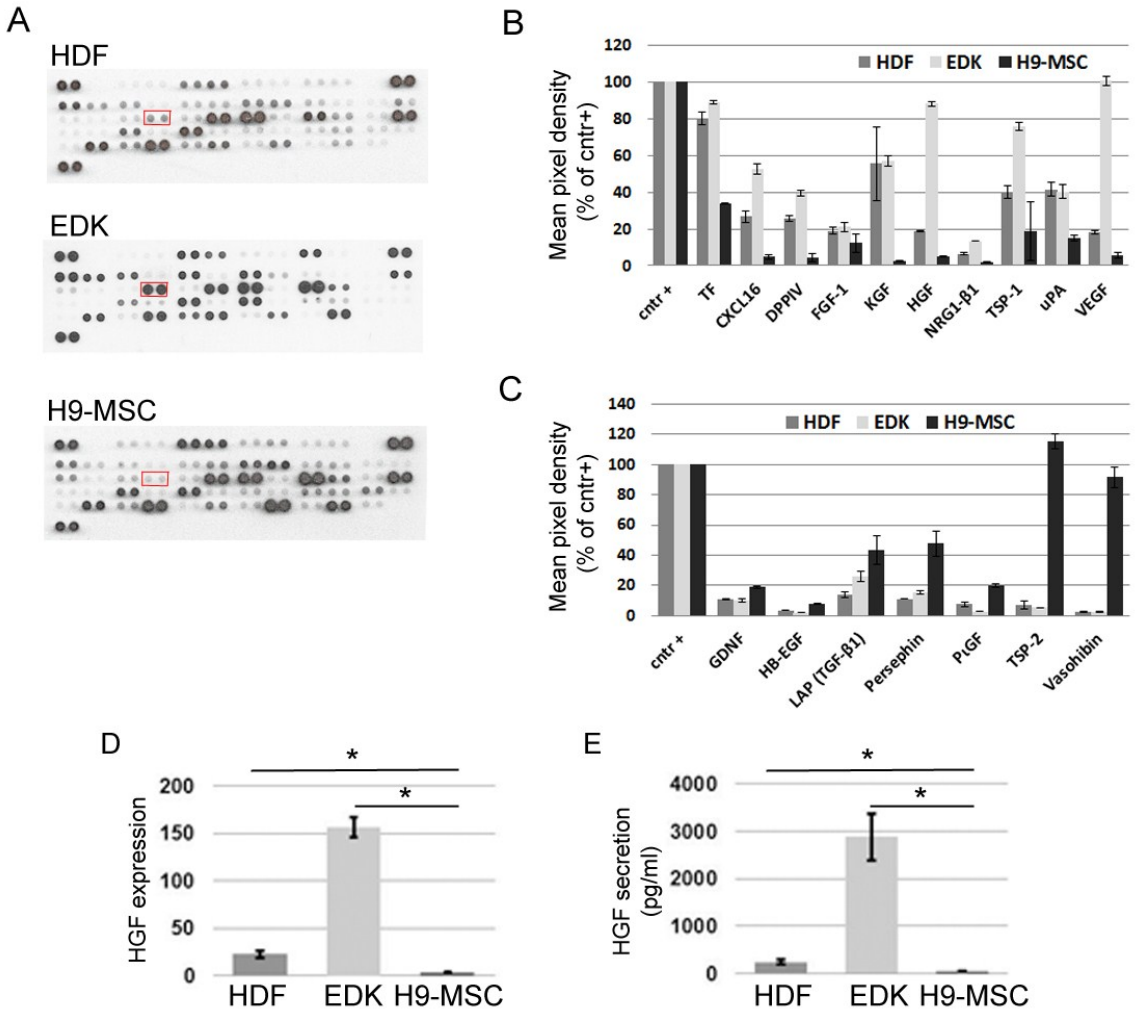

Figure 2-4. Comparison of the secretory profiles of EDK, H9-MSC, and HDF cells. A. Cytokine array membranes used to generate the secretory profiles of HDF, EDK, and H9-MSC cells shown in Table 2-2. Secretory profiles were generated by quantifying the mean spot pixel densities by Image J from the array membranes. The data are presented as percentages of the respective positive controls. HGF coordinates are highlighted. **B.** Soluble factors elevated in HDF and EDK when compared to H9-MSC. **C.** Soluble factors elevated in H9-MSC when compared to EDK and HDF. **D.** HGF mRNA expression in HDF, EDK, and H9-MSC by real-time RT-PCR. Data are normalized to GAPDH (ANOVA: *$p<0.05$). **E.** Levels of HGF in supernatants from HDF, EDK, and H9-MSC monolayer cultures by ELISA. Data are normalized per 10^4 cells (ANOVA: *$p<0.05$).

cytokine array (Figure 2-4A, Table 2-2). Secretory profiles of EDK, H9-MSC, and control HDF were generated by quantifying the mean spot pixel densities from the array membranes and normalized to the respective positive controls (Table 2-2). This analysis revealed that both EDK and HDF cells produced elevated levels of KGF, HGF, FGF-1, NRG1-β1, coagulation factor III (TF), CXCL16, DPPIV, thrombospondin-1 (TSP-1), and

Target/Control	HDF		EDK		H9-MSC	
	mean	stdv	mean	stdv	mean	stdv
Positive control	100.00		100.00		100.00	
Angiogenin	30.22	2.19	65.79	2.62	69.21	4.01
Angiopoetin-1	38.98	2.38	35.73	0.42	51.67	5.51
Amphiregulin	2.26	0.14	59.57	0.16	2.07	0.10
Coagulation factor III	80.03	3.36	88.97	0.94	33.76	0.41
CXCL16	26.79	3.16	52.87	2.83	4.69	1.15
DPPIV	25.61	1.77	39.62	1.41	4.62	2.18
EG-VEGF	14.14	2.02	59.80	2.62	8.96	1.61
Endoglin	21.83	1.47	2.87	0.39	29.71	0.39
Endostatin	68.93	1.03	70.76	3.04	56.82	1.24
Endothelin-1	49.42	7.88	8.50	2.75	73.67	8.49
FGF-1	19.04	1.64	21.10	2.51	12.30	4.90
FGF-7 (KGF)	55.57	20.13	56.98	2.93	2.39	0.33
GDNF	10.63	0.28	10.16	1.44	19.01	0.89
HB-EGF	3.65	0.22	2.13	0.13	8.00	0.44
HGF	18.67	0.44	88.21	1.34	4.85	0.20
IGFBP-1	11.16	5.69	2.13	0.13	6.73	0.81
IGFBP-2	113.28	5.96	83.83	1.62	98.21	5.92
IGFBP-3	128.52	2.38	109.21	11.96	106.04	7.29
IL-8	69.67	4.24	124.74	11.73	122.65	8.49
LAP (TGF-beta1)	13.65	2.00	25.99	3.40	43.27	9.43
MCP-1	107.20	15.61	2.31	0.13	96.71	13.04
MMP-9	48.83	1.44	29.32	0.58	63.67	5.36
NRG1-beta1	6.43	0.50	13.27	0.03	1.77	0.11
PTX3	106.79	5.55	88.51	4.27	68.04	2.13
PD-ECGF	15.92	2.72	4.78	1.10	11.61	0.09
PDGF-AA	17.26	3.55	92.30	6.07	16.18	0.20
Persephin	11.14	0.06	15.12	1.23	47.78	8.23
CXCL4	16.39	2.00	10.61	2.23	11.11	0.91
PlGF	7.65	1.50	2.68	0.13	19.66	1.20
Prolactin	10.53	3.74	2.87	0.13	0.00	0.00
Serpin E1	72.75	4.71	67.20	1.31	60.77	0.22
Serpin F1	27.92	4.49	4.85	1.10	22.57	3.13
TIMP-1	104.36	4.99	98.80	1.75	99.65	10.10
TIMP-4	25.34	3.38	45.26	1.86	28.58	1.02
Thrombospondin-1	40.34	3.41	75.85	2.12	18.99	15.98
Thrombospondin-2	7.20	2.58	5.31	0.03	115.17	4.75
uPA	41.49	3.83	40.14	3.77	15.10	1.50
Vasohibin	2.51	0.50	2.50	0.39	91.51	6.81
VEGF	18.22	1.14	100.54	2.23	5.62	1.63

Table 2-2. Secretory profiles of EDK, H9-MSC, and HDF cells. Supernatants from EDK, H9-MSC, and control HDF cultures containing equal cell numbers were harvested and assayed using an antibody-based cytokine array. Secretory profiles were generated by quantifying the mean spot pixel densities by ImageJ from the array membranes shown in Figure 2-4A. The data are presented as percentages of the respective positive controls.

VEGF when compared to H9-MSCs (Table2-2, Figure 2-4B). In contrast, H9-MSC produced higher levels of GDNF, HB-EGF, LAP (TGFβ1), persephin, uPA, and PlGF than EDK or HDF cells (Table2-2, Figure 2-4C). Notably, the level of HGF, which is known to be essential for skin development and repair (Matsumoto and Nakamura 1997; Chmielowiec, Borowiak et al. 2007) was elevated in both EDK and HDF cells but not in H9-MSCs. Using real-time PCR and ELISA, we detected 10-fold elevation of HGF expression and secretion in EDK cells compared to HDF and 100-fold elevation when compared to H9-MSC (Figure 2-4D and 2-4E). These findings indicated that the biological potential of hESC-derived mesenchymal cells was not uniform. While H9-MSCs could differentiate to osteogenic and adipogenic lineages, this cell line did not provide the paracrine support needed for epithelial development or maturation. In contrast, EDK cells demonstrated properties similar to dermal fibroblasts (HDF) based on their capacity to direct epithelial morphogenesis in an *in vivo*-like tissue environment.

EDK cells accelerate the rate of wound healing in 3D human skin equivalents linked to their HGF production

We used our previously-developed 3D tissue model of cutaneous wound healing (Garlick, Parks et al. 1996; Egles, Shamis et al. 2008) to determine whether EDK and H9-MSCs could also modulate the re-epithelialization of wounded epithelia (see detailed protocol in Appendix II). To test this, HSEs constructed using HDF were wounded with a 4mm punch and placed on the surface of a contracted collagen gel populated with either HDF, EDK, H9-MSCs, or without cells (see schematic in Figure 2-5A). HDFs have previously been shown to enable complete re-epithelialization (Garlick, Parks et al. 1996; Egles, Shamis et al. 2008) and serve as a positive control, while collagen gels generated

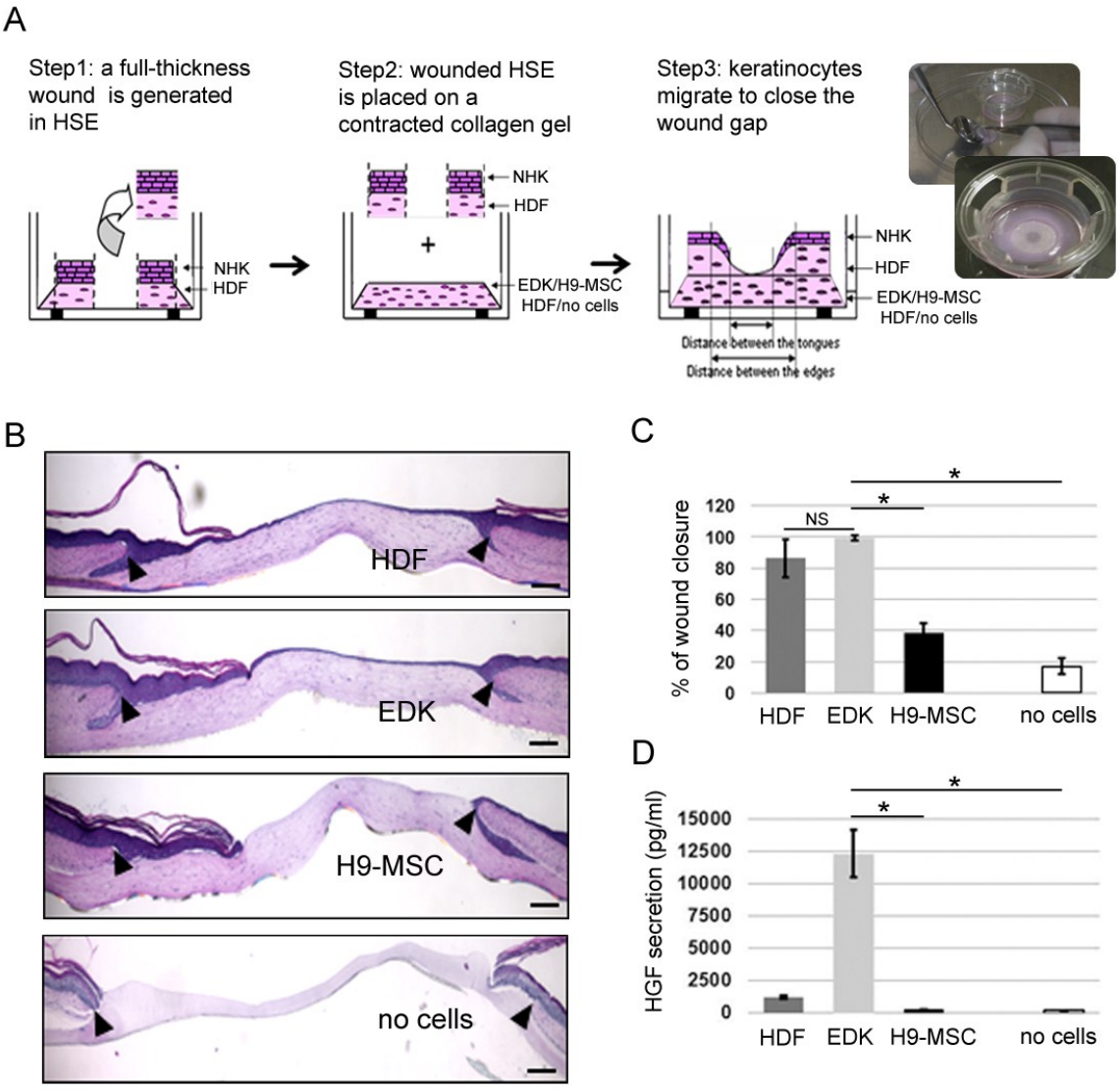

Figure 2-5. EDK cells accelerate re-epithelialization of wounded HSEs. A. Schematic of 3D tissue model of wound re-epithelialization. In Step1, a full-thickness wound is generated by excising an HSE. In Step2, the wounded HSE is placed on a second, contracted collagen gel populated with EDK, H9-MSC, HDF, or constructed without cells. In Step3, keratinocytes (NHK) undergo migration to close the wound gap and restored epithelial integrity. The far right panel is an image of 6-well insert containing HSE after wounding**. B.** Representative morphology of wounded tissues constructed with HDF, EDK, H9-MSC, or without cells 96h after wounding (black arrows demarcate the initial wound edges). Bars, 200µm. **C.** EDK showed a rate of wound closure similar to tissues in which HDF were incorporated. The degree of re-epithelialization was significantly lower in H9-MSC- and no cells-containing tissues as compared to HDF (ANOVA: *$p<0.05$). (d): Levels of HGF in supernatants of wounded tissues 96h after wounding as measured by ELISA. HDF- and EDK-containing tissues produced higher levels of HGF as compared to H9-MSC-containing tissues or tissues constructed without cells (ANOVA: *$p<0.05$).

without any cells were used as a negative control for re-epithelialization. Ninety-six hours after wounding, the wound bed was partially or completely covered by a migrating epithelial tongue towards the central area of the wound bed and by a more stratified epithelium toward the wound margins (Figure 2-5B). The degree of re-epithelialization following wounding was measured by calculating the distance separating the two epithelial tongues and was normalized to the distance between the initial wound margins and expressed graphically as the percentage of wound closure (Figure 2-5C). In general, EDK cells showed nearly complete or complete wound closure that was similar to tissues in which HDF were incorporated (HDF = 86 ± 12% and EDK = 99 ± 1.6%). In contrast, H9-MSCs-harboring tissues and the tissues constructed without any fibroblast support showed a significantly lower degree of re-epithelialization compared to HDF (H9-MSC = 39 ± 5.5% and no cells = 17 ± 5%, t-test: $p=0.003$ and $p=0.0007$, respectively) (Figure 2-5C). To test whether degree of wound re-epithelialization was linked to HGF levels, HGF concentrations in supernatants from wounded HSEs were measured by ELISA. Quantification of HGF production revealed that both HDF- and EDK-containing tissues produced significantly higher levels of HGF (5-fold and 50-fold higher, respectively) than H9-MSC-containing tissues or in tissues without cells in their stroma (Figure 2-5D). These results imply that HGF-mediated paracrine signaling may responsible, at least in part, for the wound re-epithelialization mediated by EDK cells.

Suppression of HGF production impairs the ability of EDK cells to promote wound healing in 3D human skin equivalents

To confirm that HGF secretion is necessary to optimally direct the re-epithelialization of cutaneous wound mediated by EDK cells, levels of HGF secreted

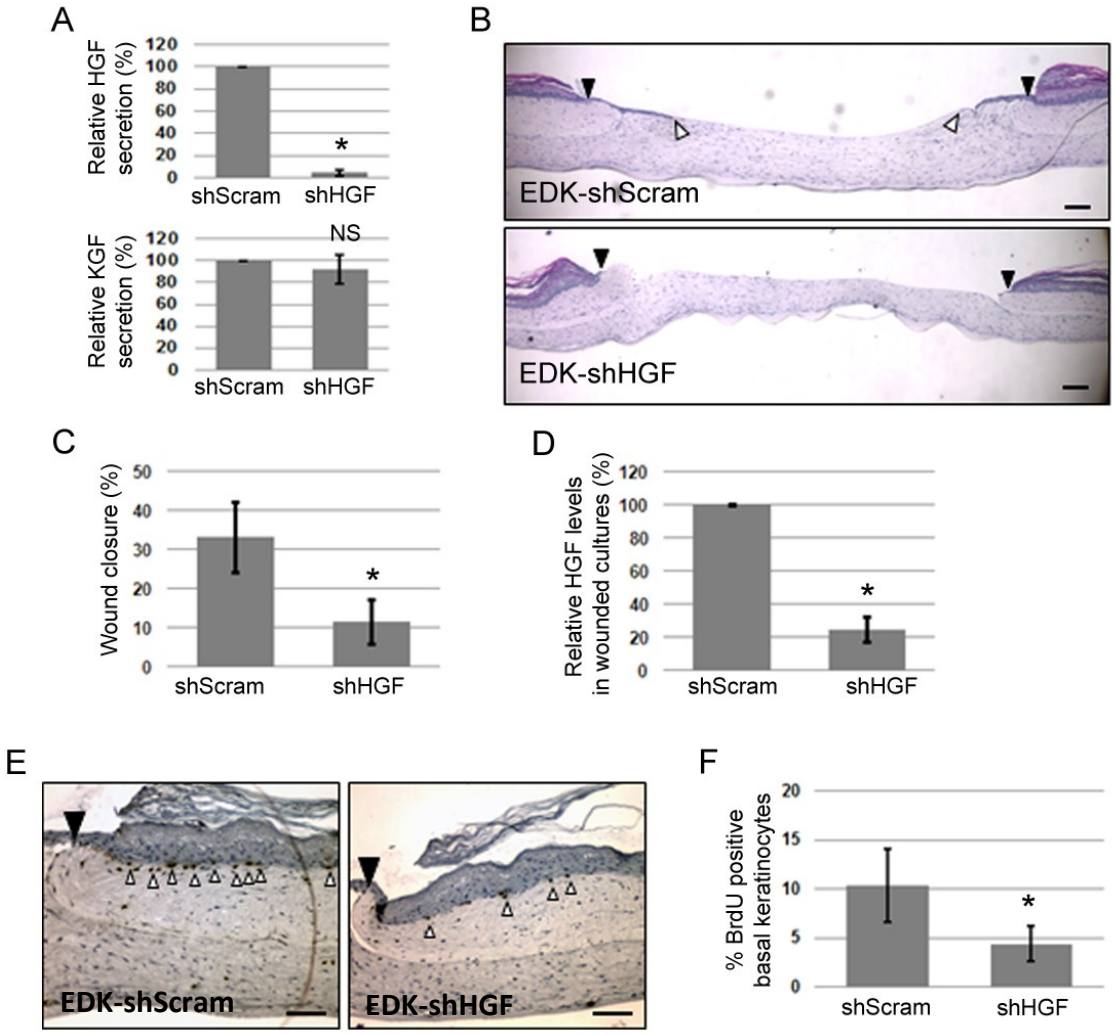

Figure 2-6. Suppression of HGF production impairs EDK-mediated re-epithelialization of wounded HSEs. A. Efficiency of shRNA knockdown of HGF (shHGF) in EDK cells relative to a scrambled, shRNA control (shScram) as measured by ELISA. Secretion of HGF (top panel) was reduced 95% relative to shScram (t-test: *p<0.01), secretion of KGF (lower panel) was not affected by shHGF. Data are normalized to shScram. **B.** Representative morphology of wounded tissues constructed with EDK-shHGF and EDK-shScram cells 72h after wounding (black arrows demarcate the initial wound edges; white arrows demarcate the tip of epithelial tongues). Bars, 200μm. **C.** The degree of re-epithelialization was significantly lower in tissues containing EDK-shHGF cells as compared to EDK-shScram (t-test: *p<0.01). **D.** Relative levels of HGF in supernatants of wounded tissues 72h after wounding as measured by ELISA. Tissues containing EDK-shHGF cells produced significantly lower levels of HGF as compared to EDK-shScram (t-test: *p<0.01). **E.** Proliferation of basal keratinocytes in tissues containing EDK-shHGF and EDK-shScram cells was analysed using immunoperoxidase staining with anti-BrdU antibody 72h after wounding (black arrows demarcate the initial wound edges; white arrows demarcate the BrdU-positive cells). **F.** Quantification of BrdU-positive basal keratinocytes. Tissues containing EDK-shHGF demonstrated significantly lower percentage of proliferating basal keratinocytes compared to EDK-shScram (t-test: **p<0.01). Bars, 100μm.

from EDK cells were significantly reduced by introducing a lentiviral shRNA construct that targeted HGF mRNA (shHGF). Efficiency of shHGF in EDK cells was measured relative to a scrambled, shRNA control (shScram) by ELISA and showed a 95% reduction in secretion of HGF from EDK cells (Figure 2-6A, top panel). This shHGF lentiviral construct did not alter secretion of other growth factors, such as KGF (Figure 2-6A, lower panel). The effect of decreased HGF secretion on the capacity of EDK cells to promote re-epithelialization of wounded HSEs was examined by incorporating EDK-shHGF and EDK-shScram into 3D tissue model of cutaneous wound repair. Tissue morphology and the degree of re-epithelialization following wounding were analysed 72h after wounding. Tissues constructed using EDK-shHGF cells showed a significantly lower degree of re-epithelialization compared to EDK-shScram (EDK-shScram = 33 ± 9% vs. EDK-shHGF = 11.6 ± 5.8%, t-test: p=0.017) (Figure 2-6B and 2-6C). HGF levels in supernatants from wounded HSEs were measured by ELISA and showed roughly 85% reduction of HGF levels in cultures containing EDK-shHGF (Figure 2-6D). To further characterize the phenotype of wounded epithelial tissues in the presence of EDK-shHGF and control EDK-shScram, we assayed proliferation of keratinocytes in the basal layer of wound margins using a BrdU-incorporation assay (Figure 2-6E). Tissues harbouring EDK-shHGF demonstrated a significantly lower percentage of proliferating basal keratinocytes compared to EDK-shScram (EDK-shScram =10 ± 3.5% and EDK-shHGF=4.4 ± 1.8%, t-test: p=0.004) (Figure 2-6F). These results support the known function of HGF as a mediator of epithelial cell proliferation in restoring epithelial integrity following wounding (Matsumoto and Nakamura 1997; Chmielowiec, Borowiak et al. 2007). This suggested that hES-derived EDK cells stimulated wound re-

epithelialization by providing paracrine signals, such as HGF, that is needed to direct the repair of a cutaneous wound.

Discussion

Our comparative characterization of two hESC-derived cell lines (EDK and H9-MSC) that were differentiated under different conditions has revealed that both cell lines exhibited similar morphology and cell surface marker expression indicative of a mesenchymal phenotype (Dominici, Le Blanc et al. 2006) . However, while EDK cells showed some phenotypic overlap with H9-MSC and adult MSCs in 2D monolayer culture, their functional properties in engineered 3D tissues and the absence of the multilineage differentiation potential seen in H9-MSC provided evidence of their fibroblast lineage commitment. Thus, we have demonstrated that engineered, 3D tissues can be used as a sensitive assay to characterize the biological potency of hESC-derived fibroblasts. Incorporation of hESC-derived cells into tissues that mimic their *in vivo* counterparts enables a more complete determination of their lineage commitment and phenotype than conventional, monolayer cultures. We have previously showed that EDK cells co-express early epithelial marker cytokeratin 18 (K18) and mesenchymal marker vimentin (Vim), however, when incorporated into 3D tissue construct, EDK cells failed to form multilayered epithelium or differentiate into keratin 14 (K14) expressing keratinocytes (Hewitt, Shamis et al. 2009). We now extend those studies using an hESC-derived cell line that produced elevated levels of HGF to provide paracrine support for tissue development and repair that mimics the functional features of dermal fibroblasts. We have shown the suppression of HGF production in EDK cells is linked to a

significant decrease in epithelial proliferation and repair, suggesting that these cells mediate epithelial tissue phenotype through a paracrine support. In contrast, hESC-derived cell line that manifests multilineage differentiation, but very low HGF levels (H9-MSC) was unable to support epithelial tissue development and repair.

Despite the critical impact of fibroblasts on tissue morphogenesis, homeostasis, and repair, gaps in our understanding of fibroblast lineage development has made the identification and reproducible isolation of specific fibroblast populations particularly challenging (Sorrell, Baber et al. 2007; Phan 2008; Sorrell, Baber et al. 2008). In this light, we expect that our findings will help address a central challenge facing clinical application of cells with properties of dermal fibroblasts for regenerative medicine by developing an efficient approach to reproducibly procure these cells from pluripotent stem cells, in a way that offers predictable and effective tissue outcomes upon their therapeutic use (Cedar, Cooke et al. 2007; Klimanskaya, Rosenthal et al. 2008).

In previous studies, MSC-like cells expressing α-SMA have been derived from hESCs (Lee, Kim et al. 2007; Jiang, Gwye et al. 2009) and fibroblast-like cells isolated from hESCs have been used as autogenic feeders to support the culture of undifferentiated hESCs (Yoo, Yoon et al. 2005; Choo, Ngo et al. 2008; Chen, Chuang et al. 2009). However, mesenchymal cells derived in these previous studies were not grown in 3D tissue microenvironments that could provide a more complete functional characterization of their identity. In addition, we have found that surface marker profile of EDK and H9-MSC is similar to those expressed on MSC-like cells previously derived from hESCs using alternative differentiation conditions to those described in our study (Barberi, Willis et al. 2005; Olivier, Rybicki et al. 2006; Lian, Lye et al. 2007; Boyd,

Robbins et al. 2009). Since the use of cell surface markers to distinguish MSCs from cells restricted to fibroblast lineage fate is limited, tissue-based, functional readouts are essential to predict the potency of hESC-derived cells differentiated into mesenchymal lineages (Sudo, Kanno et al. 2007; Summer and Fine 2008). As it is possible that EDK cells represent a heterogeneous mixture of fibroblasts and a smaller number of cells that retain MSC-like features, their future therapeutic use may require further characterization of fibroblast subpopulations. This approach has recently been demonstrated to improve the specificity of MSCs differentiated from hESCs in ways that can select for reproducible and clinically-applicable cells (Lian, Lye et al. 2007).

Transplantation of adult-derived MSCs has previously been shown to promote tissue regeneration and to improve wound repair *in vivo* (Wu, Chen et al. 2007; Stappenbeck and Miyoshi 2009; Lian, Zhang et al. 2010). Increasing evidence suggests that this repair potential is linked to the ability of MSCs to secrete paracrine-acting factors that can induce changes in their tissue microenvironment to guide healing (Phinney and Prockop 2007; Meirelles Lda, Fontes et al. 2009). We found that EDK cells secreted a broad repertoire of growth factors and cytokines linked to a variety of paracrine-mediated tissue responses, including stimulatory, paracrine factors known to accelerate the healing of epithelial wounds. Specifically, we found that this augmented re-epithelialization of wounded keratinocytes was linked to the production of HGF by EDK cells, as the diminished production of this growth factor upon shRNA infection significantly decreased tissue re-epithelialization. Since HGF is known to be induced in stromal cells in response to injury (Matsumoto and Nakamura 1997; Chmielowiec, Borowiak et al. 2007), directed differentiation of hES-derived fibroblasts may allow these

cells to be adapted for cell therapy and cutaneous regeneration. Beyond this, a decline in fibroblast numbers or function has been implicated in both skin aging and cancer development, as the age-related accumulation of senescent fibroblasts is thought to create a microenvironment that promotes squamous cell carcinoma progression (Kim, Kim et al. 2003; Mine, Fortunel et al. 2008; Kim, Cho et al. 2009; Lewis, Travers et al. 2009). Since restoration of growth factor production in fibroblasts may decrease cancer risk and sustain tissue homeostasis, the development of future cell-based treatments using hESC-derived fibroblasts can potentially augment repair and improve overall tissue health. We expect that our findings will enable future studies aimed at clarifying factors regulating fibroblast development and will help identify progenitor cells that give rise to these cells in human skin and other tissues.

Chapter 3: Human ESC- and iPSC-derived Fibroblasts Demonstrate Augmented Production and Assembly of Extracellular Matrix Proteins

Publications:

The findings of this project have been published in In Vitro Cellular & Developmental Biology – Animal, Epub ahead of print Jan 19, 2012. "iPSC-derived fibroblasts demonstrate augmented production and assembly of extracellular matrix proteins". Shamis Y, Hewitt KJ, Bear SE, Alt-Holland A, Qari H, Margvelashvilli M, Knight EB, Smith A, Garlick JA.

Author Contributions:

Yulia Shamis: designed and performed all the experiments, analyzed data, and wrote the manuscript

Kyle J. Hewitt: developed protocol for directed differentiation of hESC and iPSC to EDK and iPDK fibroblasts, respectively (see Figure 3-1A, and 3-1B) discussed the results, and commented on the manuscript

Bear SA: optimized culture conditions and protocols for preparation of 3D stromal tissues, discussed the results, and commented on the manuscript

Alt-Holland A: provided technical assistance for the western blot analysis (see Figure 3-5A), discussed the results, and commented on the manuscript

Qari H: performed flow cytometry analysis of EDK, iPDK, and HDF cells (see Table 3-2), discussed the results, and commented on the manuscript

Margvelashvilli M: performed RT-PCR analysis of EDK, iPDK and HDF cells (see Figure 3-2), discussed the results, and commented on the manuscript

Knight EB: provided technical assistance for the tissue culture, discussed the results, and commented on the manuscript

Smith A: provided technical assistance for the tissue processing and histology, discussed the results, and commented on the manuscript

Jonathan A. Garlick: supervised the project, discussed the results, and assisted in the writing of the manuscript

Abstract

Recent technological advances in cell reprogramming by generating induced pluripotent stem cells (iPSC) offer major perspectives in regenerative medicine by providing an alternative source of autologous cells for potential therapeutic applications. However, the functional properties of iPSC-derived cells and their similarities to cells differentiated from hESCs remain unclear. To address this question, we compared the production and assembly of extracellular matrix (ECM) by iPSC-derived fibroblasts to that of fibroblasts differentiated from human embryonic stem cells (hESC), and to mature dermal fibroblasts, the same cell type from which iPSCs were initially reprogrammed. Human iPSC- and hESC-derived fibroblasts demonstrated stable morphology and expression of surface markers characteristic of mesenchymal cells during prolonged culture and showed an elevated growth potential when compared to dermal fibroblasts. We found that in the presence of L-ascorbic acid-2-phosphate, iPSC- and hESC-derived fibroblasts increased their expression of collagen genes, secretion of soluble collagen, and extracellular deposition of Type I Collagen to a significantly greater degree than that seen in dermal fibroblasts. Under culture conditions that enabled the self-assembly of a 3D ECM, both iPSC- and hESC-derived fibroblasts generated a well-organized stromal tissue by depositing elevated amounts of ECM when compared to dermal fibroblasts. Immunoblot and imunohistochemical analysis of the composition of these stromal tissues revealed that ECM assembled by both iPSC- and hESC-derived fibroblasts contained significantly greater amounts of Type III Collagen than that assembled by dermal fibroblasts. By comparing the production and assembly of ECM by iPSC-derived fibroblasts to their hESC-derived counterparts, we demonstrated that human iPSCs and

hESC have similar biological potential and represent a promising, alternative source of mesenchymal cells to advance future regenerative therapies**.**

Introduction

As stromal constituents of many tissues, fibroblasts play an essential role in regulating normal tissue homeostasis and wound repair through their synthesis of extracellular matrix (ECM) proteins and secretion of growth factors. The composition and organization of ECM produced by stromal fibroblasts direct many aspects of cell behavior including growth, survival, cell recruitment, and differentiation during tissue repair and regeneration (Schultz and Wysocki 2009). Incorporation of stromal fibroblasts into tissue-engineered biomaterials has shown great promise for their application in regenerative medicine to replace damaged or diseased tissues by fabricating skin and dermal substitutes (Wong, McGrath et al. 2007), tendon and ligament tissue replacements (Gurkan, Cheng et al. 2010), corneal tissues (Proulx, d'Arc Uwamaliya et al. 2010), heart valves (Schmidt and Hoerstrup 2006), and blood vessels (Grainger and Putnam 2011). However, the therapeutic potential of stromal fibroblasts has been limited by our incomplete understanding of the precursor cells that give rise to them and by their phenotypic heterogeneity (Chang, Chi et al. 2002; Sorrell and Caplan 2004; Phan 2008). In addition, the lack of specific markers defining functional subpopulations of stromal fibroblasts has complicated their characterization for potential use in regenerative therapies (Yamaguchi, Itami et al. 1999; Koumas, King et al. 2001; Haniffa, Wang et al. 2007; Sorrell, Baber et al. 2007; Sorrell, Baber et al. 2008). In light of this, next-generation treatment strategies in tissue repair will benefit from the new technology of

generating induced pluripotent stem cells (iPSC) that can offer a plentiful and reliable source of patient-specific mesenchymal cells, which may provide more predictable tissue outcomes upon their therapeutic use.

Although the iPSC technology has the potential to provide autologous cells for regenerative medicine, there are still many challenges to overcome before cells generated from iPSCs can be used in clinic. Using protocols initially established for hESC differentiation, it has been shown that like hESCs, iPSCs can be directed to differentiate into specific cell types and lineages (Lian, Lye et al. 2007; Swistowski, Peng et al. 2010; Liu, Kim et al. 2011). However, the functional properties of iPSC-derived cells and their similarities to cells differentiated from human ESCs remain unclear. On the one hand, some studies have shown that hESC-derived cells are limited in their biological potential when compared to the same cell types differentiated from hESCs, such as they have residual methylation, limited expansion potential, and early senescence (Feng, Lu et al. 2010; Ghosh, Wilson et al. 2010). On the other hand, it has also been shown that iPSCs are undistinguishable from hESCs in their chromatin structure and gene expression patterns (Guenther, Frampton et al. 2010). Furthermore, new evidence has emerged that fibroblasts differentiated from iPSC display specific properties that exceed those of the parental fibroblasts from which these iPSC were initially reprogrammed. For example, it has been shown that it is possible to rejuvenate senescent and centenarian human cells by reprogramming through the pluripotent state (Suhr, Chang et al. 2009; Suhr, Chang et al. 2010; Lapasset, Milhavet et al. 2011). In these studies, iPSC-derived fibroblasts showed an extended replicative potential, increased telomere size, and improved mitochondrial function when compared to the parental senescent fibroblasts initially used for iPSC

reprogramming (Suhr, Chang et al. 2009; Suhr, Chang et al. 2010; Lapasset, Milhavet et al. 2011). In this light, it is particularly important to determine if specific cell types derived from iPSCs will have the same functional features when compared to hESC-derivatives and mature cell types.

We have recently reported a protocol to efficiently derive cells from hESCs that show phenotypic and functional features of dermal fibroblasts (EDK), as seen by their capacity to direct epidermal morphogenesis and wound repair upon incorporation into the stromal compartment of engineered human skin equivalents (Hewitt, Shamis et al. 2009; Shamis, Hewitt et al. 2011) (See Chapter 2). However, the production of ECM by EDK fibroblasts has not yet been characterized. In this study, using the same derivation strategy developed for hESCs, we generated fibroblasts from iPSCs (named iPDK), and compared their ECM production and assembly to that of EDK and primary human dermal fibroblasts (HDF).

Materials and Methods

Cell Culture

Human dermal fibroblasts (HDF), were purchased from ATCC Inc., the cell line known as BJ, (Manassas, Virginia) and expanded on tissue culture plastic in DMEM (Invitrogen, Carlsbad, CA) supplemented with 10% FBS (Hyclone, Logan, UT). The iPSC line (gift of the lab of Dr. Konrad Hochedlinger) (Maherali, Ahfeldt et al. 2008), was derived by reprogramming BJ fibroblasts using separate dox-inducible vectors Oct4, Sox2, Klf4, cMyc and Nanog. The H9 line of hESC was purchased from the WiCell Institute

(Madison, WI). The iPSC and hESC lines were maintained in culture as previously described (Thomson, Itskovitz-Eldor et al. 1998). EDK and iPDK fibroblast cell lines were differentiated from hESC and iPSC, respectively using our previously described protocol for the generation of fibroblasts (Hewitt, Shamis et al. 2009; Hewitt, Shamis et al. 2011). For a step-by-step protocol, see Appendix I. For all experiments, HDF, EDK and iPDK cell lines were grown on Type I Collagen-coated plates (BD Biosciences, San Jose, CA) in media consisting of 3:1 DMEM:F12 (Invitrogen, Carlsbad, CA), 5% FCII (Hyclone, Logan, UT), 0.18mM adenine, 8mM HEPES, 0.5 µg/mL hydrocortisone, 10^{-10} M cholera toxin, 10ng/mL EGF, 5µg/mL insulin (all from Sigma, St. Louis, MO). All cell lines were routinely checked for mycoplasma contamination using MycoAlert® Mycoplasma detection kit (Lonza, Rockland, ME).

Proliferation Kinetics

HDF, EDK, and iPDK fibroblasts of the same passage (p7) underwent additional passaging every 7 days upon reaching 70-80% confluence. Cell numbers were determined by counting trypsinized cells using a hemocytometer, and data were recorded as an average of three measurements for each passage. As cell numbers were first determined at p8, the number of population doublings (PD) was first calculated for p8 using the following formula: $X=[\log10(N_H)-\log10(N_1)]/\log10(2)$. The N_H is the harvested cell number and the N_1 is the plated cell number. The PD for each passage was calculated and added to the PD of the previous passages to calculate the cumulative population doublings.

Real-time RT-PCR

RNA was isolated using Qiagen RNeasy purification kit (Qiagen, Valencia, CA), and then converted to cDNA with the iScript cDNA synthesis kit (Biorad, Hercules, CA) using 0.5μg RNA. Real-time RT-PCR reactions were carried out using 20ng of cDNA, 200nM of each primer and 2X SYBRgreen Supermix (Biorad, Hercules, CA) at a total sample volume of 12.5 μL and samples were run in triplicate on a iQ5 Real-Time PCR detection system (Bioad, Hercules, CA). PCR products were amplified to 30 cycles at 94 °C for 30 s, 60 °C for 30 s and 72 °C for 60 s. The relative level of gene expression was assessed using the $2^{-\Delta\Delta C}$t method. Error bars represent standard deviation of 3 biological replicates. The following oligonucleotide primer sequences were used: GAPDH-F: 5'- tcgacagtcagccgcatcttcttt-3', GAPDH-R: 5'-accaaatccgttgacctt-3'; COL1A1-F: 5'- cctcctgacgcacggccaag-3', COL1A1-R: 5'-ccctcgacgccggtggtttc-3': COL3A1-F: 5'-cctccaactgctcctactcg-3', COL3A1-R: 5'-tcgaagcctctgtgtccttt-3'; COL4A1-F: 5'-ccaggatttcaaggtccaaa-3', COL4A1-R: 5'-tcattgccttgcacgtagag-3'; COL5A1-F: 5'-ctggggagaagggaaaactc-3', COL5A1-R: 5'-tcagtccaagagctcccact-3'; FN-F: 5'-tgaccctacagtttccca-3', FN-R: 5'-tgattcagacattcgttcccac-3'.

Histology, Immunohistochemistry, and Immunofluorescence

Self-assembled, 3D stromal tissues were fixed in 10% neutral-buffered formalin, , embedded in paraffin, sectioned at 8μm thickness and hematoxylin and eosin (H&E) staining was performed to assess tissue morphology. For immunohistochemistry, antigen retrieval was performed by steaming tissue sections in Citrate buffer for 15 min and, immunostaining was performed with antibodies against Type I Collagen, Type III collagen (Abcam, Cambridge, MA), fibronectin (BD Trunsduction, San Jose, CA),

vimentin (Abcam, Cambridge, MA), α-SMA (Chemicon, Temecula, CA). Staining localization was detected using DAB (Vector Laboratories, Burlingame, CA), and tissues were counterstained with hematoxylin (Sigma, St. Louis, MO). For immunofluorescence staining, BJ, EDK and iPDK cells were grown in 2D, monolayer cultures on glass coverslips for 1 week in the presence or absence of AA (10µg/ml), fixed in 4% paraformaldehyde, permeabilized using 0.1% triton X-100, and immunostained with against Type I Procollagen (Fitzgerald Inc, Acton, MA) or Fibronectin (BD Trunsduction,, San Jose, CA) and stain localization was detected using either Alexa Fluor 488- or Alexa Fluor 594- conjugated goat anti-mouse secondary antibody (Invitrogen, Carlsbad, CA). Microscopy was performed with a Nikon Eclipse 80i microscope and composite images were created using SPOT Advanced software (Diagnostic Instruments, Sterling Heights, MI).

Preparation of 3D Stromal Tissues

HDF, EDK, and iPDK cells were harvested at 70-80% confluence and seeded onto 24-well Millicell® (Millipore, Billerica, MA) Hanging Cell Culture inserts (1.0µm pore size) at a density of $5x10^5$ cells/cm^2. Cells were fed with the media containing 3:1 DMEM:F12 (Invitrogen, Carlsbad, CA), 5% FCII (Hyclone, Logan, UT), 0.18mM adenine, 8mM HEPES, 0.5 µg/mL hydrocortisone, 10^{-10} M cholera toxin, 10ng/mL EGF, 5µg/mL insulin with or without 10µg/ml of L-ascorbic acid-2-phosphate (Sigma, St. Louis, MO) and medium was changed every 3 days throughout the culture period of 5 weeks.

Flow Cytometry

HDF, EDK, and iPDK cells were trypsinized, pelleted, and re-suspended in 2% FBS in PBS. Cell suspensions were stained with PE-conjugated anti-CD73, -CD105, -CD90, -CD10, -CD13, -CD166, -CD146, -CD106 or Isotype control-IgG1k (BD Pharmingen, San Jose, CA). Cells were incubated for 30 min on ice and washed with 2% FBS in PBS solution. All data were acquired using a FACSCalibur (BD, San Jose, CA) and analyzed using CellQuest (BD, San Jose, CA) and Summit V4.3 software (Dako, Carpentaria, CA). Analysis was performed on 20,000 cells per sample and positive expression was defined as the level of fluorescence greater than 99% of the corresponding isotype control IgG1k (BD Biosciences, San Jose, CA).

Immunoblotting

HDF, EDK, and iPDK cells were grown for 1week in monolayer culture in the presence or absence of AA (10µg/ml). 3D stromal tissues were grown for 5 weeks in the presence of AA (10µg/ml). Proteins were extracted on ice in 4% deoxycholate (4% Sodium Deoxycholate in 20mM Tris-HCl pH 8.8, protease and phosphatase inhibitors) followed by 5 rounds of sonication. Extracts were span down at 14000 rpm for 30 min at 4^0C and protein concentrations were determined using NanoDrop2000 (Thermo Scientific, Wilmington, DE). Equal protein samples were separated by SDS-PAGE (4-20% gel) under non-reducing conditions (type I collagen and type III collagen) and reducing conditions (fibronectin). Proteins were transferred to nitrocellulose membranes in 20% methanol in running buffer. Membranes were immunoblotted with antibodies against Type I Collagen and Type III Collagen (Abcam, Cambridge, MA), Fibronectin (BD Transduction, San Jose, CA) and Erk 1/2 (Santa Cruz Biotechnology, Santa Cruz, CA).

HRP-conjugated secondary antibodies were from Jackson ImmunoResearch Laboratories (West Grove, PA). Densitometry analysis of scanned blots was performed using ImageJ software (U. S. National Institutes of Health, Bethesda, Maryland, USA).

Soluble Collagen Assay

HDF, EDK, and iPDK $0.5x10^5$ cells were seeded onto 100 mm culture dishes and maintained in 10ml of tissue culture medium with and without AA (10µg/ml) for 1 week. Before analysis, cells were fed with fresh growth medium for the final 48 hours of their incubation. For measurement of soluble collagens, tissue culture supernatants were collected and analysed by Sircol™ assay (Biocolor, Ireland) according to the manufacturer's protocol. Assays were performed in triplicate from three independent samples. Absorbance was read at 540 nm using a plate reader and the concentrations of soluble collagen were determined from a standard curve that was generated using rat tail collagen provided by the manufacturer.

Statistical Analysis

Statistical analyses were carried out using IBM SPSS Statistics 19 software (IBM, Armonk, NY). All results are reported as mean ± standard deviation of at least three independent samples. Statistical comparison between two groups was performed using Student's t-test. When comparing more than two groups One-Way Analysis of Variance (ANOVA) test was used followed by the post hoc Tukey's multiple comparison tests. Results were considered significant for $p \leq 0.05$.

Results

Comparative characterization of EDK and iPDK cells

iPSCs were initially generated and characterized by the Hochedlinger lab using retroviral transduction of the BJ line of human dermal fibroblasts (ATCC, Inc., Manassas, VA) with five retroviral reprogramming factors (BJ hiPS#1) (Maherali and Hochedlinger 2008). The protocol for derivation of fibroblasts from iPSCs (iPDK) was identical to the differentiation protocol optimized to generate cells with properties of human fibroblasts from hESCs (EDK), summarized in Figure 3-1A and described in more detail in Appendix I (Hewitt, Shamis et al. 2009). As reported by Hewitt et al., multiple cell lines were derived from both ESCs and iPSCs, which demonstrated a similar appearance during the sequential stages of differentiation as seen in representative images at days 1, 10, and 28 days after initiation of differentiation (Figure 3.1B) (Hewitt, Shamis et al. 2011). Importantly, there was a noticeable difference in the efficiency of differentiation of iPSCs compared to ESCs, with fewer cells observed at later stages using iPSCs, although the morphology was still similar using all pluripotent cell types (Figure 3-1B, day 28) (Hewitt, Shamis et al. 2011).

To characterize and compare the mesenchymal phenotype of EDK and iPDK cells, we analyzed the expression of surface markers characteristic of mesenchymal cells, their proliferation kinetics, and their functionality in 3D human skin equivalents (HSEs). Surface marker profiling of EDK and iPDK was performed by flow cytometry and compared to the profile generated for HDFs. All cell lines showed similar expression of CD73, CD90, CD166, CD146, CD10, CD13, and CD44. HDF showed low expression of CD106 when compared to both EDK and iPDK. The intensity of fluorescent labeling and

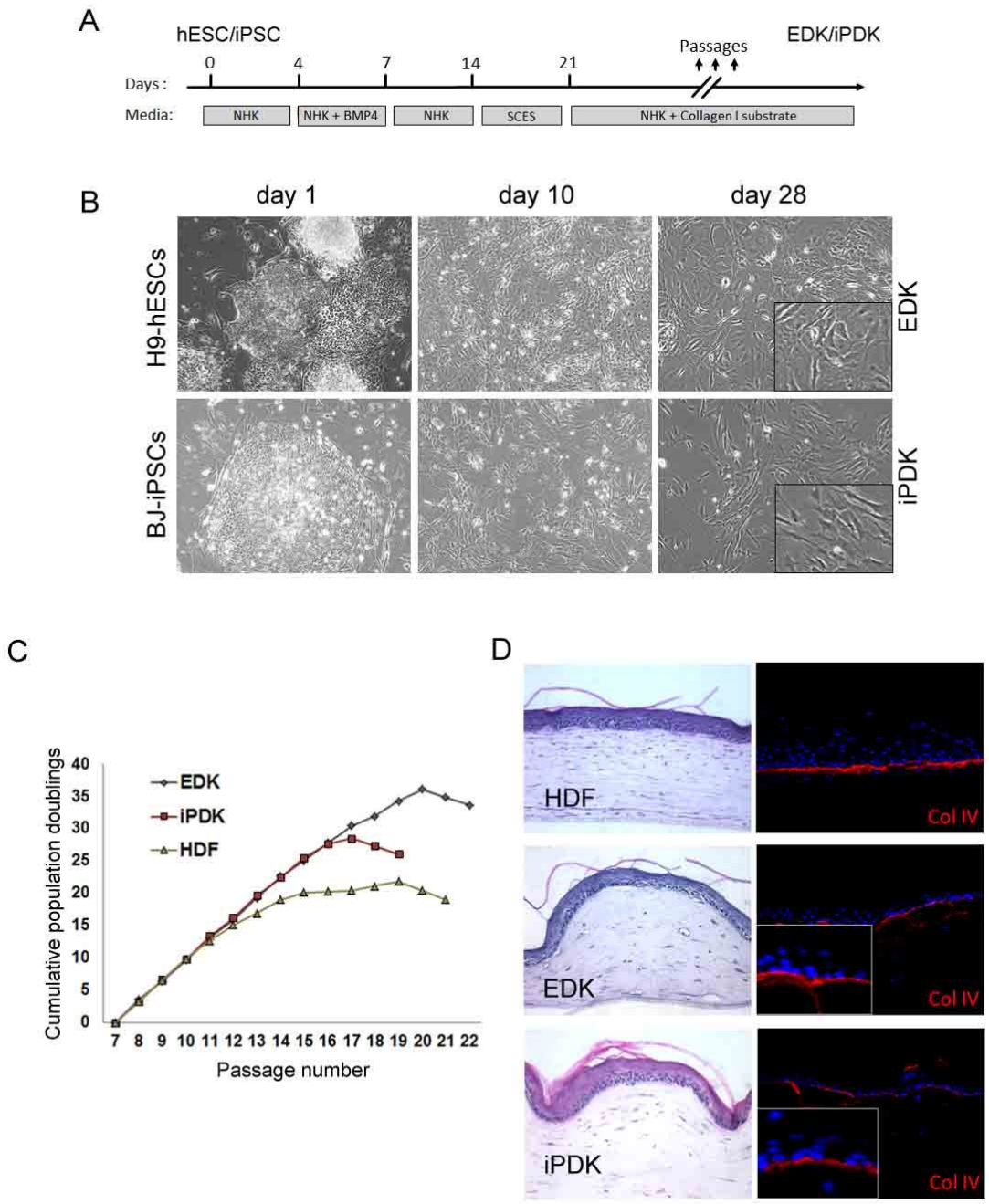

Figure 3-1. Characterization of morphology and growth potential of iPSC- and hESC-derived fibroblasts and control primary dermal fibroblasts. A. Schematic of the protocol for differentiating EDK from hESCs and iPDK from iPSCs. **B.** Human ESC and iPSC were induced to differentiate in parallel, using identical differentiation procedures, and monitored for cell morphology at various stages. Representative images of hESCs and iPSCs during differentiation showing similar morphology at days 1, 10, and 28 of differentiation. **C.** Growth capacity of EDK, iPDK and control HDF was assessed by calculating cumulative population doublings (y-axis) during serial subculture (x-axis). EDK and iPDK fibroblasts demonstrated increased growth potential when compared to HDF. **D.** EDK and iPDK support epidermal morphogenesis when incorporated into the stroma of human skin equivalents. Representative images of EDK, iPDK, and HDF-containing tissues are shown. H&E staining shows that EDK and iPDK cells support the growth and differentiation of keratinocytes similar to control HDF. Immunostaining shows the basement membrane marker, Type IV collagen (red) localized to the region between the stromal and epidermal compartment.

the distribution of labeled cells were similar for CD105 when HDF and iPDK were compared (Table 3-1).

Characterization of the proliferation kinetics of these cells revealed significant differences between these cell lines, as demonstrated by their cumulative growth curves (Figure 3-1C). *In vitro* expansion potential of EDK, iPDK, and control HDF fibroblasts was assessed by calculating population doublings (PDs) during serial subculture. All three cell lines were thawed at passage 7 and subcultured weekly over a period of 3 months. The cultures were considered to have lost their growth potential when cells underwent less than one PD per passage. As demonstrated by their cumulative growth curves, EDK, iPDK, and HDF showed significant differences in their growth kinetics (Figure 3-1C). All tested cell lines demonstrated very similar PDs until passage 11 (mean PD of 3.3 ± 0.3). The decline in PDs was first seen in HDF that occurred at passage 13 (PD = 1.8 ± 0.6) followed by gradual decline in growth potential and complete loss of growth potential at passage 19. The decline in PDs of EDK and iPDK fibroblasts

Surface marker	Antigen	HDF	EDK	iPDK
CD73	SH3, ecto-5'-nucteotidase	99	99	99
CD105	SH2, endoglin	99	60	95
CD90	Thy-1	99	99	99
CD13	Aminopeptidase N	99	98	97
CD10	CALLA	99	99	30
CD146	MCAM	60	60	90
CD106	VCAM-1	5	60	60
CD166	ALCAM	99	95	95
CD44	Hyaluronate, HCAM	99	99	99

The percentage of cells positive for the cell surface markers are shown, each experiment is normalized to isotype control and has been repeated at least two times.

Table 3-1. Comparison of surface antigen expression on HDF, EDK, and iPDK by flow cytometry. EDK, iPDK, and control HDF have similar expression of mesenchymal CD73, CD90, CD10, CD13, CD44, CD146, and CD166. HDF show low expression of CD106. EDK show low expression of CD105, while iPDK and HDF show high expression of CD105.

occurred at passage 20 and 16, respectively (EDKp20: PD = 1.8 ± 0.6; iPDKp16 PD = 2.14 ± 0.16) followed by a rapid loss of growth potential at passage 19 and 22, respectively. These results demonstrated that proliferation kinetics of iPDK was very similar to that of EDK and was markedly prolonged when compared to HDF.

Next, we incorporated iPDK cells into stromal compartment of human skin equivalents (HSE). These 3D tissues serve as an *in vitro* surrogate of human skin that have been previously used to study the functional capacity of EDK cells to support epidermal morphogenesis and wound repair (Shamis, Hewitt et al. 2011). EDK, iPDK, and control HDF cell lines were incorporated into collagen gels and were grown at an air-liquid interface for 10 days, with foreskin-derived, human keratinocytes (NHK) on their surface. Control HDFs incorporated into the stromal compartment of HSEs supported the proliferation and differentiation of keratinocytes on its surface (Figure 3-1D). Tissues incorporating either iPDK or EDK cells showed a similar degree of epithelial morphogenesis and establishment of the basement membrane as demonstrated by collagen IV staining (Figure 3-1D, inserts).

EDK and iPDK express elevated levels of ECM proteins in respond to ascorbic acid stimulation when compared to primary dermal fibroblasts

Production of extracellular matrix (ECM) proteins is an essential feature of stromal fibroblast function that is essential for tissue maintenance and repair. As it is known that L-ascorbic acid-2-phosphate (AA) induces expression and extracellular deposition of ECM proteins, specifically collagens, by dermal fibroblasts (Murad, Grove et al. 1981; Chojkier, Houglum et al. 1989), we sought to compare the response of iPSC- and hESC-derived fibroblasts to AA stimulation. To address this, we performed real time

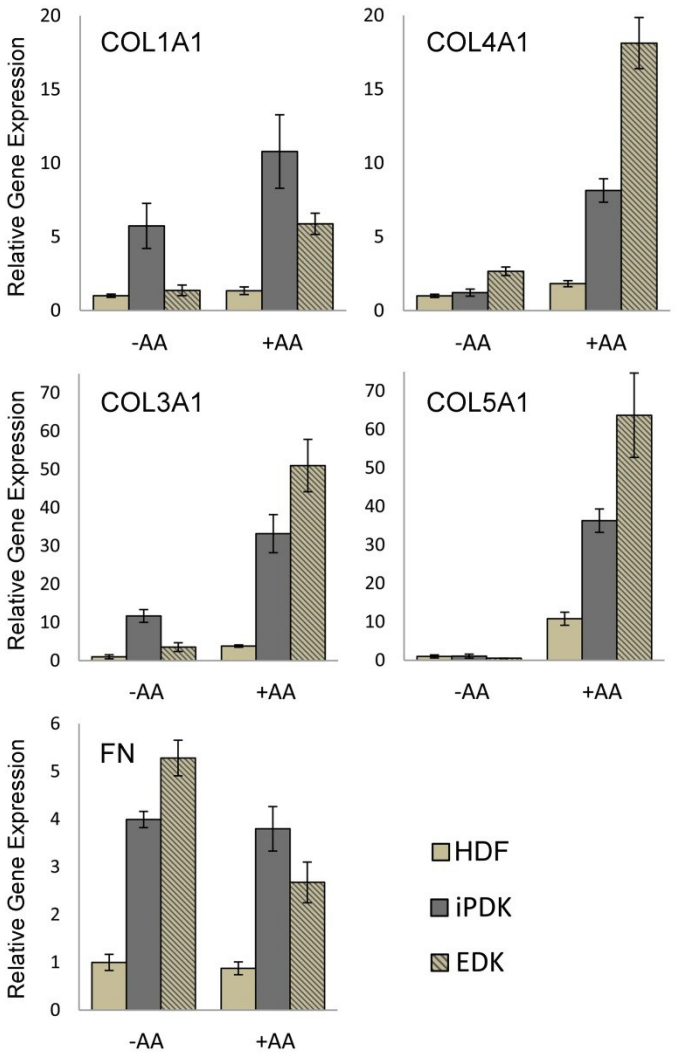

Figure 3-2. Fibroblasts differentiated from iPSC and hESC expressed elevated levels of collagenous proteins in the presence of ascorbic acid that exceeded those expressed by primary dermal fibroblasts. Real-time RT-PCR analysis of ECM proteins showed that EDK and iPDK expressed elevated levels of proα1(I) collagen (COL1A1), proα1(III) collagen (COL3A1), proα1(IV) collagen (COL4A1) and proα1(V) collagen (COL5A1) when compared to HDF in the presence of L-ascorbic acid-2-phosphate (AA). AA stimulation had no effect on expression of fibronectin (FN). Results represent the mean expression levels normalized to GAPDH; error bars represent standard deviation from three independent experiments.

RT-PCR analysis to measure the expression levels of ECM proteins in EDK, iPDK, and control HDF after growth for 1 week in the presence or absence of AA. We observed significantly greater AA responsiveness and expression of genes for ECM proteins in both iPDK and EDK cells when compared to HDF (Figure 3-2). Stimulation with AA (10µg/ml) had little or no effect on expression of pro-α1(I) collagen (COL1A1) and pro-α1(IV) collagen (COL4A1) in HDF, while expression of pro-α1(III) collagen (COL3A1) and pro-α1(V) collagen (COL5A1) were increased, 3- and 5-fold respectively. When stimulated with AA, iPDK cells demonstrated a 2-fold increase in COL1A1, a 3-fold increase in COL3A1, an 8-fold increase in COL4A1, and a 35-fold increase in COL5A1

mRNA levels when compared to cells not stimulated with AA. Similar to iPSC-derived fibroblasts, hESC-derived fibroblasts also expressed elevated levels of collagen precursors in response to AA. When stimulated with AA, EDK cells demonstrated a 5-fold increase in COL1A1, 15-fold increase in COL3A1, 6-fold increase in COL4A1, and 125-fold increase in COL5A1 mRNA levels. Stimulation with AA had a negligible effect on expression of the non-collagenous ECM protein, fibronectin (FN), in all three cell lines. However, the baseline expression levels of FN were noticeably higher in both, iPDK and EDK cells when compared to HDF. These findings demonstrated that both hESC- and iPSC-derived fibroblasts were responsive to AA, which elevated the expression of collagen genes to a significantly greater degree than those seen in primary dermal fibroblasts.

EDK and iPDK respond to ascorbic acid stimulation by increasing collagen secretion and extracellular deposition to a greater degree when compared to primary dermal fibroblasts

We compared the potential of EDK, iPDK and control HDF to secrete, process, and deposit collagen using a soluble collagen assay, immunofluorescence staining and western blot analysis. Fibroblasts were cultured for 1 week in the presence or absence of AA, and supernatants were collected after 48 hours of incubation to measure levels of total soluble collagen (type I-V collagen) using Sircol™ assay (Figure 3-3A). HDF showed reduced levels of soluble collagen protein as compared to iPDK and EDK fibroblasts. In the presence of AA, all three cell types secreted significantly higher levels of total soluble collagen when compared to cells grown in the absence of AA. However, AA increased the production of total soluble collagen to a greater extent by EDK and iPDK cells (238±28% in EDK and by 142±17% in iPDK vs. untreated control) when

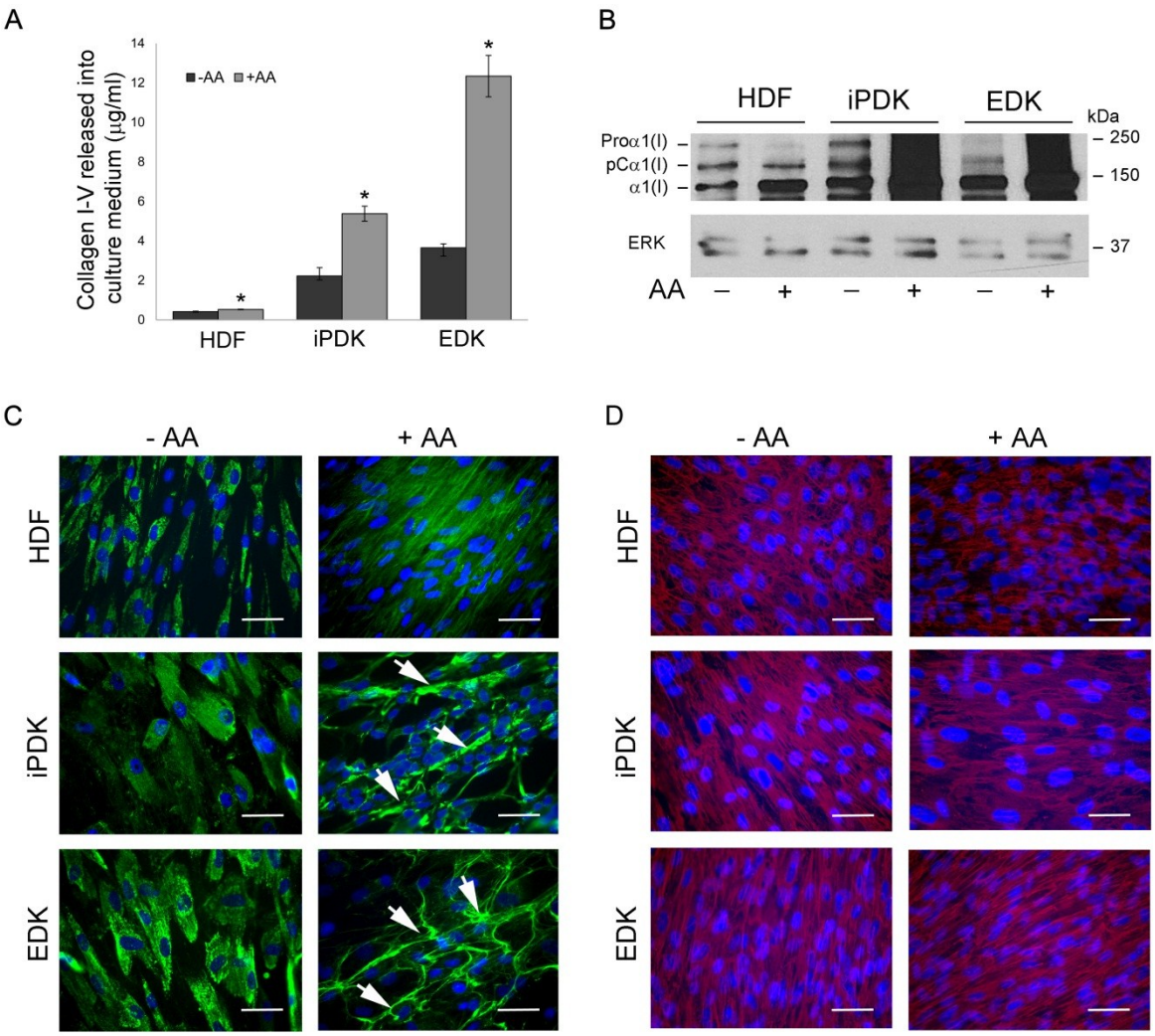

Figure 3-3. Stimulation with ascorbic acid induces secretion and deposition of collagenous proteins in iPSC- and hESC-derived fibroblasts to a greater degree than primary dermal fibroblasts. A. Soluble collagen assay (Sircol™) showed that AA induced higher secretion levels of collagens I-V in EDK and iPDK than in control HDF (t-test: *P<0.05) compared to untreated controls. **B.** Western blot analysis of Type I Collagen demonstrated that conversion of Proα1(I) collagen to the mature α1(I) form was more efficient in the presence of AA in all three cell types. However, AA increased production of α1(I) collagen to a greater extent in EDK and iPDK cells than in control HDF. **B.** Immunofluorescence analysis of Type I Pro-collagen localization in EDK, iPDK and HDF grown in the presence or absence of AA. In the presence of AA, EDK and iPDK fibroblasts deposited higher amount of Type I Pro-collagen into the extracellular space between cells (arrows, B) than BJ fibroblasts. Bars, 50µm**. C.** Immunofluorescence analysis of fibronectin in EDK, iPDK and HDF cells grown in the presence or absence of AA. There was no noticeable difference in the deposition of fibronectin in EDK, iPDK, and HDF.

compared to HDF (by 26±4% in BJ vs. untreated control). To determine if stimulation with AA increased processing of proα1(I) collagen in EDK and iPDK cells, we performed western blot analysis using an anti-collagen I antibody that recognizes all three

forms of α1(I) collagen: the unprocessed procollagen α1(I) chain (Proα1(I)), the C-terminal procollagen α1(I) chain (pC-α1(I)) and the fully processed α1(I) chain with both the N- and C- propeptides cleaved (α1(I)). Immunoblots showed that in the presence of AA, the generation of mature α1(I) collagen was more efficient in all three cell types (HDF, iPDK and EDK), as seen by the loss of the Proα1 (I) band which likely reflects AA-stimulated hydroxylation of proline and lysine residues in pro-collagen (Figure 3C). However, in the presence of AA, EDK and iPDK cells generated significantly greater amount of α1(I) collagen when compared to HDF (Figure 3-3B). To confirm that AA increased extracellular deposition of collagen, we performed imunofluoresence staining to compare the localization of Type I Pro-collagen in EDK, iPDK, and control HDF that were grown in 2D monolayer cultures in the presence or absence of AA (Figure 3-3C). In the absence of AA, all three cell types demonstrated a similar cytoplasmic localization of Type I Pro-collagen without extracellular deposition. In the presence of AA, both, iPDK and EDK cells demonstrated elevated accumulation of Type I Pro-collagen in the extracellular space when compared to Type I Pro-Collagen deposited by HDF (Figure 3-3C, arrows). There was no noticeable difference in the deposition of fibronectin between EDK, iPDK, and HDF (Figure 3-3D). Taken together, these results demonstrated that iPSC-derived fibroblasts showed elevated secretion and extracellular deposition of collagen when compared to primary dermal fibroblasts, yet were similar to levels produced by hESC-derived fibroblasts.

3D stromal tissues assembled by EDK and iPDK cells

Since AA induced an increase in production and deposition of ECM proteins in EDK and iPDK in 2D monolayer culture, we next assessed the potential of EDK, iPDK,

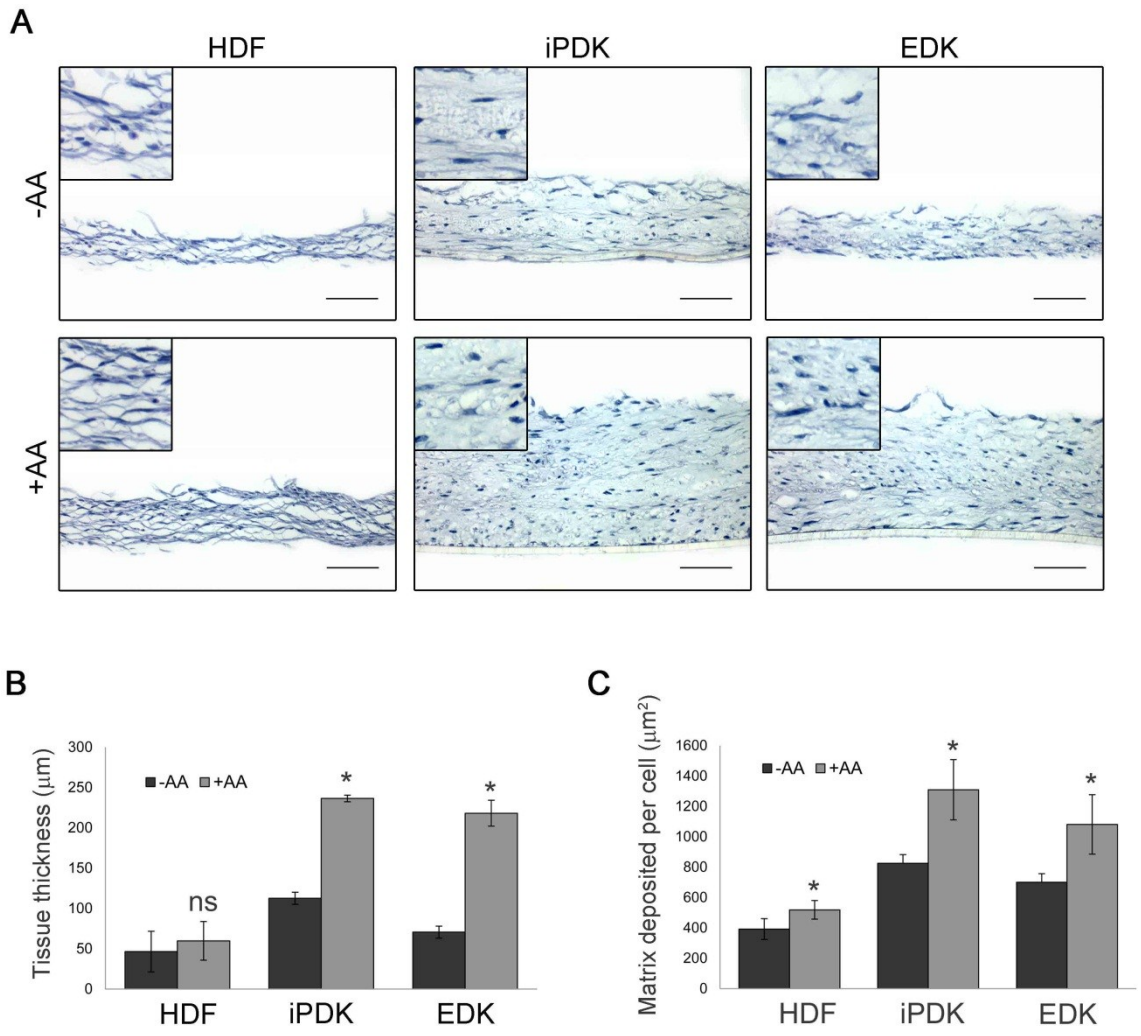

Figure 3-4. hESC- and iPSC-derived fibroblasts assemble a 3D stromal tissues. A. Representative H&E stains of tissue constructs assembled by EDK, iPDK, and control HDF. Bars, 100μm. **B.** Measurements of tissue thickness showed that EDK and iPDK and EDK assembled significantly thicker tissues than HDF in both the presence and absence of AA (t-test: *P<0.05). **C.** Quantification of ECM deposition on a per cell basis showed that stimulation with AA increased ECM deposition and assembly in all three cell types (t-test: *P<0.05). However, the capacity of AA to increase deposition of ECM was greater in EDK and iPDK than HDF.

and control HDF to deposit and organize a 3D ECM under conditions that enabled assembly of a stroma-like tissue. These three cell types were seeded at high density on a porous polycarbonate membrane in a transwell and cultured for 5 weeks in the presence or absence of AA. In this way, it was possible to assess the production and assembly of ECM produced by EDK, iPDK and HDF under more stringent experimental conditions

than in 2D monolayer culture. Tissues harboring each of these three cell types were examined for the degree to which they could organize stromal architecture and for thickness of tissues generated upon assembly of 3D ECM. Histological analysis of these tissues demonstrated the presence of fibroblasts aligned in a dense collagenous matrix (Figure 3-4A, inserts). Tissue constructs assembled by HDF showed a more fibrillar connective tissue that was less compact compared to those assembled by iPDK and EDK cells (Figure 3-4A). To quantify differences in the amount of ECM produced by these cell lines in these tissues, we measured the thickness and the amount of ECM deposited on a per cell basis using multiple sections from three independent experiments. Tissue thickness measurements revealed that iPDK and EDK assembled significantly thicker tissues than HDF when grown in the presence of AA (Figure 3-4B). To quantify the amount of ECM deposited on a per cell basis in each construct, we measured the area of each tissue that was normalized to the number of cells present (Figure 3-4C). These measurements demonstrated that significantly greater amounts of ECM were deposited and assembled when all cell types were grown in the presence of AA. However, the addition of AA to EDK and iPDK cells increased ECM deposition to a greater extent (by 54±28% in EDK and by 59±24% in iPDK vs. untreated control) than was seen for HDF (by 32±15% in HDF vs. untreated control). To ensure that no changes occurred in the mesenchymal phenotype of EDK, iPDK and HDF as the result of prolonged growth conditions and exposure to AA, we used flow cytometric analysis to characterize the CD surface antigen profile of these cells after growth in 2D monolayer cultures in the absence or presence of AA for 3 and 5 weeks (Table 3-2). All three cell lines showed stable morphology and expression of surface markers CD90, CD73, CD10, and CD166 typical

Cell type	Surface marker	3wk		5wk	
		-AA	+AA	-AA	+AA
HDF	CD73	98	99	97	99
	CD90	98	97	99	98
	CD10	98	99	99	99
	CD166	91	97	93	87
iPDK	CD73	97	97	97	98
	CD90	97	96	95	94
	CD10	97	97	96	94
	CD166	93	94	91	94
EDK	CD73	91	99	98	98
	CD90	99	97	99	99
	CD10	99	98	99	99
	CD166	99	93	98	98

The percentage of cells positive for the cell surface markers are shown, each experiment is normalized to isotype control and has been repeated at least two times.

Table 3-2. Stable expression of CD markers characteristic of stromal fibroblasts are seen in long term culture of EDK, iPDK, and HDF by flow cytometry. EDK, iPDK and HDF maintained stable mesenchymal phenotype when cultured over prolong period of time (up to 5 weeks) in the presence of AA as shown by the expression of CD markers typical of stromal fibroblasts.

of stromal fibroblasts. These surface markers were found in greater than 90% of EDK, iPDK, and HDF grown in the presence and absence of AA, indicating that neither prolonged time in culture nor exposure to AA resulted in the selection of subpopulations linked to a loss of fibroblast properties. These data demonstrate that fibroblasts differentiated from hESC and iPSC demonstrated augmented production and assembly of ECM when compared to primary dermal fibroblasts.

3D stromal tissues assembled by EDK and iPDK cells are enriched in Type III Collagen when compared to tissues assembled by primary dermal fibroblasts

In addition to overall matrix production, it is known that the organization and structure of stromal tissues is dependent on the levels of production of individual ECM proteins (Sottile, Shi et al. 2007). To further compare the composition of 3D stromal tissues assembled by EDK, iPDK and HDF, we analyzed levels of Type I Collagen (COL1), Type III Collagen (COL3) and fibronectin (FN) by immunoblot and

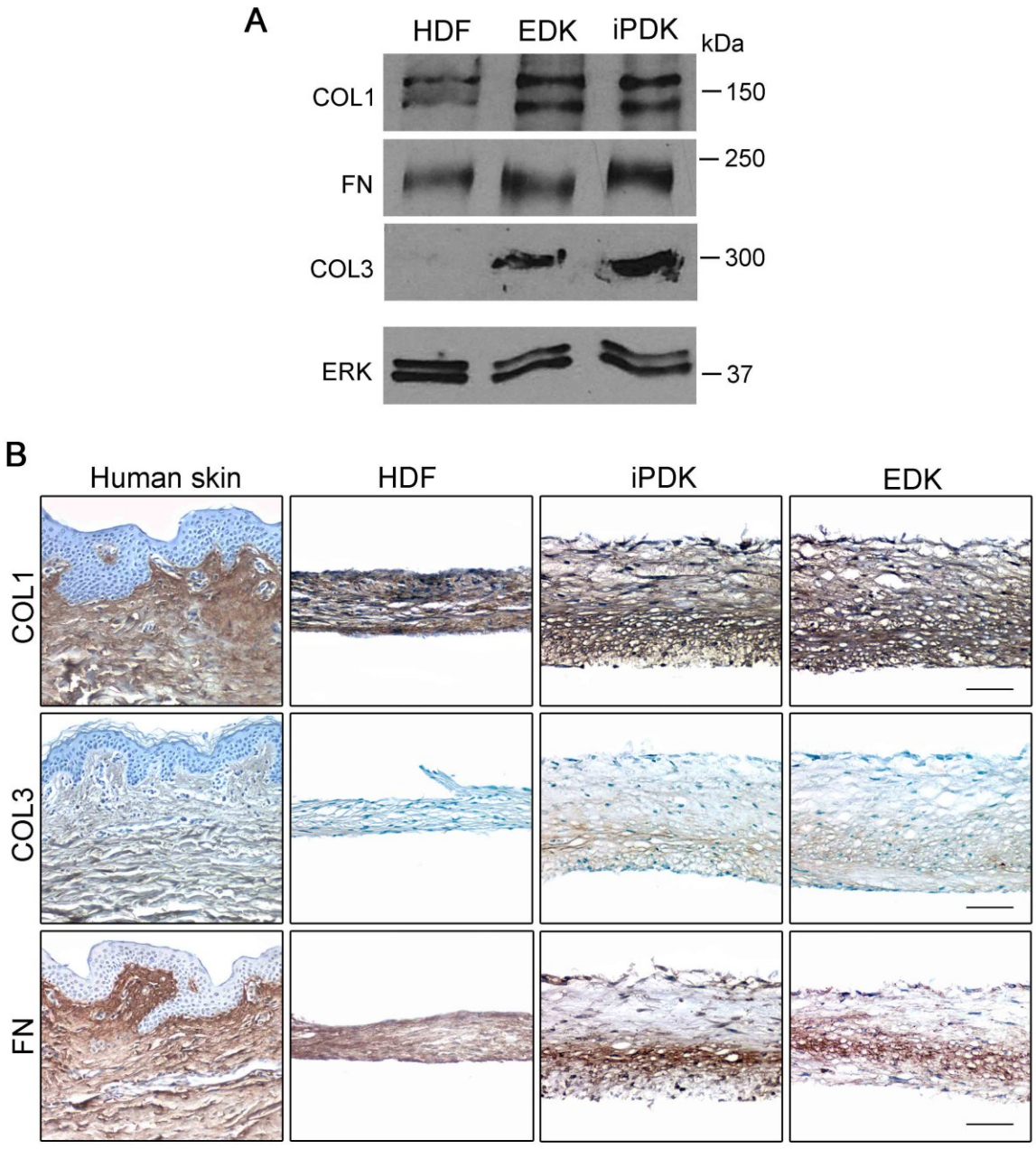

Figure 3-5. Tissues assembled by hESC- and iPSC-fibroblasts are enriched in Type III Collagen compared to those assembled by HDF. A. Representative western blot of Type I Collagen (COL1), Type III Collagen (COL3), and fibronectin (FN) within 3D ECM assembled by EDK, iPDK and HDF after 5 weeks of growth in presence of AA. Stromal tissues assembled by EDK and iPDK containe high levels of COL3 when compared to tissued assembled by HDF. **B.** Immunohistochemical staining of tissues assembled by EDK, iPDK and HDF compared to control sections of human skin. Consistent with the western blot analysis, COL3 was detected in tissues assembled by EDK and iPDK fibroblasts but not in tissues assembled by HDF. Bars, 100µm.

immunohistochemical analysis (Figure 3-5). These tissue constructs were solubilized and subjected to western blot analysis, which revealed that levels of both COL1 and FN were similar in tissues assembled by EDK, iPDK and HDF (Figure 5A-5C). Western blot analysis of COL3 demonstrated that tissues assembled by both EDK and iPDK contained higher levels of COL3 when compared with tissues assembled by HDF (Figure 3-5A). The presence of COL1, COL3, and FN was further verified by immunohistochemistry (Figure3-5B). Similar to neonatal human skin, COL1 and FN were present throughout the tissues assembled by all three cell types (EDK, iPDK and HDF). Consistent with the western blot analysis, COL3 was detected in tissues assembled by EDK and iPDK fibroblasts but not in tissues assembled by HDF (Figure 3-5B). The increased expression of Type III Collagen is characteristic of fetal fibroblasts and has been shown to facilitate scarless wound repair (Beanes, Hu et al. 2002; Larson, Longaker et al. 2010). In addition, Type III Colagen is a main component of the provisional matrix seen during the early stages of wound repair (Namazi, Fallahzadeh et al. 2011). Thus, the elevated levels of Type III Collagen in tissues harboring EDK and iPDK cells are indicative of the repair-competent phenotype of these cells.

Discussion

Fibroblasts represent a diverse population of mesenchymal stromal cells that play an essential role in regulating normal tissue homeostasis and wound repair (Schultz and Wysocki 2009). However, the utility of these cells for wound repair therapy has been limited by difficulties to acquire sufficient numbers of donor cells upon *ex vivo* expansion and by their heterogeneity that leads to unpredictable clinical outcomes (Koumas, King et

al. 2001; Sorrell and Caplan 2004; Sorrell, Baber et al. 2007; Wong, McGrath et al. 2007; Phan 2008). In this light, the development of approaches aimed at generating clinically-relevant quantities of fibroblasts with significant repair potential from pluripotent stem cells, such as hESCs and iPSC, may provide plentiful and reliable alternative sources of fibroblasts for tissue repair and regeneration. In this study, we have begun to explore the potential of hESC- and iPSC-derived fibroblasts for such therapeutic applications by comparing the production and assembly of ECM by hESC- and iPSC-derived fibroblasts to those of primary dermal fibroblasts. We have found that hESC- and iPSC-derived fibroblasts exceeded the growth potential of primary dermal fibroblasts and showed an augmented capacity to deposit collagen proteins in 2D monolayer culture and to organize and assemble a 3D stroma-like tissue.

To accomplish this, we compared BJ line of dermal fibroblasts (HDF) to fibroblasts derived from iPSC (iPDK) and hESC (EDK) by growing these cells in 2D monolayer culture and as 3D tissues in the presence of ascorbic acid (AA). AA is known to increase collagen synthesis by stimulating transcription of collagen genes and by acting as co-factor in post-translational pro-collagen hydroxylation that is essential for the stabilization of collagen triple helical structure (Peterkofsky 1972; Murad, Grove et al. 1981; Chojkier, Houglum et al. 1989). In addition, it has been found that dermal fibroblasts exposed to AA can assemble stroma-like tissues, composed of a multilayer of fibroblasts surrounded by dense accumulations of mature collagen fibrils in the extracellular space (Hata and Senoo 1989). Such stroma-like structures have been defined in previous studies as “self-assembled” or cell-derived ECM (Pouyani, Ronfard et al. 2009; Throm, Liu et al. 2010), where fibroblasts deposit and organize an ECM,

comprised primarily of Type I Collagen and fibronectin, that displays features of a provisional matrix seen during the early stages of wound repair (Pouyani, Ronfard et al. 2009). We have found that both, hESC- and iPSC-derived fibroblasts (EDK and iPDK, respectively) were highly responsive to AA, which demonstrates that these cells retain this important functional property of stromal fibroblasts following their differentiation from pluripotent stem cells. For example, when cultured in 2D monolayer culture in the presence of AA, EDK and iPDK fibroblasts increased their expression of collagen genes, secretion of total soluble collagen, and the extracellular deposition of Type I collagen to a significantly greater degree than those seen in HDF. When grown in the presence of AA under culture conditions that enabled the organization of a 3D ECM, EDK and iPDK fibroblasts acquired a highly synthetic phenotype that was characterized by elevated ECM production and organization that generated stroma-like tissues that showed significantly greater amounts of ECM than were found to be deposited by HDF. The analysis of the composition of these stromal tissues revealed that EDK- and iPDK-harboring tissues contained greater amounts of Type III Collagen when compared to HDF-harboring tissues, indicating their similarities to fetal dermis and provisional matrix seen during the early stages of wound repair (Beanes, Hu et al. 2002; Larson, Longaker et al. 2010; Namazi, Fallahzadeh et al. 2011). The elevated levels of Type III Collagen seen in fetal tissues has been suggested to facilitate scarless fetal wound healing by promoting cellular migration and proliferation, see Chapter 1.1. (Larson, Longaker et al. 2010). These differences were seen in spite of the morphologic similarities and overlap in expression of CD surface markers that were seen when EDK, iPDK and parental BJ fibroblasts were grown in 2D culture for up to 5 weeks. This phenotypic stability

demonstrates that the dramatic changes seen in collagen production in 2D culture and in 3D tissue assembly were not due to changes that occurred in these cells during prolonged culture or upon AA exposure. Taken together, our findings revealing a greater degree of ECM production and assembly and an increased Type III Collagen deposition in tissues harbouring EDK and iPDK fibroblasts when compared to HDF, suggests that hESC- and iPSC-derived fibroblasts represent a replenishing source of potent fibroblasts that may be useful for repair of wounds.

Importantly, functional differences between iPSC- and hESC-derived cells and primary dermal fibroblasts were only fully revealed when these cells were grown in a complex, 3D tissue environment. This suggests that evaluation of the biological potential of hESC- and iPSC-derived cells will require the development of reliable methods to evaluate their functional properties before they can be translated for human therapy. Such analysis of cell potency is currently limited by the nature of 2D, monolayer cultures, that cannot fully evaluate cellular function due to the absence of in an *in vivo*-like tissue context. By characterizing the properties of hESC- and iPSC-derived, differentiated cells using bioengineered 3D tissues as more predictive models of *in vivo* tissue responses, it will be possible to better assess cellular behavior before future therapeutic transplantation. Such tissue surrogates can therefore serve as a platform to assess the developmental capacity of hESC- and iPSC-derived cells to become functional cell types and will enable identification of iPSC-derivatives optimized for future regenerative therapies.

Furthermore, our findings extend recent studies showing that fibroblasts derived from iPSC (BJ-iPSC) acquire phenotypic properties that exceed those of fibroblasts from

which they were initially reprogrammed (BJ line of dermal fibroblasts). For example, iPSC-derived fibroblasts display an extended replicative potential (Suhr, Chang et al. 2009) and improved mitochondrial function (Suhr, Chang et al. 2010) when compared to the parental fibroblasts used to reprogram the iPSC from which they were differentiated. In addition, we recently found that hESC-derived fibroblasts manifest a repair-competent phenotype following wounding of 3D human skin equivalents (Shamis, Hewitt et al. 2011). Based on these findings, future therapies using iPSC-derived cells may be targeted to improve repair of non-healing wounds. For example, it is known that fibroblasts from non-healing wounds maintain their pathogenic phenotype due to premature senescence (Falanga 2005; Telgenhoff and Shroot 2005), failure to respond to growth factors (Loot, Kenter et al. 2002; Galkowska, Wojewodzka et al. 2006) and an inability to recruit cellular precursors needed to direct granulation tissue formation (Telgenhoff and Shroot 2005). During reprogramming to pluripotency, iPSC acquire elongated telomeres, to evade premature replicative senescence (Marion and Blasco 2010). As chronic wounds are recalcitrant to repair due to senescence-mediated cell cycle arrest of wound fibroblasts (Telgenhoff and Shroot 2005), overcoming this senescent phenotype may be important in generating wound repair-competent cells to improve healing. Taken together with our findings of improved ECM growth and production in iPSC-derived fibroblasts, our approach may lay the foundation through which somatic fibroblasts may undergo "recalibration" of their repair phenotype (Suhr, Chang et al. 2009; Suhr, Chang et al. 2010; Shamis, Hewitt et al. 2011) upon reprogramming to iPSC in a way that can revert fibroblast to a more functional state leading to restoration of tissue health. By comparing the biological potential of iPSC-

derived fibroblasts to fibroblasts from which iPSC were originally reprogrammed (BJ line of dermal fibroblasts), we have taken an important step towards understanding how iPSC-derived fibroblasts may demonstrate improved efficacy and function for future regenerative therapies.

Chapter 4: Human ESC- and iPSC-derived Fibroblasts Promote Angiogenesis In vitro and In vivo

Author Contributions:

Shamis Y: designed and performed all the experiments and analyzed data

Hewitt KJ: developed protocol for directed differentiation of hESC and iPSC to EDK and iPDK fibroblasts, respectively (see Appendix I and Figure 4-1A), discussed the results, and commented on the project

Silva EA: performed 3D in vitro sprouting assay (see Figure 4-3D-F), provided technical assistance for the transplantation of EDK cells into ischemic hindlimbs (see Figure 4-8), performed LDPI analysis of ischemic hindlimbs (see Figure 4-9), discussed the results, and commented on the project

Levenberg S. and Brudno Y: provided consultation and technical assistance for the preparation of 3D vascular networks (see Figure 4-4) discussed the results, and commented on the project

Mooney D: supervised the project, discussed the results and implications

Garlick JA: supervised the project, discussed the results and implications

Abstract

Vascular tissue engineering requires a ready source of endothelial cells and perivascular mesenchymal cells. While many reports have shown the derivation of endothelial cells from pluripotent stem cell sources, such as human embryonic stem cells (hESCs) and induced pluripotent stem cells (iPSCs), an efficient protocol for directed differentiation of pericytes have not been yet described. We have recently reported an efficient and reproducible protocol to generate mesenchymal cells from both hESCs and iPSCs (EDK and iPDK) with phenotypic and functional properties of pericytes.

Temporal gene expression and flow cytometry analysis during differentiation of hESCs and iPSCs towards EDK and iPDK cells revealed a progressive induction of pericyte markers NG2, PDGFRβ, CD105, and CD73, as well as transient induction of αSMA and markers of pericyte progenitors CD31, CD34, and FLK1/KDR. When stimulated with TGF-β1, EDK and iPDK cells showed the potential to differentiate into vascular vSMCs by upregulating the expression of contractile proteins αSMA, SM22α, SM-MHC, calponin, and caldesmon. EDK and iPDK cells showed further similarities to pericyte lineage by secreting elevated levels of soluble angiogenic regulators, including VEGF, HGF, IL-8, Angiopoetin-1, and PDGF-AA. When incorporated into 3D *in vitro* model of angiogenesis, EDK and iPDK provided necessary paracrine factors that induced endothelial sprouting. When co-cultured with endothelial cells in 3D fibrin-based constructs, EDK and iPDK cells promoted self-assembly of vascular networks and deposition of vascular basement membrane proteins. Furthermore, transplantation of these cells into mouse model of severe hindlimb ischemia reduced tissue necrosis and

improved perfusion of ischemic hindlimbs, demonstrating the potential of these cells to induce regeneration of vasculature in *vivo*.

Considering limitations associated with existing sources of pericytes, our differentiation protocol can be used for derivation of well-characterized pericyte populations for disease modeling, tissue engineering, and development of novel strategies in regenerative medicine.

Introduction

Angiogenesis, the growth of new capillary blood vessels, is required for the successful wound healing and for the vascularization of tissue-engineered grafts. The process of angiogenesis is initiated by the release of pro-angiogenic growth factors, including vascular endothelial growth factor (VEGF), platelet-derived growth factor (PDGF), transforming growth factor (TGF-α,TGF-β), basic fibroblast growth factor (bFGF), angiopoietin-1 (Ang-1), interleukin-8 (IL-8), and insulin-like growth factor 1 (IGF-1), that bind to their receptors on endothelial cells activating signal transduction pathways and stimulating endothelial proliferation, migration, and patterning (Gerhardt and Betsholtz 2003; Gurtner, Werner et al. 2008). The newly formed vasculature is initially unstable and subsequently become stabilized through the recruitment of pericytes, which control capillary morphology and function by regulating endothelial proliferation and differentiation, stimulate formation of a permeability barrier, and deposition of basal lamina (Gerhardt and Betsholtz 2003; Jain 2003).

Despite the critical role of pericytes in regulating angiogenesis, our understanding of pericyte phenotype and function is still limited. This is in part because pericytes are

difficult to identify (Gerhardt and Betsholtz 2003; Armulik, Genove et al. 2011). Pericytes constitute a heterogeneous population of mesenchymal cells that display plasticity as they can differentiate into other cell types within the surrounding connective tissue, including vascular smooth muscle cells (vSMC), fibroblasts, myocytes, osteoblast, chondrocytes, and adipocytes (Armulik, Genove et al. 2011). Since pericytes share many of the characteristics of MSCs, it has also been suggested that MSC found throughout fetal and adult tissues are in fact pericytes (Au, Tam et al. 2008; Crisan, Yap et al. 2008). The derivation of mesenchymal cells with characteristics of pericytes from both hESCs and iPSCs has been recently reported (Lian, Zhang et al. 2010; Boyd, Nunes et al. 2011; Dar, Domev et al. 2012). These cells have been shown to stabilize endothelial cell networks *in vitro* and promote re-vascularization and functional recovery of ischemic tissues *in vivo* (Lian, Zhang et al. 2010; Boyd, Nunes et al. 2011; Dar, Domev et al. 2012).

We have recently reported an efficient and reproducible protocol to generate mesenchymal cells from both hESC and iPSC (EDK and iPDK, respectively) that may have broad applicability for future therapeutic use in tissue engineering and regenerative medicine (Hewitt, Shamis et al. 2009; Hewitt, Shamis et al. 2011; Shamis, Hewitt et al. 2011; Shamis, Hewitt et al. 2012). Temporal gene expression and flow cytometry analysis during differentiation of hESC and iPSC towards EDK and iPDK cells have revealed a progressive induction of pericyte markers NG2, PDGFRβ, CD105, and CD73 as well as transient induction of αSMA and markers of pericyte precursors CD31, CD34, and FLK1/KDR. In addition, the analysis of secretory profiles of EDK and iPDK cells has demonstrated the elevated secretion of angiogenic soluble mediators, including

VEGF, HGF, IL-8, PDGF-AA, and Ang-1. The objective of this study was to further characterize the pro-angiogenic potential and pericyte functionality of EDK and iPDK cells using *in vitro* and *in vivo* models of angiogenesis.

Materials and Methods

Cell Culture

Adult dermal-derived human blood microvascular endothelial cells (HMVEC-dBlAd) were purchased from Lonza Inc., (Lonza, Basel, CH). Human umbilical vein endothelial cells (HUVEC) and RFP expressing human umbilical vein endothelial cells (RFP-HUVEC) were purchased from Angio-Proteomie (Angio-Proteomie, Boston, USA). All endothelial cells were expanded and maintained on tissue culture plastic in EGM-2MV media (Lonza, Basel, CH). EDK and iPDK cell lines were differentiated from H9 line of hESC and BJ-derived line of iPSC, respectively, using our previously described protocol for the generation of fibroblasts (Hewitt, Shamis et al. 2009; Hewitt, Shamis et al. 2011). For a step-by-step protocol, see Appendix I. For all experiments, HDF, EDK and iPDK cell lines were grown on Type I Collagen-coated plates (BD Biosciences, San Jose, CA) in media consisting of 3:1 DMEM:F12 (Invitrogen, Carlsbad, CA), 5% FCII (Hyclone, Logan, UT), 0.18mM adenine, 8mM HEPES, 0.5 µg/mL hydrocortisone, 10^{-10} M cholera toxin, 10ng/mL EGF, 5µg/mL insulin (all from Sigma, St. Louis, MO). All cell lines were routinely checked for mycoplasma contamination using MycoAlert® Mycoplasma detection kit (Lonza, Rockland, ME).

Real-time RT-PCR

RNA was isolated using Qiagen RNeasy purification kit (Qiagen, Valencia, CA), and then converted to cDNA with the iScript cDNA synthesis kit (Biorad, Hercules, CA) using 0.5μg RNA. Real-time RT-PCR reactions were carried out using 20ng of cDNA, 200nM of each primer and 2X SYBRgreen Supermix (Biorad, Hercules, CA) at a total sample volume of 12.5 μL and samples were run in triplicate on a iQ5 Real-Time PCR detection system (Bioad, Hercules, CA). PCR products were amplified to 30 cycles at 94 °C for 30 s, 60 °C for 30 s and 72 °C for 60 s. The relative level of gene expression was assessed using the $2^{-\Delta\Delta C}$t method. Error bars represent standard deviation of 3 biological replicates. The following oligonucleotide primer sequences were used: GAPDH-F: 5'-TCGACAGTCAGCCGCATCTTCTTT-3', GAPDH-R: 5'-ACCAAATCCGTTGACCTT-3'; CD31-F: 5'-CAACGAGAAAATGTCAGA-3' , CD31-R: 5'-GGAGCCTTCCGTTCTAGAGT-3'; CD34-F: 5'-TGAAGCCTAGCCTGTCACCT-3', CD34-R: 5'-CGCACAGCTGGAGGTCTTAT-3'; VEGFR-F: 5'-GGCCCAATAATCAGAGTGGCA-3', VEGFR-R: 5'-TGTCATTTCCGATCACTTTTGGA-3'; CD146-F: 5'-CTCGACTCCACAGTCTGGGAC-3', CD146-R: 5'-AAGGCAACCTCAGCCATGTCG-3'; PDGFRβ-F: 5'-GTGGTGATCTCAGCCATCCT-3', PDGFRβ-R: 5'-CCGACATAAGGGCTTGCTT-3'; NG2-F: 5'-GCTTTGACCCTGACTATGTTGGC-3', NG2-R: 5'-TCCAGAGTAGAGTCGCAGCA-3'; SM-MHC-F: 5'-CGCCAAGAGACTCGTCTGG-3', SM-MHC-R: 5'-TCTTTCCCAACCGTGACCTTC -3'; Calponin: 5'-CAGTCCACCCTCCTGGCTTTG-3', Calponin: 5'-GATGTTCCGCCCTTCTCTTAG-3'; Caldesmon-F: 5'-AGTATGTGGGAGAAAGGGAATG-3', Caldesmon-R: 5'-

AGGTTTGGGAGCAGGTGA-3'; SM22α-F: 5'- AGGAGCGGCTGGTGGAGTGGAT -3', SM22α-R: 5'- CATGTCAGTCTTGATGACCCCATAGTC-3'; ACTA2-F 5'-CATCTCCAGAGTCCAGCACA -3', ACTA2-R: 5'-ACTGGGACGACATGGAAAAG-3'.

Flow Cytometry

EDK and iPDK cells were trypsinized, pelleted, and re-suspended in 2% FBS in PBS. Cell suspensions were stained with PE-conjugated anti-CD73, -CD105, -CD140b, - or Isotype control-IgG1k (BD Pharmingen, San Jose, CA). Cells were incubated for 30 min on ice and washed with 2% FBS in PBS solution. For αSMA staining, EDK and iPDK cells were trypsinized, pelleted, and fixed in 0.01% paraformaldehyde, permeabilized using 0.5% Saponin, and immunostained against αSMA (Abcam, Cambridge, MA) followed by Alexa Fluor 594-conjugated goat anti-mouse secondary antibody (Invitrogen, Carlsbad, CA) . All data were acquired using a FACSCalibur (BD, San Jose, CA) and analyzed using CellQuest (BD, San Jose, CA) and Summit V4.3 software (Dako, Carpentaria, CA). Analysis was performed on 20,000 cells per sample and positive expression was defined as the level of fluorescence greater than 99% of the corresponding isotype control IgG1k (BD Biosciences, San Jose, CA).

ELISA

EDK, iPDK, EDK-shScram, and EDKshPDGFRβ cells were grown either in normoxic or hypoxic conditions (1% O_2) for 48 hours. Tissue culture supernatants were harvested and processed using DuoSet VEGF, HGF, bFGF, and IL-8 ELISA kits (R&D Systems, Minneapolis, MN) according to manufacturer's protocol. Media was assayed in triplicates

from at least three independent samples. The values were normalized according to cell numbers counted in the respective cultures at the time of supernatant harvesting and expressed in pg/ml per 10^4 cells.

Antibody-based Cytokine Array

EDK and iPDK 10^6 cells were plated onto 100mm tissue culture plates and grown to 80-90% confluence in tissue culture medium consisting of 3:1 DMEM:F12 (Invitrogen, Carlsbad, CA), 5% FCII (Hyclone, Logan, UT), 0.18mM adenine, 8mM HEPES, 0.5 µg/mL hydrocortisone, 10^{-10} M cholera toxin, 10ng/mL EGF, 5µg/mL insulin (all from Sigma, St. Louis, MO). All cells were fed with 5ml of fresh tissue culture media 24 hours prior the experiment. Tissue culture supernatants were harvested, and the supernatants from the plates containing equal cell numbers were processed using Proteome Profiler Human Angiogenesis Antibody Array (R&D Systems, Minneapolis, MN) according to manufacturer's protocol. Histogram profiles were generated by quantifying the mean spot pixel densities from the array membrane using ImageJ software (U. S. National Institutes of Health, Bethesda, Maryland, USA).

3D In Vitro Sprouting Assay

HMVEC-dBlAd cells were cultured to confluence at in complete EGM-2MV medium (Lonza, Basel, CH). Dextran beads microcarriers (Cytodex™ 3) with a dry weight of 50 mg were swollen in PBS and autoclaved. The microcarriers were washed in EGM-2MV medium and seeded with 3×10^6 HMVECs in a spinner flask. Before the experiment spinner flasks were coated with Sigmacoat solution (Sigma, St. Louis, MO), drained, and washed thoroughly with PBS. The microcarriers and cell mixture were stirred for 2 min

out of 30 min for 3 h at 37 °C incubation. After 3 h, the beads and cells mixture were continuously stirred and incubated for an additional 21 h. The cell-coated beads were then seeded in fibrin gel in a 24-well-plate. The composition of the fibrin gel in each well was 0.68 mg fibrinogen (Sigma, St. Louis, MO), 11.4 μg aprotinin (Sigma, St. Louis, MO), 0.455U thrombin (Sigma, St. Louis, MO) in 393 μL of PBS and 57 μL of basal EGM-2MV. Mixtures were incubated at 37 °C for 30 min to gel. The basal EGM-2MV media, the basal EGM-2MV media containing VEGF (50ng/ml), or the basal EGM-2MV media containing EDK or iPDK cells ($0.5x10^4$ cells/cm^2) were added into each insert and incubated for 48 hours. Media were changed every 24 hours. After 48 hours, the gels were rinsed with PBS, and fixed with 4% paraformaldehyde (Electron Microscopy Sciences, Hatfield, PA), and visualized at 10X objective magnification with an Olympus IX2 microscope. Sprouts were identified as continuous multi-cellular structures extended from the microcarrier beads with a minimum of two cells in the structure.

GFP Labelling of EDK and iPDK Cells

Lentiviral particles carrying GFP (gift of the lab of Dr. Larry Feig) were generated in 293FT cells using ViraPower™ Lentiviral Expression System (Invitrogen, Carlsbad, CA) according to manufacturer's protocol. The pLenti-CMV-GFP-puro vector was purchased from Addgene (Addgene, Cambridge, MA). GFP-EDK and GFP-iPDK cell lines were generated by infection of 50,000 cells with 1 MOI of lentivirus carrying GFP sequence. Stable cell lines were selected with puromycin (2μg/ml) (Sigma, St. Louis, MO).

Preparation of 3D Vascular Networks

Endothelial cells (RFP-HUVEC: 0.3×10^6, 0.15×10^6, or 0.06×10^6) and fibroblasts cells (HDF, EDK or iPDK: 0.06×10^6) were used to generate each construct. Endothelial cells and fibroblasts were mixed together, pelleted, and resuspended with 60 μl of fibrin solution. The composition of the fibrin solution in each was 7 mg/ml fibrinogen (Sigma, St. Louis, MO), 50 μg/ml aprotinin (Sigma, St. Louis, MO), and 20U/ml thrombin (Sigma, St. Louis, MO). Mixtures were pipetted into glass-bottom 12-well plates and incubated at 37 °C for 15 min to gel. EGM-2MV media (Lonza, Basel, CH) were added into each well and incubated for 7 days hours. Media were changed every other day.

Immunofluorescence and Confocal Imaging

3D fibrin constructs were scanned by Leica™ TCS SP2 confocal microscope after 1, 4, and 8 days in culture. Lenses in use were ×20, ×40 (oil). Laser excitation wavelengths included 488 nm and 561 nm. Emission spectrum was freely tunable between 425 nm and 740 nm. For x20 magnification, sample scanning was recorded every 10 μm, which generated 25 ± 2.5 optical slices, depending on the variation of the thickness. For x40 magnification, sample scanning was recorded every 1 μm, which generated 15 ± 2 optical slices. For immunofluorescence, after 10 days in culture, 3D fibrin constructs were fixed with 4% paraformaldehyde for 10 min and permeabilized using 0.3% Triton X-100 for 10 min, and immersed overnight in blocking solution containing 10% goat serum and 0.1% Triton X-100 at 4 °C. Constructs were immunostained overnight using primary antibodies directed against Type IV Collagen (Sigma, St. Louis, MO) followed by 3 hours incubation with Alexa Fluor 488 -conjugated goat anti-mouse secondary antibodies

(Invitrogen, Carlsbad, CA). After final washes in PBS, the constructs were stored in 24-wells plates in PBS at 4 °C before imaging.

Quantification of 3D Vascular Networks

3D fibrin constructs were scanned by Leica™ TCS SP2 confocal microscope after 8 days in culture using ×20 lenses. Sample scanning was recorded every 10 μm, which generated 25 ± 2.5 optical slices, depending on the variation of the thickness. The resulting image stacks of RFP-HUVEC were subjected to a series of image analyses using SPOT Advanced software (Diagnostic Instruments, Sterling Heights, MI) allowing for manual determination of vessel length and thickness. Vessel length was calculated between proximity branches. Vessel thickness was calculated in the middle of each sprout. Two independent constructs and three z-stacks of images taken at different focus depths per construct were analyzed for each condition.

shRNA Knockdown

Stable shRNA knockdowns of PDGFRβ in EDK cells were generated by infection of 50,000 cells with 1 MOI of lentiviral particles carrying predicted PDGFRβ-interacting sequences or non-target shRNA control sequence. Following infection, stable cell lines were selected with puromycin (2μg/ml) (Sigma, St. Louis, MO) for 4 days. Viruses were obtained from MISSION shRNA Lentiviral Particles (Sigma, St. Louis, MO). Out of 5 predicted sequences, one was selected for future experiments (TRCN1999-shβ1) based on degree of knockdown, verified by real-time PCR and flow cytometry.

Cell Migration Assay

Migration was assessed using a 96-well transwell migration plate (Millipore, Bellerica, MA) with 8 μm pore size. Polycarbonate membranes were coated one day prior to seeding cells with 10μg/mL fibronectin (BD Biosciences, Bedford, MA) diluted in PBS. EDK-shScram and EDK-shPDGFRβ were prepared by serum-starvation in serum-free media overnight . Adult dermal-derived human blood microvascular endothelial cells (HMVEC-dBlAd) were grown to confluence in EGM-2MV media (Lonza, Basel, CH). Before the experiment the EGM-2MV media was replaced with serum-free media and incubated for 24hours to generate HMVEC-conditioned serum-free media. Serum-free media (SFM) or HMVEC-conditioned serum-free media (HMVEC-SFM) was added to the lower chamber, and 1x104 cells per insert were added to the upper chamber. Cells were incubated at 37ºC for 6 hrs, washed in PBS and fixed with 2% paraformaldehyde. Using a cotton-swab, non-migrated cells were removed from the top of membrane, and the membrane was then stained with 0.1% Crystal Violet for 10 minutes, and counted manually near the center of the membrane at 10x magnification. Data represents an average of 3 experiments, and 6 technical replicates per experiment.

Preparation of RGD-coupled Alginate Scaffolds

Alginate scaffolds (gift of the lab of Dr. David Mooney) (Vacharathit, Silva et al. 2011) were prepared using high molecular weight (~250 kDa) ultrapure sodium alginate powder (Novamatrix Pronova UP MVG alginate) enriched (≥60%) in G blocks. Briefly, a 2% w/v alginate solution in dH_2O was oxidized by 1% with sodium periodate to create hydrolytically labile bonds. Oxidized alginates were coupled with oligopeptides containing the Arg-Gly-Asp cell adhesion sequence (Commonwealth Biotechnologies,

Richmond, VA) following aqueous carbodiimide chemistry. Hydrogels were prepared by mixing the alginate solution with calcium sulfate slurry and the mixture was injected between glass plates with a spacer of 1 mm. After curing for 20 min, gel disks with diameter of 10 mm were punched out. These gel disks were frozen and stored at −20°C, and after 24 h, gel disks were lyophilized to yield macroporous materials.

Ischemic Hindlimb Model in SCID Mouse

All procedures were carried out at Harvard Universirt and were approved by the Experimental Animal Committee of Harvard University. SCID mice were subjected to femoral artery and vein ligation to induce hindlimb ischemia. Immediately after ligation cell-loaded alginate scaffolds (5×10^6 cells per scaffold) were transplanted on the medial side of thigh muscle. The groups ($n = 5$ per condition) were as follows: (*i*) blank scaffold, (*ii*) EDK-loaded scaffolds (with $VEGF_{121,}$ 3 μg per scaffold) (5×10^6 cells), and (*iii*) EDK-shPDGFRβ-loaded scaffolds (with $VEGF_{121}$, 3 μg per scaffold) (5×10^6 cells). Transplantation of blank scaffolds without cells had little benefit, because autoamputation of the ischemic limbs was noted in three days, and these mice were euthanized one week after surgery. Before the surgery (day 0), and 1 day, 7 days, 2, 4 and 6 weeks postsurgery, hindlimbs subjected to surgery were visually examined, and each received a score based on the evaluation of the degree of necrosis (5=normal 4=presenting nail discoloration, 3=multiple necrotic toes, 2=necrotic foot, 1=necrotic leg, 0=complete amputation). In addition, measurements of the ischemic/normal limb blood flow ratio were performed on anesthetized animals (n = 5/time point/experimental condition) by using a Periscan system blood perfusion monitor laser Doppler equipment (Perimed Instruments, Ardmore, PA).

Statistical Analysis

Statistical analyses were carried out using IBM SPSS Statistics 19 software (IBM, Armonk, NY). All results are reported as mean ± standard deviation of at least three independent samples. Statistical comparison between two groups was performed using Student's t-test. When comparing more than two groups One-Way Analysis of Variance (ANOVA) test was used followed by the post hoc Tukey's multiple comparison tests. Results were considered significant for $p \leq 0.05$.

Results

Emergence of pericyte markers following differentiation of hESCs and iPSCs towards EDK and iPDK

We have recently reported an efficient and reproducible protocol for generating mesenchymal cells from both hESC and iPSC (EDK and iPDK, respectively) that may have broad applicability for future therapeutic use in tissue engineering and regenerative medicine (Hewitt, Shamis et al. 2009; Hewitt, Shamis et al. 2011; Shamis, Hewitt et al. 2011; Shamis, Hewitt et al. 2012). The directed differentiation protocol is summarized in Figure 4-1A and described in more detail in Appendix I. Human ESC and iPSC were induced to differentiate in parallel using identical differentiation procedures and were monitored for expression of pericyte markers during the sequential stages of differentiation. The change in mRNA and protein expression following differentiation from hESCs and iPSCs was analyzed at days 0, 7, 14, and 28 days by real-time RT-PCR and flow cytometry (Figure 4-1). Data analysis revealed a transient induction of FLK1/KDR, CD34, and CD31, markers of vasculogenic progenitors, following BMP4

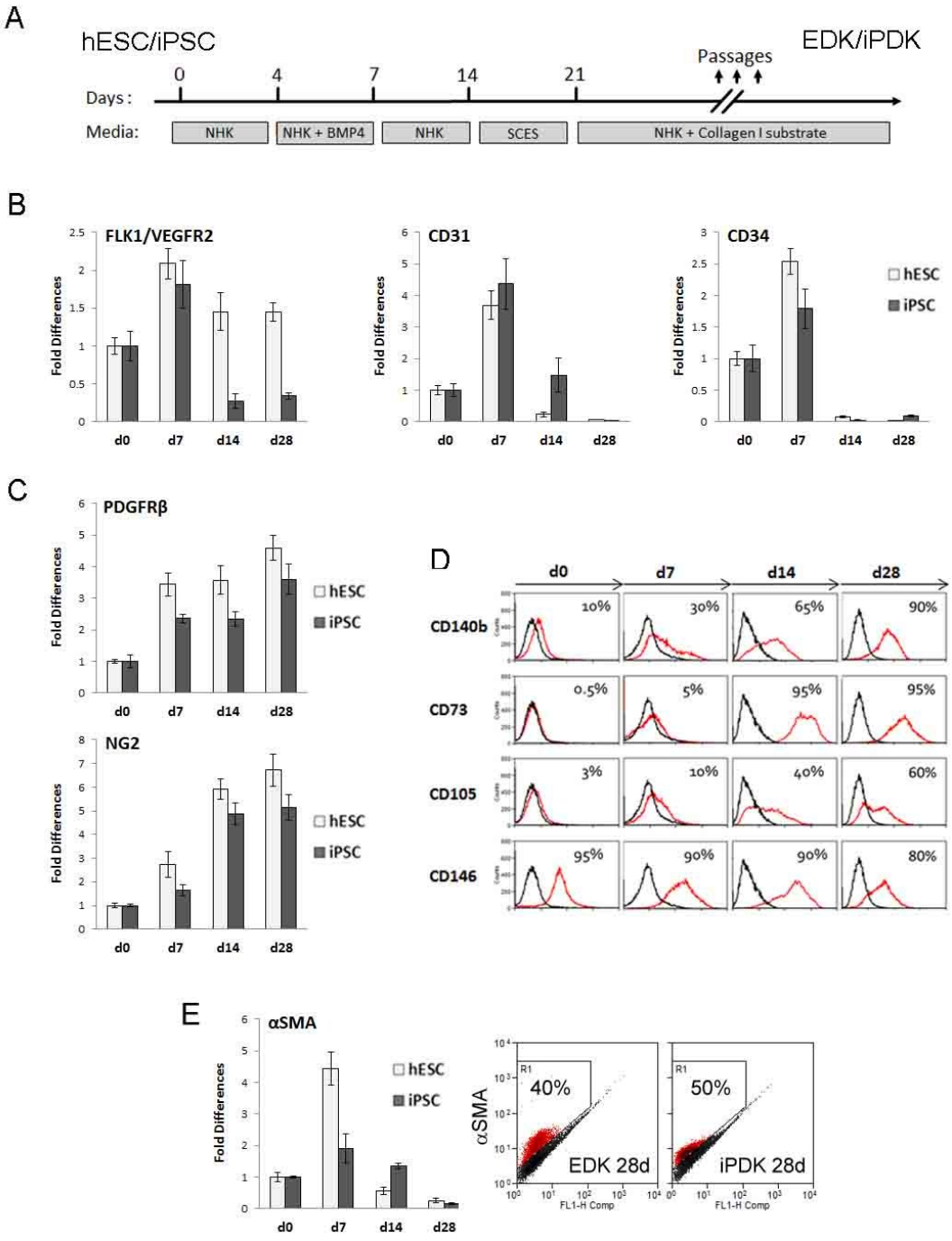

Figure 4-1. Emergence of pericyte markers following differentiation from hESCs and iPSCs. A. Summary of directed differentiation protocol for derivation of EDK and iPDK cells **B.** Quantitative RT-PCR analysis demonstrating a transient induction of vasculogenic precursor markers FLK1/VEGFR2, CD34, and CD31 following differentiation from hESCs and iPSCs. **C.** Quantitative RT-PCR analysis demonstrating a gradual increase in expression levels of pericyte markers PDGFRβ and NG2 following differentiation from hESCs and iPSCs. **D.** Flow cytometry analysis demonstrating a graduate increase in protein levels of pericyte markers CD140b, CD73, CD105, and stable expression of CD146 following differentiation from hESCs (marker expression-red profiles are shown relative to isotype control-black profiles). **E.** Analysis of pericyte marker αSMA gene and protein expression following differentiation from hESCs and iPSCs by real time RT-PCR and flow cytometry.

treatment at day 7 (Figure 4-1B). Analysis of pericyte markers revealed a gradual increase in expression levels of NG2, PDGFRβ, CD73, and CD105 (Figure 4-1C and 1D, Table 4-1). Analysis of protein levels of CD146 showed a slight decrease in percentage of CD146+ cells from 95% to 75% and 95% to 80% throughout the differentiation of hESC and iPSC, respectively (Figure 4-1D, Table 4-1). The gene expression level of αSMA was significantly upregulated at day 7 of differentiation, however dropped below the level of hESC and iPSC by day 28 of differentiated (Figure 4-1E). Analysis of protein levels of αSMA showed that 40% of EDK and 50% of iPDK cell population stained positive for αSMA (Figure 4-1E). Together, the temporal gene and protein expression data suggest that the culture conditions are conductive to differentiation of hESC and iPSC towards vasculogenic precursors may be producing cells of the pericyte lineage.

Surface marker	Antigen	Cell type	% of positive cells*			
			d0	d7	d14	d28
CD140b	PDFGRβ	hESC	10%	30%	65%	90%
		iPSC	30%	50%	60%	90%
CD73	SH3, ecto-5'-nucteotidase	hESC	0.5%	5%	95%	95%
		iPSC	5%	-	-	99%
CD105	SH2, endoglin	hESC	3%	10%	40%	60%
		iPSC	10%	-	-	90%
CD146	MCAM	hESC	95%	90%	90%	80%
		iPSC	95%	-	-	75%

* The percentages of cells positive for the cell surface markers are shown. Each experiment is normalized to isotype control, and has been repeated at least 2 times.

Table 4-1. Flow cytometry analysis of surface markers characteristic of pericytes. Human ESC and iPSC were induced to differentiate in parallel using identical differentiation procedures and the expression of CD73, CD105, CD146, and CD140b during the sequential stages of differentiation was analyzed by floe cytometry.

EDK and iPDK cells have the potential to differentiate into vascular smooth muscle cells

Pericytes have been shown to modulate their phenotype along the pericyte–vascular smooth muscle cell (vSMCs) axis in conjunction with vessel growth and remodeling (Armulik, Genove et al. 2011). In addition to their ability to differentiate into vSMCs, pericytes may also give rise to other types of mesenchymal cells, including fibroblasts, osteoblasts, chondrocytes, and adipocytes (Collett and Canfield 2005; Crisan, Yap et al. 2008; Armulik, Genove et al. 2011). The adipogenic and osteogenic differentiation potential of EDK cells have been analyzed before (See Chapter 2, Figure 2-2E and Figure 2-2F), and the same methods have been later used to analyze the differentiation potential of iPDK cells. The osteogenic differentiation of EDK and iPDK cells was induced using the β-glycerophosphate method, followed by Alzarin Red staining. The adipogenic differentiation was induced using the 3-isobutyl-1-methylxanthine method followed by Oil Red O staining. Similar to results obtained for EDK cells, iPDK did not appear to have oseogenic or adipogenic differentiation potential (data not shown). TGF-β1 has been previously reported to induce lineage commitment of hESC to vSMC, therefore we used TGF-β1 to stimulate the differentiation of EDK and iPDK cells towards vSMC phenotype. Upon stimulation with TGF-β1 (5ng/ml) for 1 week, EDK and iPDK cells showed the potential to differentiate into vSMC by upregulating the expression of contractile proteins αSMA, SM22α, SM-MHC, calponin, and caldesmon by more than 2-fold (Figure 4-2A and 4-2B). To confirm the gene expression data, the change in protein level of αSMA in response to TGF-β1 stimulation was also analyzed by flow cytometry. Flow cytometry analysis showed an increase in αSMA positive population from 35% to 60% and 50% to 70% for EDK and iPDK cells,

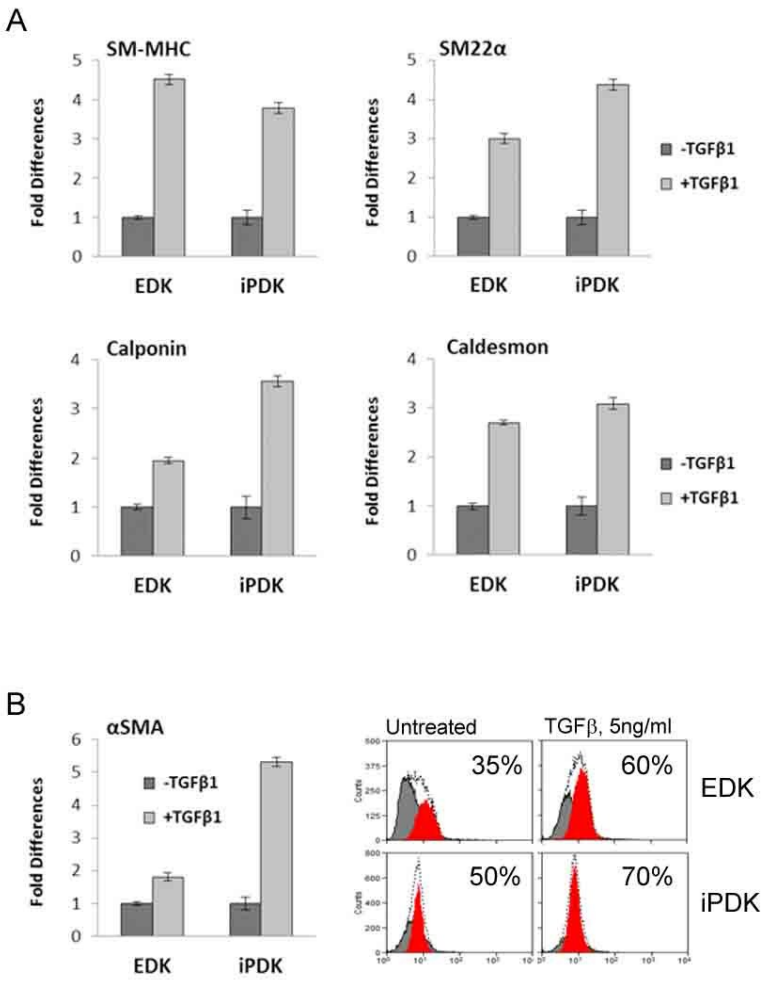

Figure 4-2. Vascular smooth muscle cell (vSMC) differentiation of EDK and iPDK cells. A. EDK and iPDK cells were cultured for 1 week in serum-reduced control media (-TGFβ1) or media supplemented with 5ng/ml of TGFβ1 (+TGFβ1). TGFβ1 treatment led to upregulation of contractile proteins expression as shown by quantitative RT-PCR revealed. **B.** Quantitative RT-PCR and flow cytometry analysis revealed upregulaation of αSMA in both EDK and iPDK cells as a result of TGFβ1 treatment (αSMA-positive cells - red profiles; αSMA-negative cells – grey profiles)

respectively (Figure 4-2B). These data suggest that EDK and iPDK cells retain a certain level of stem cell plasticity as indicated by vSMC differentiation potential.

EDK and iPDK cells promote angiogenesis in vitro

Angiogenesis is controlled by net balance of pro-angiogenic and anti-angiogenic soluble mediators (Armulik, Genove et al. 2011). To analyze the angiogenic potential of EDK and iPDK, their secretion profiles were generated using antibody-based cytokine array, which was designed to detect soluble mediator of angiogenesis (Figure 4-3A). Secretory profiles of EDK and iPDK were generated by quantifying the mean spot pixel

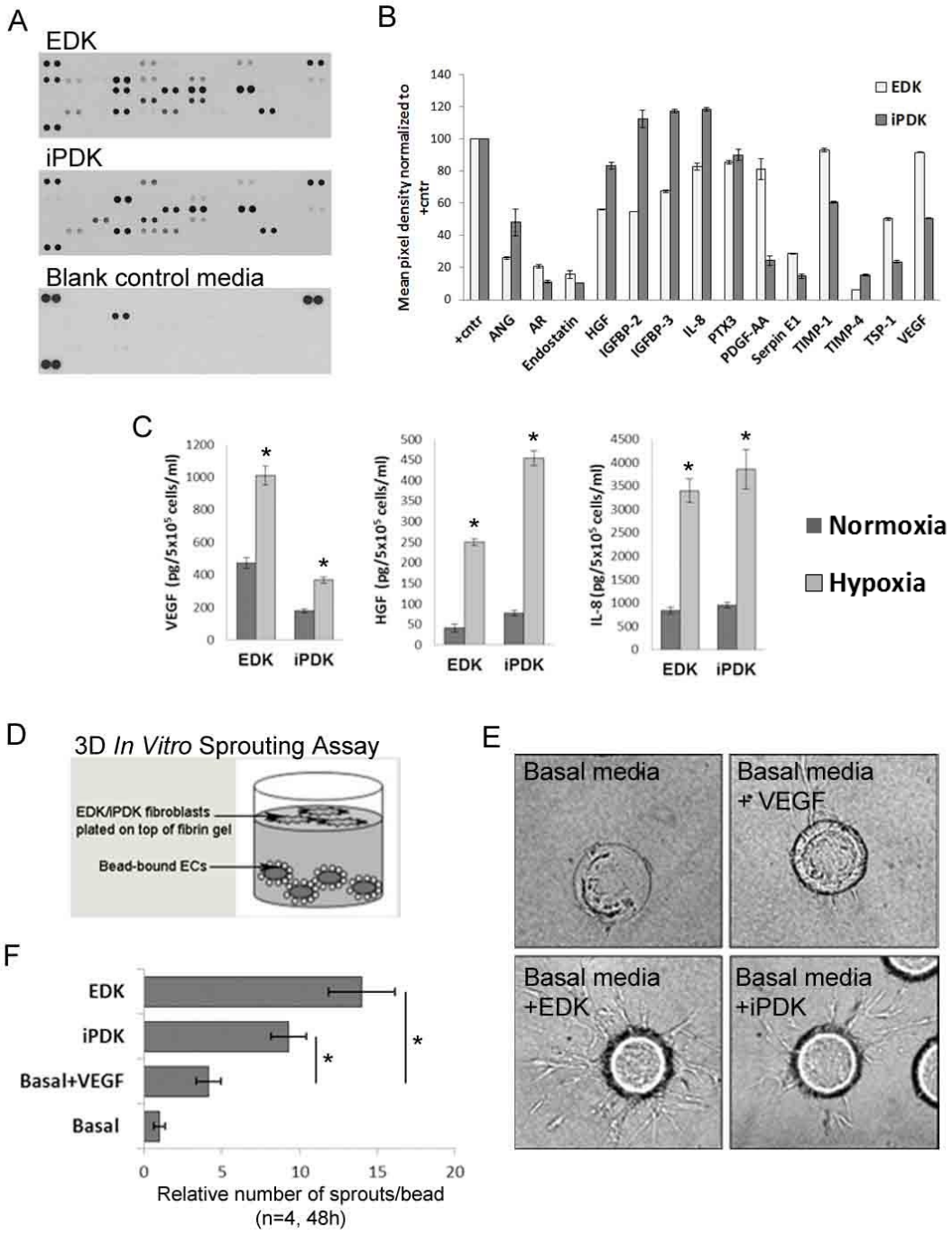

Figure 4-3. Angiogenic factors secreted by EDK and iPDK cells promote endothelial sprouting. A. Cytokine array membranes used to generate the secretory profiles of EDK and iPDK cells shown in Table 4-2. Secretory profiles were generated by quantifying the mean spot pixel densities by Image J from the array membranes. **B.** Angiogenic factors elevated in both EDK and iPDK cells. **C.** Expression of selected pro-angiogenic factors VEGF, HGF, and IL-8 in response to hypoxia was analyzed by ELISA (t-test: *$p<0.05$). **D.** Schematic of 3D *in vitro* sprouting assay to test angiogenic potential of EDK and iPDK cells **D.** Representative images of endothelial sprouts formed in EDK, iPDK, and control cultures. **E.** Quantification of endothelial sprouts revealed that sprout formation was significantly increased in both EDK- and iPDK-containing cultures when compared to control cultures (ANOVA: *$p<0.05$).

Target/Control	EDK		iPDK	
	mean	stdv	mean	stdv
control (+)	100.00		100.00	
Angiogenin-1 (Ang-1)	25.93	0.74	48.13	8.31
Amphiregulin (ER)	20.55	1.06	11.30	0.64
Coagulation factor III (TF)	44.82	0.25	3.98	0.68
CXCL16	7.44	0.74	1.11	0.00
EG-VEGF	12.48	0.02	1.00	0.00
Endostatin	15.74	2.52	10.42	0.00
FGF-7 (KGF)	6.55	0.95	1.13	0.11
HGF	56.14	0.30	83.19	2.13
IGFBP-2	54.82	0.21	82.36	5.18
IGFBP-3	67.50	0.85	87.27	1.04
IL-8	82.86	2.03	88.31	0.98
MCP-1	0.97	0.11	8.83	0.17
MMP9	3.22	0.44	70.36	4.00
PTX3	85.58	1.17	90.05	3.56
PDGF-AA	81.40	6.44	24.44	2.96
Serpin E1	28.70	0.38	14.70	1.28
TIMP-1	93.18	1.21	60.72	0.77
TIMP-4	3.34	0.06	15.54	0.55
Thrombospondin-1 (TSP-1)	50.21	0.59	23.61	0.94
VEGF	91.73	0.25	50.69	0.30

Table 4-2. Secretory profiles of EDK and iPDK cells. Supernatants from EDK and iPDK cultures containing equal cell numbers and blank control media were harvested and assayed using an antibody-based cytokine array. Secretory profiles were generated by quantifying the mean spot pixel densities by ImageJ from the array membranes shown in Figure 4-3A. The data are presented as percentages of the respective positive controls.

densities from the array membranes and normalized to the respective positive controls (Figure 4-3A and 4-3B, Table 4-2). EDK and iPDK cells showed very similar but not identical secretion profiles (Table 4-2). Both EDK and iPDK expressed elevated levels of pro-angiogenic factors Angiogenin-1 (Ang-1), Amphiregulin (AR), HGF, IGFBP-2, IGFBP-3, IL-8, PDGF-AA, Trombospondin-1 (TSP-1), and VEGF, as well as anti-

angiogenic factors Endostatin, PTX3, and Serpin E1 (Figure 4-3B). In addition, both EDK and iPDK showed proteolytic activity essential for matrix degradation during angiogenic sprouting by secreting elevated levels of MMP regulators TIMP1 and TIMP4 (Figure 4-3B). There was a noticeable difference in levels of Coagulation factor III (TR), CXCL16, KGF, MCP-1, and MMP9 in EDK when compared to iPDK cells (Table 4-2). In response to hypoxia, both EDK and iPDK cells significantly upregulated the expression of VEGF, HGF, and IL-8 as shown by ELISA (Figure 4-3C).

To determine whether soluble factors provided by EDK and iPDK cells were capable to promote endothelial sprouting, EDK and iPDK were incorporated into 3D *in vitro* sprouting assay that recapitulate the key steps of early angiogenic process (Vailhe, Vittet et al. 2001). For this assay, microcarriers beats were coated with adult dermal-derived human blood microvascular endothelial cells (HMVEC) and embedded into a fibrin gel, and EDK and iPDK cells were layered on the gel surface to provide soluble factors that promote endothelial sprouting from the surface of the beads (Figure 4-3D). After 48 hours of incubation, numerous sprouts were present in EDK- and iPDK-containing cultures that could easily be observed under phase-contrast microscopy (Figure 4-3E). In contrast, in control cultures grown in basal media or basal media supplemented with 50 ng/ml of VEGF, the sprout formation was limited (Figure 4-3E). Quantification of endothelial sprouts revealed that sprout formation was significantly induced in both EDK- and iPDK-containing cultures when compared to control cultures (Figure 4-3F). These findings indicate that EDK and iPDK cell have the potential to promote angiogenesis through paracrine mechanisms.

EDK and iPDK cells support in vitro vascular network formation

Next, we studied the ability of EDK and iPDK cells to support in vitro vascular network formation within 3D fibrin-based constructs. Fibrin-based constructs were prepared by mixing RFP-expressing human umbilical vein endothelial cells (RFP-HUVEC) with EDK and iPDK cells at ratios 5:1, 3:2, and 1:1 within fibrin matrix and culturing for 8 days (Figure 4-4A). Confocal microscopy analysis showed that after 8 days, formation of interconnected endothelial networks was observed in all conditions (Figure 4-4B). The assessment of network morphology revealed a significant increase in mean vessel length and a decrease in vessel thickness as the ratio of RFP-HUVEC to EDK and iPDK decreased (Figure 4-4C).

In order to obtain further insights on interaction between fibroblasts and endothelial cells during culture time, EDK and iPDK cells were labeled with GFP and incorporated into fibrin constructs with RFP-expressing HUVEC at ratio 3:1 (HUVEC:EDK/iPDK). Fibrin constructs were monitored on 1, 4, and 8 days postseeding using confocal microscopy. During 8 days period, RFP-HUVEC co-seeded with GFP-EDK and GFP-iPDK underwent a series of phenotypic changes that resulted in formation of stable interconnected vascular networks (Figure 4-5A). After 1 day in culture, GFP-EDK and GFP-iPDK cells began spreading in the matrix while RFP-HUVECs were primarily rounded. After 4 days in culture, RFP-HUVEC cells elongated and form disorganized partially connected vascular networks co-localizing with GFP-expressing EDK and iPDK cells situated at various points both above and below the focal plane. After 8 days in culture, RFP-HUVEC cells assembled into stable vascular networks with segments of uniform diameter (~15-20μm) co-localizing with GFP- expressing EDK and iPDK cells

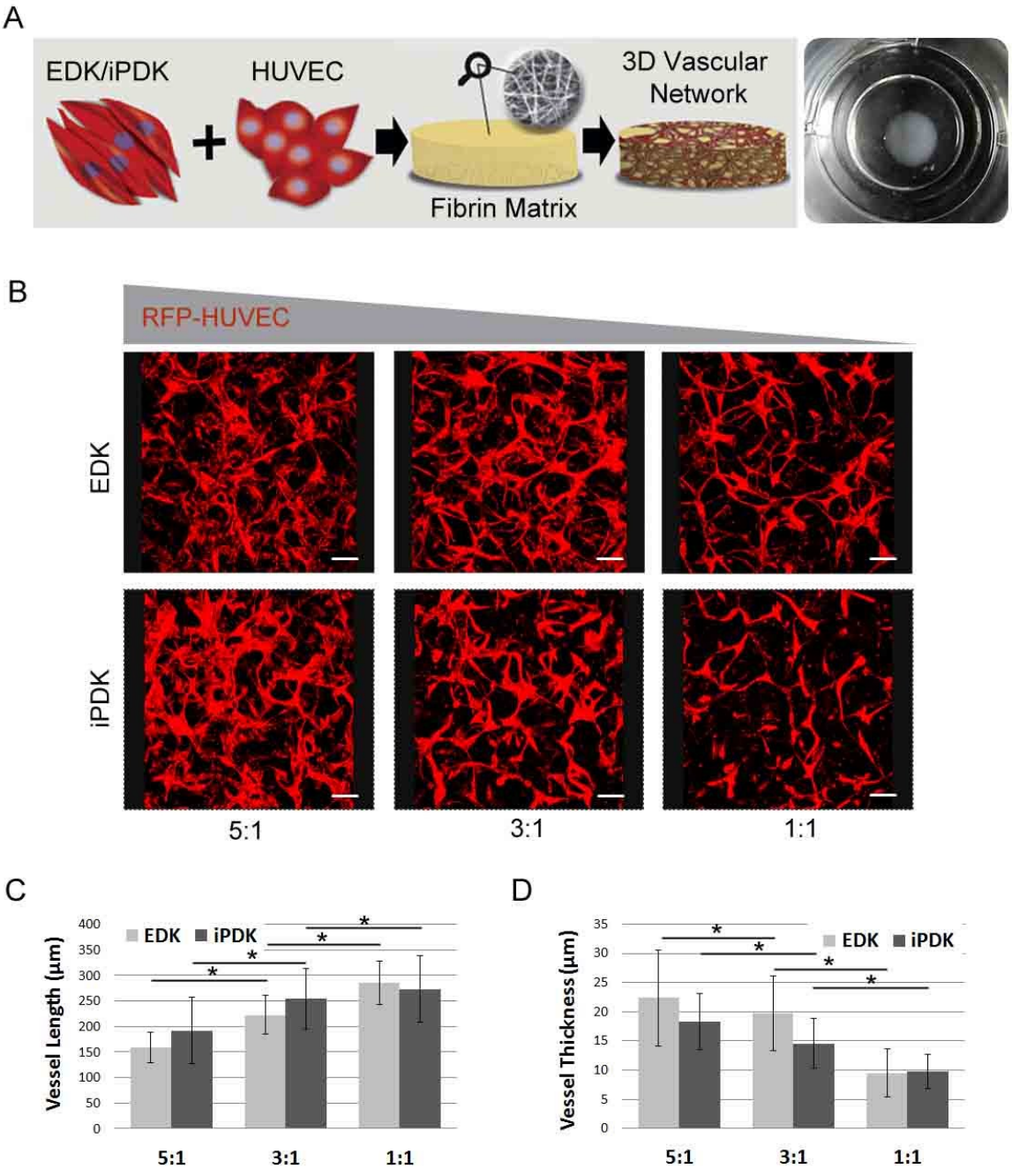

Figure 4-4. Endothelial cells co-cultured with EDK and iPDK form vascular networks. A. Schematic showing engineering of 3D vascular network in vitro. RFP-HUVEC are co-cultured with EDK or iPDK cells within fibrin matrix and allowed to spontaneously assembly into vessel networks. The image of the fibrin construct is shown on the right panel. Representative image of a fibrin constract is shown (tipical dimensions: 5mm diameter and 0.25mm height). **B**. Representative confocal images (collapsed Z-stacks of total 250± 25 µm) of 3D vascular networks formed within fibrin matrix following seeding RFP-HUVEC cells with EDK and iPDK at ratios of 5:1, 3:1, and 1:1. Bar, 100 µm **C**. Vascular network morphology assessment revealed a tendency towards forming longer and thinner vessels with decreasing HUVEC concentrations (ANOVA: *$p<0.05$).

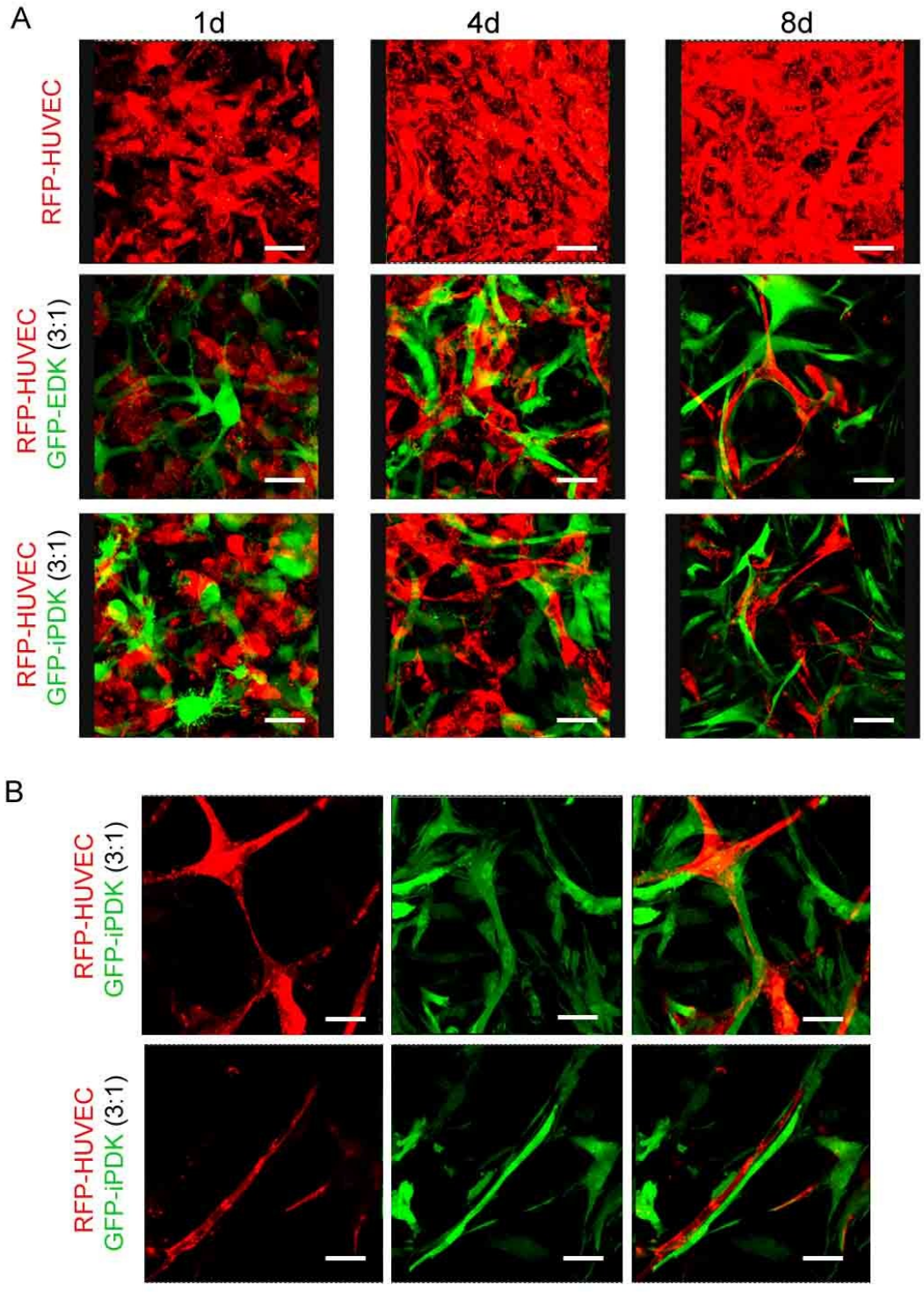

Figure 4-5. Vascular network maturity levels *in vitro*. A. Organization of RFP-expressing HUVEC and GFP-expressing EDK and iPDK cells within 3D fibrin constructs over time. Representative confocal images (collapsed Z-stacks of total 250± 25 μm) of 3D vascular networks formed within fibrin constructs 1, 4, and 8 days following seeding. Bars, 50 μm. **B.** Confocal images taken at higher magnification (collapsed Z-stacks of total 15± 2 μm) illustrating EDK and iPDK cells co-localizing with of vascular networks at day 8 following seeding. Bars, 25 μm.

(Figure 4-5A, see higher magnification in Figure 4-5B). Heterotypic cell contact was required for vascular network formation as neither monoculture of RFP-HUVEC in complete endothelial media (Figure 4-5A) nor monoculture of RFP-HUVEC in EDK- and iPDK-conditioned media (data not shown) resulted in formation of interconnected vascular networks.

Formation of the vascular basement membrane is a hallmark of vessel maturation (Jain 2003). Therefore, we studied the formation of vascular basement membrane structure in 3D fibrin-based constructs prepared with RFP-HUVEC and EDK and iPDK

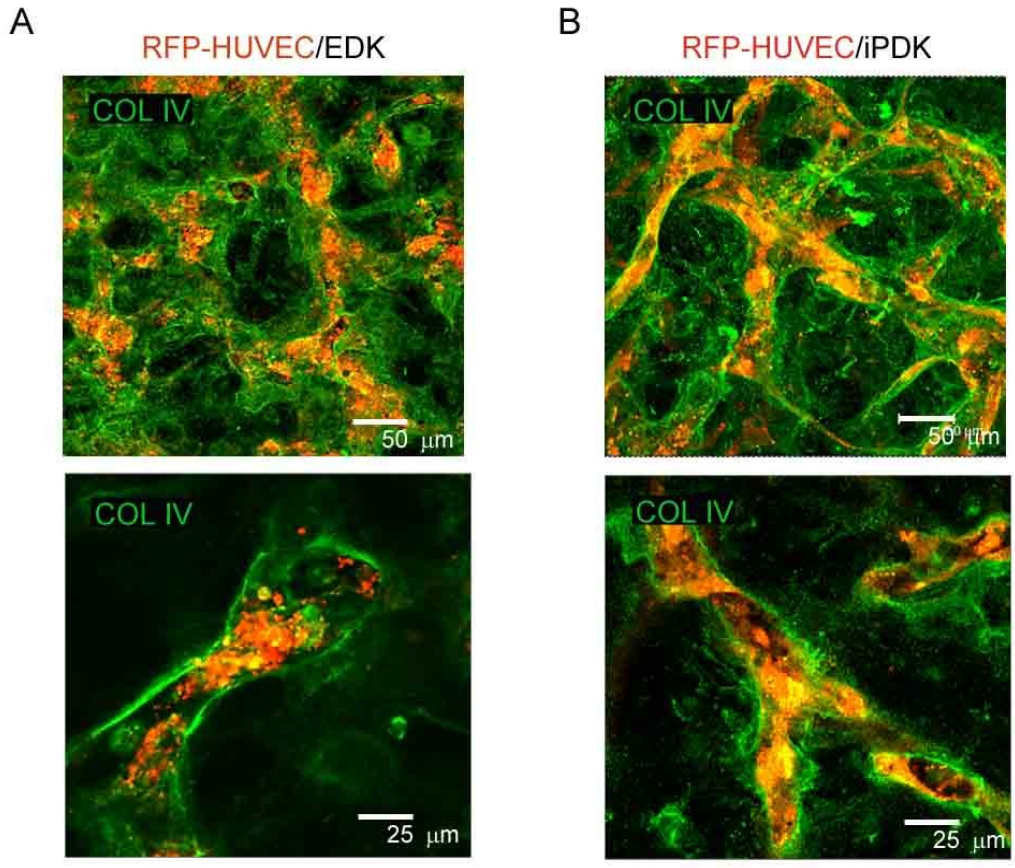

Figure 4-6. Vascular networks are stabilized by basement membrane protein deposition. Type IV Collagen (COL IV, green) is deposited at RFP-expressing HUVEC in EDK **(A)** and iPDK **(B)** co-cultures. Top panels show representative confocal images (collapsed Z-stacks of total 250± 25 μm) of 3D vascular networks formed within fibrin constructs 8 days following seeding. Bars, 50 μm. Bottom panels show confocal images taken at higher magnification (collapsed Z-stacks of total 15± 2 μm). Bars,25 μm.

cells at 8 days postseeding. Whole were stained with immunofluorescently-labeled antibodies specific to Type IV Collagen, the main constituent of vascular basement membrane. Confocal immunofluorescence analysis of fibrin constructs revealed that Type IV Collagen is deposited at RFP-expressing HUVEC cells in EDK and iPDK co-cultures, completely enveloping the vascular networks (Figure 4-6A and 4-6B). These results indicate that EDK and iPDK cells provide specific set of signals that support the organization of 3D vascular network and the deposition of vascular basement membrane i*n vitro*.

Transplantation of EDK cells to ischemic limb reduced tissue necrosis and improved blood perfusion

Since the recruitment of pericytes is regulated through PDGF-BB/PDGFRβ signaling pathway (Gerhardt and Betsholtz 2003; Armulik, Genove et al. 2011), for in vivo transplantation experiment we generated EDK and iPDK cells with decreased expression of PDGFRβ. Cells were infected with shRNA lentiviral constructs directed against the PDGFRβ gene (shPDGFRβ) and cells infected with non-specific shRNA constructs (shScram) were used as control. The extent of the knockdown in infected EDK was determined by flow cytometric and RT-PCR analysis for PDGFRβ (Figure 4-7A and 4-7B). To show that PDGFRβ knockdown could alter PDGFRβ-related function, the infected cells were incorporated into a Boyden Chamber assay to compare the migration of EDK-shScram and EDK6-shPDGFRβ cells towards either serum-free media (SFM) or SFM conditioned for 24 hours by adult dermal-derived human blood microvascular endothelial cells (HMVEC-SFM) (Figure 4-7C). The analysis PDGFRβ knock down cells revealed that levels of PDGFRβ on the cell surface were decreased in at

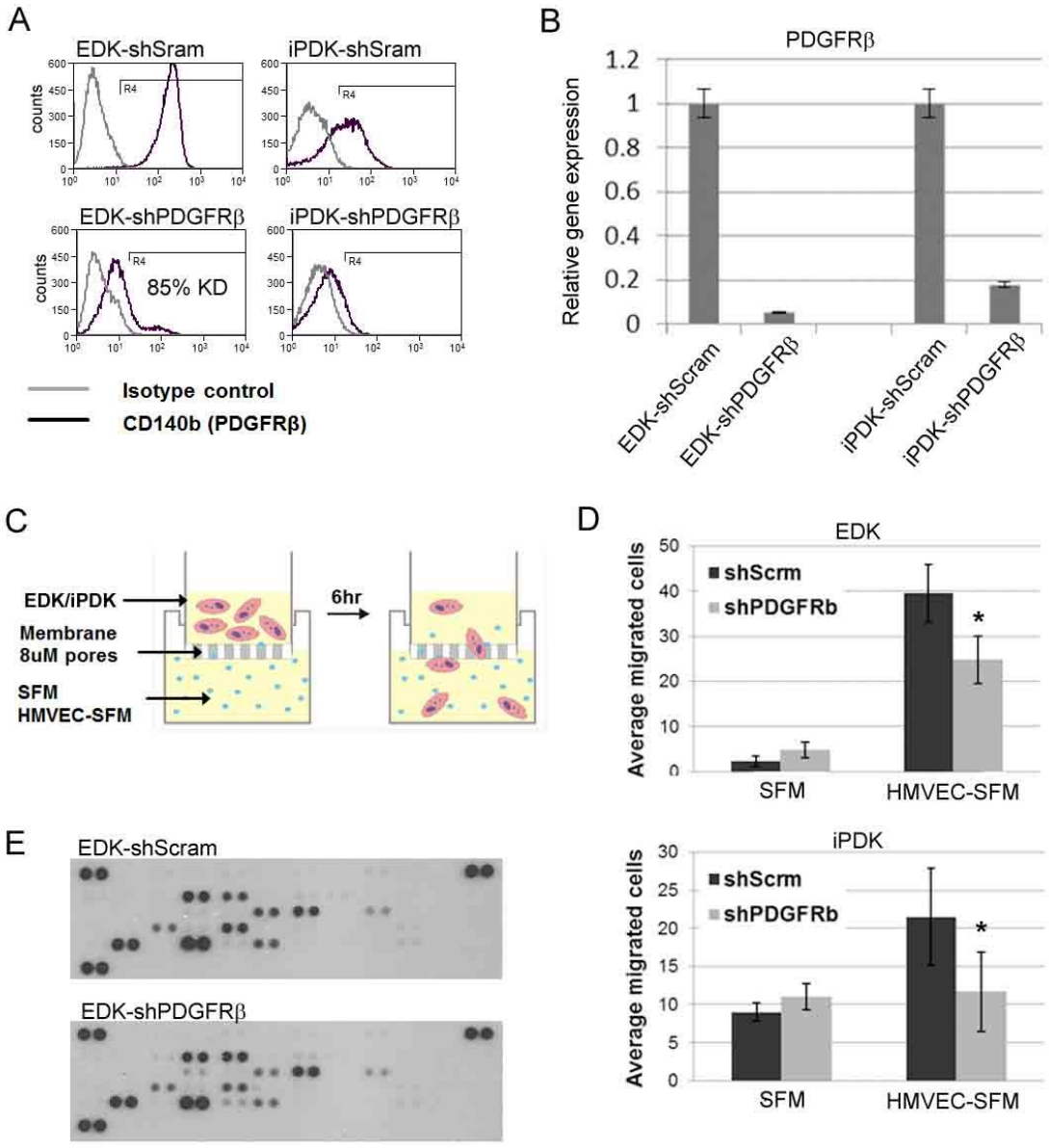

Figure 4-7. shRNA-mediated knockdown of PDGFRβ results in downregulation of PDGFRβ in EDK and iPDK cells and decreased cell migration. EDK and iPDK cells were infected with shRNA lentiviral construct directed against the PDGFRβ gene (shPDGFRb) and the effect of this knockdown was compared to cells infected with a non-specific, scrambled shRNA (shScrm). Flow cytometric **(A)** and RT-PCR **(B)** analysis demonstrated that levels of PDGFRβ were downregulated in at least 85% of EDK and 75% in iPDK cells. **C.** Schematic of a Boyden Chamber assay to compare the migration of EDK-shScram and EDK- shPDGFRβ cells towards serum-free media (SFM) or SFM conditioned for 24 hours by HMVEC (HMVEC-SFM). **D.** EDK-shScram and iPDK-shScram cells demonstrated 15-fold and 2-fold induction of migration towards HMVEC-SFM. The number of migrating EDK- and iPDK- shPDGFRβ cells towards HMVEC-SFM was significantly reduced compared to correspondent shScram controls (t-test:*P<0.05). **E.** There was no noticeable difference in secretory profiles of EDK-shScram and EDK-shPDGFRβ as shown by antibody-based cytokine array. Array membranes are shown.

least 85% (Figure 4-7A and 4-7B) that was sufficient to significantly reduce the migration of EDK and iPDK across a fibronectin-coated membrane towards HMVEC-SFM (Figure 4-7D). Secretory profiles of EDK-shScram and EDK-shPDGFRβ were generated using antibody-based cytokine array, which confirmed that PDGFRβ knockdown has no significant effect on the secretion of angiogenic mediators in these cells (Figure 4-7D). These results indicate that EDK and iPDK cells can be recruited toward endothelial cells and this response is mediated, at least in part, through PDGF-BB/PDGFRb signaling.

To compare the potential of pluripotent stem cell derived fibroblasts for induction of vascular regeneration *in vivo*, we used animal model of peripheral arterial disease, the hindlimb ischemia model in SCID mice that was created by femoral artery and vein ligation. These studies have been performed in collaboration with the lab of Dr. David Mooney and Harvard Medical School. As cell delivery vehicle we utilized RGD-coupled alginate scaffolds that were developed in the Mooney lab, which allowed us to deliver cells into ischemic area in a spatiotemporally controllable manner while protecting them in the early stages of tissue reintegration (Figure 4-8A) (Silva, Kim et al. 2008). Three experimental groups were set up as follows: 1) alginate scaffolds seeded with $0.5x10^6$ of EDK6-shScram cells (n=5), 2) alginate scaffolds seeded with $0.5x10^6$ of EDK6-shPDGFRβ cells (n=5), and 3) blank scaffolds (n=5), which were transplanted subcutaneously into area of femoral artery ligation (Figure 4-8B), and the mice were followed up for 6 weeks after the procedure. Hindlimbs subjected to surgery were visually examined at day 1, day 3 and weeks 1, 2, 4, and 6 following surgery, and each received a score based on the evaluation of the degree of necrosis (5=normal

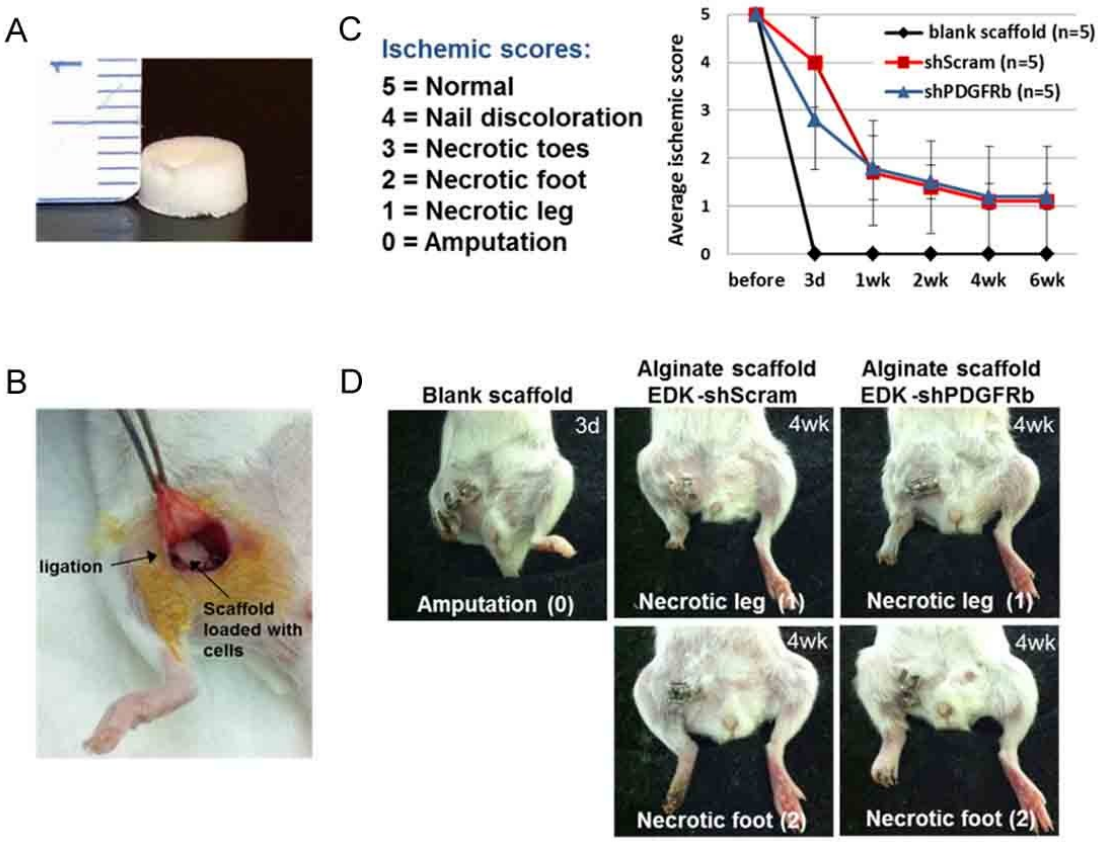

Figure 4-8. Transplantation of EDK cells into ischemic hindlinmbs. A. RGD-coupled alginate scaffold that was used as a vehicle for cell transplantation. **B.** Image demonstrating the transplantation of alginate scaffold seeded with cells into ischemic hindlimbs. **C.** Average ischemic scores given by visual examination of ischemic limbs following cell transplantation. Transplantation of EDK cells attenuated tissue necroasis and prevented limb amputation. There was no difference between the effects of EDK-shScram and EDK-shPDGFRβ cells. **D.** Representative images of ischemic limbs 3 days after transplantation with blank scaffolds and 4 weeks after transplantation with either EDK-shScram or EDK-shPDGFRβ.

4=presenting nail discoloration, 3=multiple necrotic toes, 2=necrotic foot, 1=necrotic leg, 0=complete amputation). Visual examination of hindlimbs revealed that animal treated with blank scaffolds rapidly suffered from extreme necrosis and loss of the ischemic hindlimbs in three days after surgery and were not used in any further analysis. In contrast, transplantation of EDK-shScram and EDK-shPDGFRβ cells prevented autoamputation and the level of necrosis was reduced. Both ED-shScram and EDK-shPDGFRβ groups demonstrated very similar ischemic scores over time (Figure 4-8C).

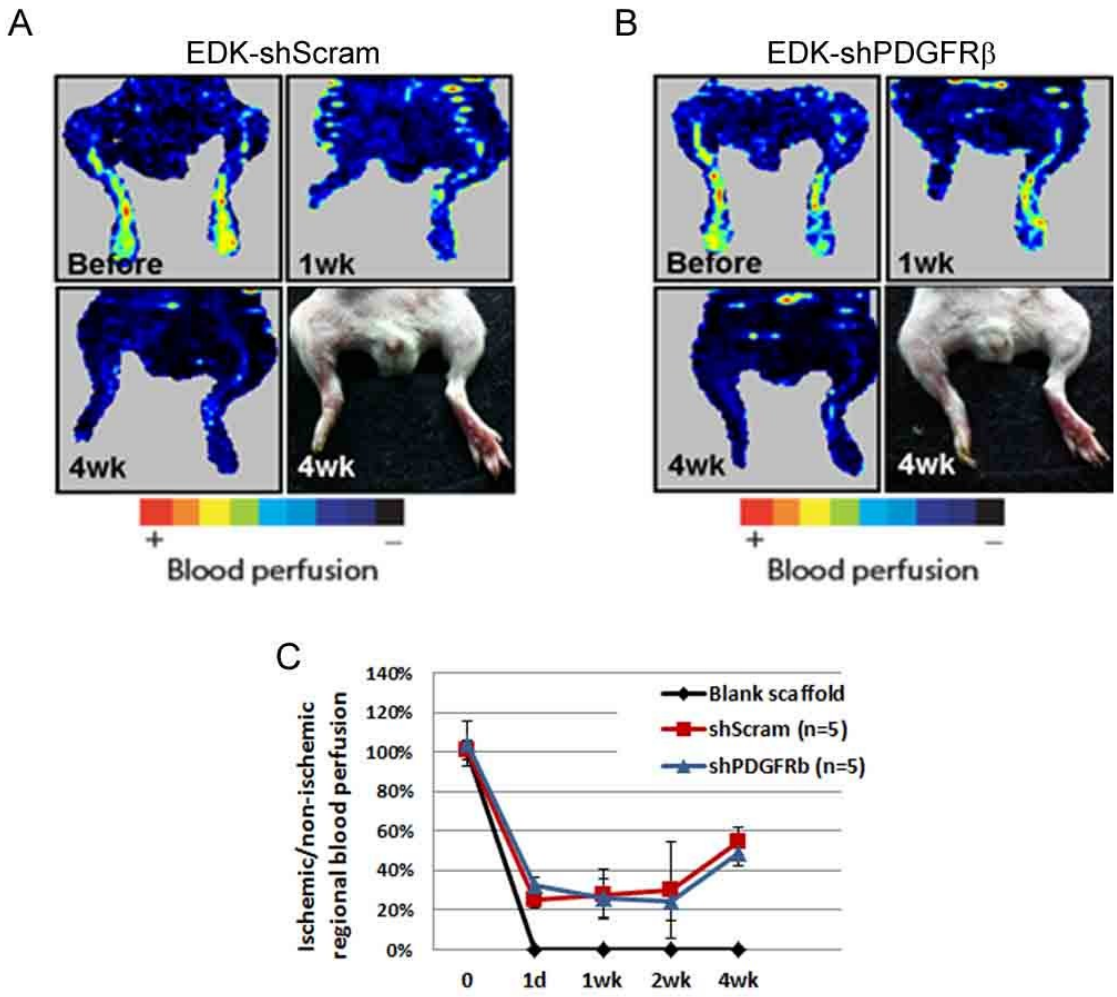

Figure 4-9. Laser Dopler perfusion image (LDPI) analysis of ischemic hindlimbs as a function of time postsurgery. Serial LDPI analysis in hindlimb ischemia mice. After 1 week, animals treated with EDK6-shScram **(A)** and EDK6-shPDGFRb **(B)** cells showed decreased perfusion levels compared to day0 control. After 4 weeks, significant blood flow recovery was observed in both week, animals treated with EDK6-shScram and EDK6-shPDGFRb treated groups. **C.** Quantitative analysis of hindlimb blood flow after treatment with EDK6-shScram and EDK6-shPDGFRb by calculating the ischemic/normal limb perfusion ratios.

By week four after surgery ischemic hindlimes in both EDK-shScram and EDK-shPDGFRβ groups stabilized at either necrotic foot or necrotic leg (Figure 4-8D).

To analyse the perfusion of ischemic hindlimb after cell transplantation, Laser Dopler perfusion image (LDPI) analysis was performed at day 1, day 3 and weeks 1, 2, and 4 following surgery. Femoral artery and vein ligation led to a rapid loss in perfusion

to the ligated limbs, and animals treated with blank scaffolds demonstrated rapid limb necrosis and no perfusion images were obtained. Animals treated with EDK-shScram and EDK-shPDGFRβ fibroblasts demonstrated rapid loss in perfusion as a result of induction of hindlimb ischemia (~30% of normal perfusion levels), which stayed constant for 2 weeks following surgery. By 4 weeks, significant blood flow recovery was observed in both EDK-shScram and EDK-shPDGFRβ groups reaching ~60% of normal perfusion levels (Figure 4-9A and 4-9B).

Transplantation of EDK-shScram and EDK-shPDGFRβ cells to iscemic hindlimbs demonstrated similar therapeutic effect charachterized by increased blood perfusion over time and partial recovery of ischemic limbs. Hovewer, EDK-shScram cells showed no advantage over EDK-shPDGFRβ cells *in vivo*, possibly due to insufficient knockdown of PDGFRβ (85%). Since there were no noticeable difference in secretory profiles of EDK-shScram and EDK-shPDGFRβ, the therapeutic effect of these cells that was seen *in vivo* was likely mediated through paracrine mechanisms.

Discussion

By controlling the differentiation conditions it is possible to induce hESCs and iPSCs to differentiate into any cell type in the human body, and it is hoped that this ability can be harnessed to generate therapeutically relevant cell types for repairing or replacing damaged cells and tissues. Specifically, differentiation into pericytes would be essential for therapeutic tissue regeneration, due to their ability to promote angiogenesis and support tissue vascularization. In our previous reports, we described an efficient and reproducible protocol for generating mesenchymal cells from both hESC and iPSC (EDK

and iPDK, respectively) that may have broad applicability for future therapeutic use in tissue engineering and regenerative medicine (Hewitt, Shamis et al. 2009; Hewitt, Shamis et al. 2011; Shamis, Hewitt et al. 2011; Shamis, Hewitt et al. 2012). In current study, we have further characterized the pericyte functionality of EDK and iPDK cells and their potential to support tissue vascularization using *in vitro* and *in vivo* models of angiogenesis. By analyzing the marker expression, differentiation potential, secretory profile, and interactions with endothelial cells, we have established that EDK and iPDK cells can function as pericytes. Considering limitations associated with existing sources of pericytes our differentiation protocol can be used for derivation of well-characterized pericyte populations for disease modeling, tissue engineering, and development of novel strategies in regenerative medicine.

In parallel, we have generated EDK and iPDK cell lines from hESCs and iPSCs, respectively, using the same differentiation conditions, and analyzed the marker expression during sequential stages of differentiation. This analysis revealed a transient induction of vasculogenic precursors FLK1/KDR, CD34, and CD31, following BMP4 treatment, and a gradual increase in expression of pericyte markers NG2, PDGFRβ, CD73, and CD105 all through differentiation. Because EDK and iPDK cells showed phenotypic similarity to pericytes, we hypothesized that the mesenchymal cells derived using our differentiation protocol may be of pericyte lineage. Since TGFβ signaling have long been associated with vascular development (Armulik, Genove et al. 2011) and, specifically, the regulation of the contractile phenotype in pericytes (Hirschi, Rohovsky et al. 1998; Sinha, Hoofnagle et al. 2004; Boyd, Nunes et al. 2011), we have analyzed the potential of EDK and iPDK cells to modulate their phenotype along the pericyte–

vSMCs axis upon TGFβ1 stimulation. We have shown that EDK and iPDK cells upregulate αSMA expression levels of mRNA and protein. αSMA is a commonly used marker for vSMCs, however, it is not specific, and can be expressed by cardiomyocytes, skeletal muscle, and myofibroblats (Armulik, Genove et al. 2011). Here we show that upon stimulation with TGFβ1, both EDK and iPDK cells upregulate the expression of contractile proteins SM-MHC, Calponin, Caldesmon, and SM22α, which are more specific of vSMC. Although the mechanism mediating the response of EDK and iPDK cells to TGFβ1 is unclear, these results indicate that EDK and iPDK cells retain a certain level of plasticity as demonstrated by vSMC differentiation.

One of the major challenges in vascular tissue engineering is developing efficient and reproducible protocols for generating specific cell types, such as endothelial cells and pericytes, with high efficiency, purity, and minimal manipulation. Although the protocol for generating of pericytes from iPSCs using embryoid bodies has been recently reported (Dar, Domev et al. 2012), it is not clear whether the embryoid bodies approach is practical and can generate sufficient numbers of pericytes with stable phenotype and extended proliferation potential. We have developed the directed differentiation approach to generate stable lines of pericyte-like cells from both pluripotent stem cell sources (EDK and iPDK cell lines) using defined culture conditions and have begun to explore their angiogenic potential *in vitro* and *in vivo*. We have shown that both EDK and iPDK cells can be robustly expanded up to 20 passages (See Chapter 3) while maintaining phenotypic stability. Both EDK and iPDK cells demonstrated very similar secretory profiles of angiogenic-related growth factors and cytokines, including VEGF, HGF, IL-8, PDGF-AA, known to control endothelial cell proliferation, migration, and

differentiation. When incorporated into 3D *in vitro* angiogenesis assay, these cells induced sprouting of human dermal-derived microvascular endothelial cells (HMVEC) indicating their potential for therapeutic angiogenesis. In addition by co-culturing EDK and iPDK cells with endothelial cells in 3D fibrin-based tissue constructs, we have shown that these cells can promote the formation of vascular networks. These results are consistent with previous reports showing that interactions between endothelial cells and pericytes are essential for development and stabilization of vascular networks *in vitro* (Evensen, Micklem et al. 2009; Vo, Hanjaya-Putra et al. 2010; Boyd, Nunes et al. 2011).

PDGFRβ/PDGF-BB signalling is known to play a role in pericyte recruitment to newly formed capillaries during angiogenesis (Gerhardt and Betsholtz 2003; Armulik, Genove et al. 2011). During angiogenesis PDGF-BB is expressed by the sprouting endothelium and PDGFRβ is expressed by the pericytes and vSMCs, suggesting a paracrine mode of interaction between these cell types (Gerhardt and Betsholtz 2003; Armulik, Genove et al. 2011). By generating PDGFRβ-deficient EDK and iPDK cell lines and by assaying the migration of these cells toward paracrine signals produced by HMVEC, we have demonstrated that EDK and iPDK can be recruited towards endothelial and this response is mediated, at least in part, through PDGF-BB/ PDGFRβ signaling. Animal model studies have previously demonstrated the role of PDGF-BB/PDGFRβ signaling pathway in the development of vasculature (Leveen, Pekny et al. 1994; Soriano 1994; Lindahl, Johansson et al. 1997; Crosby, Seifert et al. 1998; Hellstrom, Gerhardt et al. 2001; Enge, Bjarnegard et al. 2002). For example, it has been shown that the knockout of PDGF-B or PDGFRβ leads to perinatal lethality due to abnormal vascular morphogenesis caused by lack of pericytes (Leveen, Pekny et al. 1994;

Soriano 1994; Hellstrom, Gerhardt et al. 2001) . In chimeras composed of PDGFRβ-positive and -negative cells, only the positive cells were able to populate the pericyte compartment, demonstrating that that these cells depend on PDGFRβ for their development (Crosby, Seifert et al. 1998). However, the role of PDGFRβ in wound neovascularization remains unclear. In effort to understand the function of PDGFRβ-positive and -negative pericytes during wound healing, we transplanted EDK-shScram and EDK-shPDGFRβ cells into the mouse model of peripheral arterial disease using alginate scaffolds as cell carriers. Although, there was no noticeable difference in the recovery of mice transplanted with either EDK-shScram or EDK-shPDGFRβ cells, we have shown that the transplantation of these cells attenuated tissue necrosis and improved perfusion of ischemic hindlimbs. However, there was no noticeable difference in recovery of mice transplanted with EDK-shScram or EDK-shPDGFRβ cells. It is possible that the level PDGFRβ knockdown (~85%) was not sufficient to allow us to detect the difference upon transplantation. Nevertheless, these results demonstrate the potential of EDK cells to induce neovascularization *in vivo*, possibly through paracrine mechanisms. Additional *in vivo* studies are necessary, to confirm that EDK and iPDK cells are able to incorporate into recovered vasculature and to show the role of PDGFRβ in this process.

Chapter 5: Summary and Future Directions

Summary

A central challenge that must be overcome before therapeutic application of pluripotent stem cell derived cells is the development of reliable and sensitive methods to evaluate their safety and efficacy. While hESC and iPSCs can undergo directed differentiation to numerous cell types, progress towards their clinical application has been limited by the lack of tools and platforms to evaluate their stability in an *in vivo*-like tissue context. It is therefore critical to fully-characterize the properties of differentiated cells derived from hESCs and iPSCs by developing engineered, pre-clinical tissue models that will better predict their behaviour following future therapeutic transplantation to humans. I hypothesized that pluripotent stem cells could be directed to differentiate along mesenchymal lineage, and that these cells would demonstrate functionality 3D *in vitro* tissue models. To achieve these goals I generated mesenchymal lineage cells from hESCs and iPSCs and explored their functionality and wound healing potential using 3D *in vitro* models of dermal regeneration and angiogenesis.

I started this project by generating two distinct mesenchymal cell lines from pluripotent stem cell sources using alternative differentiation protocols (H9-MSC and EDK). The H9-MSC derivation protocol was based on spontaneous differentiation of hESCs followed by selective isolation of CD73-positive mesenchymal cells (Seda Tigli, Ghosh et al. 2009). The EDK derivation protocol was based on directed differentiation approach previously developed in our laboratory by culturing hESCs under defined substrate and media condition and exposure to BMP4 (Hewitt, Shamis et al. 2009). Next, I characterized the phenotype, secretion profile, and surface antigen profile of H9-MSC, EDK and control dermal fibroblasts and compared their ability to support epidermal morphogenesis and

wound re-epithelialization by incorporating them into a bioengineered skin-like tissue. The key findings of this project include: Finding #1 – Multilineage differentiation analysis revealed that despite morphological similarity EDK did not share the same mesenchymal cell properties with H9-MSC. While H9-MSC differentiated to osteoblasts and adipocytes, EDK did not show multilineage differentiation potential under tested conditions and were restricted to fibroblast lineage. Finding #2 – Analysis of soluble growth factors revealed that EDK and H9-MSC have significantly different secretory profiles. EDK but not H9-MSC produced elevated levels of growth factors implicated in epithelial wound healing and angiogenesis, including HGF, KGF, PDGF-AA, and VEGF. Finding #3 – Incorporation of EDK and H9-MSC into bioengineered human skin revealed that only EDK but not H9-MSC could support epidermal tissue development and stratification. Finding #4 – Incorporation of EDK and H9-MSC into a novel 3D tissue assay of cutaneous wound repair revealed that EDK induced faster wound re-epithelialization than H9-MSC, which was also linked to their elevated production of HGF. Finding #5 – Suppression of HGF secretion in EDK fibroblasts using shRNA confirmed that re-epithelialization stimulated by EDK was mostly mediated through HGF signaling. These findings demonstrate that hESCs could be directed to specified and alternative mesenchymal cell fates whose function could be distinguished in engineered human skin equivalents (HSEs). Characterization of hESC-derived mesenchymal cells in 3D, engineered HSEs demonstrates the utility of this tissue platform to predict the functional properties of hESC-derived fibroblasts before their therapeutic transplantation.

Following the development of iPSC technology, our laboratory obtained iPSCs and induced them to differentiate into mesenchymal cells using the same protocol optimized for derivation of EDK cells (named iPDK). While the iPSCs technology offers major perspectives in regenerative medicine by providing an alternative source of autologous cells for potential therapeutic applications, the functional properties of iPSC-

derived cells and their similarities to cells differentiated from hESCs remain unclear. To address this question, in my next project, I compared the production and assembly of extracellular matrix (ECM) by iPSC-derived fibroblasts (iPDK) to that of fibroblasts differentiated from hESC (EDK), and to primary dermal fibroblasts (HDF). In this study I used L-ascorbic acid 2-phosphate (AA) to induce synthesis and increase deposition of ECM by EDK, iPDK and HDF cells, characterized their ability to assemble 3D dermal-like tissues, analyzed the composition of these tissues. The key findings of this project include: Finding #1 – Characterization of proliferation kinetics of EDK, iPDK, and control HDF revealed significant differences in their replicative potential, as hESC- and iPSC-derived fibroblasts demonstrated a prolonged life span when compared to HDF. Finding #2 – Quantitative RT-PCR analysis showed that in response to AA both, EDK and iPDK fibroblasts expressed elevated levels of collagen genes when compared to HDF. Finding #3 – Collagen analysis using soluble collagen assay, immunofluorescence staining and western blot revealed that both, EDK and iPDK fibroblasts respond to AA stimulation by increasing collagen secretion and extracellular deposition when compared to HDF. Finding #4 – Under culture conditions that enabled the self-assembly of 3D ECM, EDK and iPDK fibroblasts were able to assemble a well-organized and physically substantial dermal-like tissues. Finding #5 – Characterization of protein composition of 3D ECM assembled by EDK, iPDK, and HDF using western blot and immunohistochemical analysis showed abundance of Type III Collagen in EDK and iPDK-derived tissues, indicating their similarity to fetal dermis and provisional ECM assembled during granulation tissue formation. By comparing the production and assembly of ECM by iPSC-derived fibroblasts to their hESC-derived counterparts, we

demonstrated that human iPSCs and hESC have similar biological potential and represent a promising, alternative source of mesenchymal cells to advance future regenerative therapies**.** Importantly, functional differences between EDK and iPDK cells and primary dermal fibroblasts were only fully revealed when these cells were grown in a complex, 3D tissue environment. This suggests that evaluation of the biological potential of hESC- and iPSC-derived cells will require the development of reliable methods to evaluate their functional properties before they can be translated for human therapy.

Temporal gene expression and flow cytometry analysis during differentiation of hESC and iPSC towards EDK and iPDK cells revealed a progressive induction of pericyte markers NG2, PDGFRβ, CD105, and CD73, as well as transient induction of αSMA and markers of pericyte progenitors CD31, CD34, and FLK1/KDR. Because EDK and iPDK cells showed phenotypic similarity to pericytes, I hypothesized that the mesenchymal cells derived using our differentiation protocol may be of pericyte lineage. In the next study, I analyzed the pericyte functionality of EDK and iPDK cells using in vitro and in vivo models of angiogenesis. The key finding of this project include: Finding #1 – When stimulated with TGF-β1, EDK and iPDK cells showed the potential to differentiate into vascular vSMCs by upregulating the expression of contractile proteins αSMA, SM22α, SM-MHC, calponin, and caldesmon. Finding #2 – EDK and iPDK cells showed further similarities to pericyte lineage by secreting elevated levels of soluble angiogenic regulators, including VEGF, HGF, IL-8, Angiopoetin-1, and PDGF-AA. Finding #3 – When incorporated into 3D *in vitro* model of angiogenesis (fibrin bead sprouting assay), EDK and iPDK provided necessary paracrine factors that induced endothelial sprouting. Finding #4 – When co-cultured with endothelial cells in 3D fibrin-

based constructs, EDK and iPDK cells promoted self-assembly of vascular networks and deposition of vascular basement membrane proteins. Finding #5 – Generation of PDGFRβ knockdown in EDK and iPDK cells (EDK- shPDGFRβ and iPDK-shPDGFRβ, respectively) and incorporation of these cells into migration assay revealed that EDK and iPDK cells can be recruited towards paracrine signals produced by endothelial cells and this response is mediated, at least in part, through PDGF-BB/PDGFRb signaling pathway. Finding #6 –Transplantation of EDK- shPDGFRβ and control EDK-shScram cells into mouse model of severe hindlimb ischemia led to significant reduction in tissue necrosis and improved perfusion of ischemic hindlimbs, demonstrating the potential of these cells to promote vascular regeneration *vivo.* Since no significant diference was observed between EDK-shScram and EDK-shPDGFRβ groups at any stages of the experiment, the therapeutic effects of these cells is likely to be mediated through the secretion of pro-angiogenic factors and not through the stabilization of blood vessels**.** These findings demonstrated the potential of EDK and iPDK cells to function as pericytes by promote angiogenesis and vascular regeneration *in vitro* and *in vivo.* Considering limitations associated with existing sources of pericytes, our differentiation protocol can be used for derivation of well-characterized pericyte populations for disease modeling, tissue engineering, and development of novel strategies in regenerative medicine.

Future Directions

Comparative characterization of neural crest and mesodermal mesenchymal progenitors

While the majority of mesenchymal cells in the adult originate from the mesoderm, embyrology studies have shown that mesenchymal cells that form the connective tissue within the head and neck arise from the neural crest (Breau, Pietri et al. 2008). During early embryonic development neural crest and non-neural epithelium in the ectoderm give rise to mesenchymal cells, termed ectomesenchyme, that plays a critical role in the formation of the hard and soft tissues of the head and neck such as bones, muscles, teeth, and branchial arches (Breau, Pietri et al. 2008). While mesoderm derived and neural crest derived mesenchymal cells have different developmental functions, it is still unknown in humans whether these two populations of mesenchymal cells will demonstrate different phenotypes and function *in vitro* or *in vivo*.

Continuation of this thesis work towards development of sources of mesenchymal cells with specific regenerative properties, such as tooth development, will require the isolation of cells of neural crest origin. Temporal gene expression analysis of EDK cells during differentiation demonstrated transient induction of mesodermal markers GATA4, T brachyury homolog, MSGN1, TBX4, and RUNX1 and downregulation of neural crest markers NHK1, p75NRT, and Sox10 suggesting mesodermal origin of EDK fibroblasts (see Figure 2-1D). By differentiating hESC and iPSCs towards neural crest and by differentiating them towards mesenchymal cells we can enrich for fibroblasts that are likely derived from the neural-crest lineage. The separation of fibroblasts derived from neural-crest and mesodermal lineages, and a comparison of their phenotypic and functional properties, may provide insights into the differences and similarities between

these two lineages. Using the assays presented in this thesis, as well as others that include the ability of mesenchymal cells to differentiate into tooth-forming odontoblasts, will be important for understanding the broader utility of these cells for regenerative medicine.

Assess functionality of ESC- and iPSC-derived fibroblasts in vivo

The *in vitro* studies described in this thesis project have established the potential therapeutic value of hESC- and iPSC-derived fibroblasts, however *in vivo* engraftment of cells and tissues is a critical next step towards determining their capability to integrate and associate with host tissue, as well as their potential in wound healing and tissue regeneration. The follow-up studies are necessary to examining therapeutic potential of these cells using different in *vivo* systems. Selections of these experiments are described below:

1. EDK and iPDK fibroblasts and primary human keratinocytes can be used to construct 3D skin equivalent tissues, which can be then grafted onto nude mice and grown for several months while maintaining barrier function. We can then examine the ability of EDK and iPDK fibroblasts to regenerate stromal tissue and support the formation of stratified squamous epithelium *in vivo.*

2. EDK and iPDK fibroblasts and human endothelial cells can be incorporated into fibrin gels and transplanted subcutaneously into nude mice and grown for several weeks. We can then examine the ability of EDK and iPDK fibroblasts to promote formation of functional blood vessels *in vivo.*

3. To monitor for survival, migration and localization *in vivo,* EDK and iPDK fibroblasts tagged with GFP will allow easy identification of the transplanted cells following engraftment. Injections of GFP-expressing EDK and iPDK cells can be used to

test for stable tissue integration, expression of mesenchymal markers, and address safety concerns related to teratoma and other tumor formation.

4. Chronic wound healing is a critical issue in the health care community, and treatments in dealing with these wounds are limited. Current treatment modalities include a live *in vitro*-grown skin substitutes placed on the wound that provides instructive signals to induce wound healing. The *in vitro* studies described in this thesis project have demonstrated that EDK and iPDK cells are capable of producing ECM proteins important for granulation tissue formation, such as Type III Collagen and to promote angiogenesis. The use of EDK and iPDK fibroblasts for generating skin substitutes may provide improvements over existing care of chronic wounds.

Appendix I. Protocol for Directed Differentiation of ESCs and iPSCs

This protocol has been developed in the laboratory of Jonathan A. Garlick by Kyle J. Hewitt and described in (Hewitt, Shamis et al. 2009; Hewitt, Shamis et al. 2011)

Differentiation of EDK/iPDK Cells

1. Two days prior to start of differentiation, gelatin coat each well of 6-well plate with 1 mL 0.1% Gelatin. Incubate at 37C overnight.

2. One day prior to start of differentiation:
    a. Remove excess gelatin, and seed mouse embryonic fibroblasts (MEF) (earlier than passage 5) onto gelatin-coated plate. Density should be approximately 1x106 cells per 6-well dish or 10cm plate.
    b. Clean up ESCs and iPSCs by selecting and manually removing colonies that have differentiated.

3. Day 0 of differentiation: plate ESCs/iPSCs
    a. Dislodge colonies of ESCs/iPSCs using Collagenase Type IV. Manually dislodge and spin down at 1000rpm to remove collagenase (enzyme is not inactivated by serum).
    b. Fix MEF feeder layer by incubating in 4% paraformaldehyde at RT for 10 min, and thoroughly wash on rocking platform 3X 5 min with PBS and 1X 5min w/ media.
    c. Passage ESCs at a 1:4 ratio onto fixed MEFs
        i. Application Note: keep one cell fraction for day 0 control for cell counting/mRNA/protein etc.

4. Feed daily with 2.5 mL WWE media and monitor morphology.

5. Day 4 of differentiation: treat with BMP-4
    a. Dilute 1uM BMP-4 stock solution 1:2000 in WWE media, for a final
    b. concentration of 0.5 nM (e.g. for 1 6-well, dilute 7.5 µL in 15 mL media,
    c. and feed 2.5 mL per well)
    d. Continue treatment daily for days 4-7 of differentiation

6. Day 7 of differentiation: split cells to freshly fixed MEF feeders
    a. Prepare fixed feeders as before (steps 1+2)
    b. Trypsinize and split cells 1:3 (may vary depending on condition of ESCs/iPSCs during plating) for approximately 1x105 cells per well of 6-well.

i. Application Note: If possible, it is best to split cells at a range of densities, as the differentiation efficiency will vary depending on quality and type of ESC/iPSC.

c. Feed cells M/W/F with SCES media.

7. Day 14 of differentiation: split cells to tissue-culture plastic dish
   a. Trypsinize and split cells 1:3 onto tissue-culture plastic (approximately 1x105 cells per well of 6-well)
      i. Application Note: If possible, it is best to split cells at a range of densities, as the differentiation efficiency will vary depending on quality and type of ESC/iPSC.
   a. Feed cells M/W/F with WWE media

8. Day 21 of differentiation: split cells to Type I Collagen-coated plate (BD BioCoat cat# 653450)
   a. Trypsinize, count, and split cells to Type I Collagen -coated plate at 5x105 cells per plate.
   b. Expand and split cells regularly according to normal growth conditions (see below)
   c. Continue to monitor morphology and growth

9. Day 28 of differentiation: expand cells (at this stage they are passage 0).

Maintenance of EDK/iPDK Cells

Thawing cells

1. Remove vial containing 1M cells from liquid nitrogen and warm at 37C
2. Add 4 mL media and spin cells at 1000 rpm for 5 min to remove DMSO
3. Resuspend pelleted cells in 10 mL media and transfer to 10cm Type I collagen-coated plate (BD BioCoat cat# 653450)
4. Grow cells in 5% CO2 at 37C
5. Feed with 8-10 mL on the following day, and every other day

Splitting cells

1. Wash plate with PBS and add 2 mL 0.05% trypsin/EDTA (Invitrogen)
2. Incubate at 37C for 3-5 min until all cells have detached.
3. Add 8 mL media, mix and count cells with hemacytometer.
4. Spin cells down to remove trypsin
5. Plate cells at a density of 0.5M per 10 cm Type I Collagen-coated plate

Freezing cells

1. Trypsinize cells as described above
2. Prepare a 2X freeze media using 20% DMSO, 40% FCII serum, 40% media
3. Resuspend pellet at 2M cells/mL
4. Add 0.5 mL cells to freeze vial, then add 0.5 mL freeze media drop-wise and mix

5. Freeze in cryotank at -80 and store in liq. Nitrogen

Medium Components

HEPES, 800 mM
Sigma - Cat no. H-4034.
Dissolve 47.24 g HEPES in 250 ml H2O. Store up to 1 year at −20◦C.

Hydrocortisone, 0.25 mg/ml (500×)
Sigma - Cat no. H-4881
Dissolve 0.0538 g hydrocortisone (Sigma) in 200 ml H2O. Store up to 1 year at -20◦C. The concentration in this solution is 0.55 mM.

Insulin, 5 mg/ml
EMD Biosci. - Cat no. 407709
Dissolve 50 mg insulin (Sigma) in 10 ml of 0.005N HCl. Store up to 1 year at −20◦C.

Adenine, 18 mM
MP Biomedicals - Cat no. 100190
Dissolve 0.972 g adenine in 2.4 ml 4 N NaOH. Bring to 400 ml with water. Store up to 1 year at −20◦C.

Cholera toxin, 10−7 M
Sigma - C-8052
Dissolve cholera toxin at 9 ng/ml in water and store up to 1 year at −20◦C.

EGF, 10 μg/ml
Sigma - I-2643
Dissolve human recombinant epidermal growth factor at 10 μg/ml in 0.1% (v/v) bovine serum albumin (BSA; tissue culture tested); storeup to 1 year at −20◦C.

WWE Culture Medium

338 ml	Dulbecco's modified Eagle medium, serum-free, low-glucose
112 ml	F12 nutrient mixture (Ham), containing L-glutamine (Invitrogen)
25 ml	Fetal Clone II serum (FCII; Hyclone, cat. no. SH30066; 5% final)
5 ml	18 mM Adenine (see recipe; 0.18 mM final)
5 ml	800 mM HEPES (see recipe; 8 mM final)
1 ml	0.25 mg/ml hydrocortisone (see recipe; 0.5 μg/ml final)
0.5 ml	10-7 M cholera toxin (see recipe; 10-10 M final)
0.5 ml	10 μg/ml EGF (see recipe; 10 ng/ml final)
0.5 ml	5 mg/ml insulin (see recipe; 5 μg/ml final)

Store up to 2 weeks at 4◦C
CAUTION: Cholera toxin is very toxic. Use appropriate precautions when handling stock solutions.

SCES Culture Medium

450 mL	DMEM:F12 1:1 ratio
50 mL	Fetal Bovine Serum
5 mL	Non-essential amino acids
2.5 mL	L-glutamine

Appendix II. Protocol for Fabrication of 3D Model of Wounded Skin

This protocol has been developed in the laboratory of Jonathan A. Garlick and described in (Egles, Shamis et al. 2008; Egles, Garlick et al. 2010)

Fabrication of Collagen Matrix

1. Culture primary human dermal fibroblasts (HDF) in monolayer culture so that they are almost confluent one day before incorporation into the collagen.

2. The day before incorporation, passage fibroblasts at a 9:10 split ratio so they will be mitotically active the next day when incorporated into the collagen gel.

3. Prepare acellular collagen on ice (see recipe). Add 1 ml of acellular collagen to each insert of 6-well plate. Ensure that the matrix coats the entire bottom surface of the insert and allow it to gel at room temperature for 20 min.

4. Trypsinize, count, and resuspend HDFs to a final concentration of 3×10^5 cells/ml. Prepare the cellular collagen (see recipe) on ice. Fibroblasts should be added last after collagen has been neutralized so that the cells will not be damaged by the alkaline pH. Gently triturate the cellular matrix and add 3 ml into each insert on top of the gelled acellular collagen matrix. Gently transfer the mixture to the incubator for 30 min.

5. When the cellular matrix is completely gelled, feed the gels with 12 ml of fibroblast medium (see recipe) by adding 10 ml of medium to the well around the insert and 2 ml of medium directly onto the insert. Incubate the gels for 5–7 days to allow complete gel contraction.

> *Application Note: During the first few days, the sides of the gel contract and will form a plateau in the center. Gels are stable between 5 and 10 days after initial construction. Collagen matrix prepared with dermal fibroblasts can be used for fabrication of human skin equivalents (HSEs) or as a second contracted collagen gel onto which the wounded epithelium will be transferred.

Fabrication of Human Skin Equivalents (HSEs)

1. Culture normal human keratinocytes (NHK) on a feeder layer of mitotically inactivated mouse 3T3 fibroblasts in NHK media (see recipe). Keratinocytes should be grown to no more than 50% confluence to minimize the number of differentiated cells seeded onto the collagen gel.

2. Remove the 3T3 feeder cells from the culture by incubating the plates in PBS/EDTA for 5 min at 37°C. 3T3's can then be displaced by gentle pipetting so that keratinocytes will remain attached. As soon as the 3T3 cells have begun to detach, replace the PBS/EDTA with PBS, gently rinse the plate with PBS until all 3T3 cells have been completely removed and only keratinocyte colonies attached to the plate.

3. Trypsinize, count, and resuspend NHK to a final concentration of 1 $x10^7$ cells/ml in Epidermalization I medium (see recipe). Remove all fibroblast medium from the trays with the contracted collagen and seed NHKs directly onto the contracted collagen gels in an aliquot of 50 µl containing 5×10^5 cells. Do not move the tray for 15 min to allow the keratinocytes to attach. Constructs are then incubated at 37°C for 30–60 min. without any medium to allow the keratinocytes to fully adhere.

4. Add 12 ml of Epidermalization I medium (see recipe) to each insert by adding 10 ml to the bottom of the well and 2 ml gently into the insert on top of the keratinocytes. Incubate at 37°C.

5. Cultures are fed with medium every 2 days as follows (see recipes for organotypic culture media):

a. Epidermalization I medium (Epi I) – 12 ml per well for the first 2 days.
b. Epidermalization II medium (Epi II) – 12 ml per well for the next 2 days.
c. Cornification medium (Cornification) – At this point, cultures are raised to the air–liquid interface by adding 7 ml per well to the bottom of the well so that the insert just contacts the medium. Aspirate medium from the inside of the insert so that tissues can be grown at the air–liquid interface. Additional feedings with Cornification medium are done every 2 days until termination of the experiment.

Fabrication of 3D Wound Healing Model of Human Skin

This protocol requires that HSEs fabricated with dermal fibroblasts (HDF) and normal human keratinocytes (NHK) and a second contracted collagen gel onto which the wounded epithelium will be transferred will first be simultaneously constructed (see the protocols above)

1. Aspirate all medium from the HSE after 7–10 days of culture. Remove the insert from the tray and place it in a sterile dish. Cut out the central part of the collagen gel covered by keratinocytes using a 14mm dermatological punch.

2. Generate an excisional wound in the center of the tissue through the epidermis, collagen, and membrane using 6mm disposable biopsy punch.

3. Use forceps to gently lift the edge of the wounded tissue by separating the collagen gel from the membrane. Drag the tissue onto a dental mirror while leaving the membrane behind.

4. Carry the mirror directly over the second contracted collagen matrix so that the edge of the mirror and wounded tissue are in contact with the matrix. Slide the tissue onto the second collagen gel by teasing it gently with a closed forceps as the mirror is slowly pulled away, leaving the culture on the contracted collagen gel.

5. Maintain the tissue at an air–liquid interface by adding 8 ml of Cornification medium (see recipe) beneath the insert during re-epithelialization, change the medium every 2 days until the end of the experiment.

> *Application Note: Use the protocol above for the preparation of the second contracted collagen gel onto which the wounded epithelium will be transferred. The type of fibroblasts and l number of cells incorporated into collagen matrix can be modified.

Materials

1. 6-well tissue culture tray with 3 μm porous polycarbonate membrane inserts (Organogenesis, Canton, MA, cat.# MS-10-305)

2. Bovine tendon Type I collagen (Organogenesis, cat.# 200-055)

3. 0.5 M EDTA, pH 8.0 (Invitrogen, Carlsbad, CA, cat.# 15575)

4. PBS (Invitrogen, Carlsbad, CA, cat.#14190)

5. 0.05% Trypsin/EDTA (Invitrogen, Carlsbad, CA, cat.# 25300054)

6. 5 mM EDTA; add 5 ml of 0.5 M EDTA to 500 ml PBS

7. 10% EDTA/PBS; mix 50 ml of 5 mM EDTA with 450 ml PBS

8. 14 mm stainless steel dermatological punch (Delasco, Council Bluffs, IA, cat.# KP-14)

9. 6 mm disposable biopsy punch (Miltex inc, cat.# 33-36)

10. Dental mirror for transfer of wounded culture

Medium Components

1. 100× HEPES (800 mM) – dissolve 47.24 g in 250 ml ddH_2O, store at −20°C for up to 1 year (Sigma, St. Louis, MO, cat.# H-4034)

2. 100× Adenine (18 mM) – dissolve 0.972 g in 2.4 ml 4 N NaOH, q.s. to 400 ml with ddH_2O, store at −20°C for up to 1 year (MP biomedicals, Solon, OH, cat.# 100190)

3. 500× Hydrocortisone (0.25 mg/ml) – dissolve 0.0538 g in 200 ml ddH_2O, store at −20°C for up to 1 year (Sigma, St. Louis, MO, cat.# H-4881)

4. 1,000× Cholera toxin (10^{-7} M) – dissolve 9 ng/ml in ddH_2O, store at −20°C for up to 1 year (Sigma, St. Louis, MO, cat.# C-8052)

5. 1,000× EGF (10 μg/ml) – dissolve 10 μg/ml in 0.1% BSA, store at −20°C for up to 1 year (Austral Biological, San Ramon, CA, cat.# GF-010-9)

6. 1,000× Insulin (5 mg/ml) – dissolve 50 mg in 10 ml of 0.005 N HCl, store at −20°C for up to 1 year (Sigma, St. Louis, MO, cat.# I-2643)

7. 10 nM triiodothyronine (T3) – add 1 ml T3 to 99 ml ddH_2O for 500× stock (Sigma, cat # T-5516)

8. 2 μM progesterone – dissolve 1 mg in 1 ml absolute ethanol, add 14.7 ml ddH_2O, dilute 1 ml in 100 ml DMEM for 1,000× stock (Sigma, St. Louis, MO, cat.# P-8783)

9. Chelated BCS – Chelate serum by adding 10 g CHELEX 100 (Sigma, St. Louis, MO, cat.# C-7901) to 100 ml serum and stirring for 3 h at 4°C, then filter through Whatman paper, then through a sterile filter.

10. Transferrin (5 mg/ml) – (BioSource cat. # 352-020, 200 ml)

11. 500× PES – contains O-phosphorylethanolamine (0.01 mM final), ethanolamine (10 μM final), and selenium (10 μg/ml final) (BioSource, cat.# P02-45-100)

12. Calcium Chloride ($CaCl_2$) (BioSource, 0.5 M, 100 ml, cat. no. 391-100)

13. 10X Minimum essential medium with Earle's salts (Cambrex, Walkersville, MD, cat. no. 12-684F)

14. L-glutamine (200mM) (BioWhittaker, 100ml, cat. No. 17-605E).

15. Sodium bicarbonate (71.2 mg/ml) (Cambrex, cat. No. 17-613E,)

16. DMEM (Gibco, cat. No.11885)

17. F12 Nutrient Mixture (HAM) (Gibco, cat. No. 11765-054)

010 medium

43 g DME powder (JRH Biosciences, this is a special order medium base that is prepared in bulk) contains no glucose and no $CaCl_2$
5 L ddH_2O

0.5 g $MgSO_4$
18.5 g $NaHCO_3$

Keratinocyte Culture Medium (NHK)

338 ml DME medium (Invitrogen, Carlsbad, CA, cat.# 11885)
112 ml F12 medium (Invitrogen, Carlsbad, CA, cat.# 11765)
25 ml FBS (Hyclone, Logan, UT, cat.# SH30071.03) (5% final)
5 ml 18 mM adenine (0.18 mM final)
3.4 ml 100× penicillin/streptomycin (Invitrogen, Carlsbad, CA, cat.# 15140-122)
5 ml 800 mM HEPES (8 mM final)
1 ml 0.25 mg/ml hydrocortisone (0.5 µg/ml final)
0.5 ml 10^{-7} M cholera toxin (10^{-10} M final)
0.5 ml 10 µg/ml EGF (10 ng/ml final)
0.5 ml 5 mg/ml insulin (5 µg/ml final)
Store up to 2 weeks at 4°C.

Fibroblast Culture Medium (HDF)

500 ml DME medium (Invitrogen, Carlsbad, CA, cat.#11885)
55.6 ml FBS (Hyclone, Logan, UT, cat.# SH30071.03) (10% final)
5.6 ml 800 mM HEPES (8 mM final)
3.4 ml 100× Penicillin/Streptomycin (Invitrogen, Carlsbad, CA, cat.#15140-122)
Store up to 2 weeks at 4°C.

3T3 Medium

500 ml DME medium (Invitrogen, Carlsbad, CA, cat.# 11885)
55.6 ml Bovine Calf Serum (Hyclone, Logan, UT, cat.# SH30072.03) (10% final)
3.4 ml 100× Penicillin/Streptomycin (Invitrogen, Carlsbad, CA, cat.#15140-122)

Acellular Collagen Matrix

No. of inserts / Materials	6	12	18	24
10XEMEM	0.6ml	1.2ml	1.8ml	2.4ml
L-Glutamine	54µl	108µl	163µl	217µl
FBS	0.68m	1.35ml	2.02ml	2.7ml
Na bicarbonate	187µl	374µl	561µl	748µl
Collagen	5ml	10ml	15ml	20ml

Cellular Collagen Matrix

No. of inserts / Materials	6	12	18	24
10XEMEM	1.8ml	3.6ml	5.34ml	7.12ml
L-Glutamine	162.5µl	325µl	487.5µl	650µl
FBS	2.02ml	4.04ml	6.06ml	8.08ml
Na Bicarbonate	0.56ml	1.12ml	1.68ml	2.24ml
Collagen	15ml	30ml	45ml	60ml
Fibroblsts ($3.0x10^5$/ml)	1.65ml	3.3ml	4.5ml	6.6ml

Organotypic culture media

Media Type / Materials	[Stock]	Epi I	Epi II	Cornification
O1O		362.5mL	362.5mL	237mL
F-12		120mL	120mL	237mL
L-Glutamine	200mM	10mL	10mL	10mL
Adenine	18mM	1mL	1mL	1mL
Hydrocortisone	0.55mM	1mL	1mL	1mL
$CaCl_2$	0.5M	-	1.8mL	1.8mL
T3	10nM	1mL	1mL	1mL
Transferrin	5mg/mL	1mL	1mL	1mL
PES	X500	1mL	1mL	1mL
Insulin	5mg/mL	1mL	1mL	1mL
Progesterone	2nM	0.5mL	0.5mL	-
Serum		0.5mL (cBCS)	0.5mL (FBS) Lot#ALG14153	10mL (FBS) Lot#ALG14153

References

*Abe, R., S. C. Donnelly, et al. (2001). "Peripheral blood fibrocytes: differentiation pathway and migration to wound sites." J Immunol **166**(12): 7556-7562.*

*Aberdam, D., K. Gambaro, et al. (2007). "Embryonic stem cells as a cellular model for neuroectodermal commitment and skin formation." C R Biol **330**(6-7): 479-484.*

*Alaish, S. M., D. Yager, et al. (1994). "Biology of fetal wound healing: hyaluronate receptor expression in fetal fibroblasts." J Pediatr Surg **29**(8): 1040-1043.*

*Alvarez-Diaz, C., J. Cuenca-Pardo, et al. (2000). "Controlled clinical study of deep partial-thickness burns treated with frozen cultured human allogeneic epidermal sheets." J Burn Care Rehabil **21**(4): 291-299.*

*Andriani, F., A. Margulis, et al. (2003). "Analysis of microenvironmental factors contributing to basement membrane assembly and normalized epidermal phenotype." J Invest Dermatol **120**(6): 923-931.*

*Angel, P. and A. Szabowski (2002). "Function of AP-1 target genes in mesenchymal-epithelial cross-talk in skin." Biochem Pharmacol **64**(5-6): 949-956.*

*Armulik, A., G. Genove, et al. (2011). "Pericytes: developmental, physiological, and pathological perspectives, problems, and promises." Dev Cell **21**(2): 193-215.*

*Au, P., J. Tam, et al. (2008). "Bone marrow-derived mesenchymal stem cells facilitate engineering of long-lasting functional vasculature." Blood **111**(9): 4551-4558.*

*Badiavas, E. V., M. Abedi, et al. (2003). "Participation of bone marrow derived cells in cutaneous wound healing." J Cell Physiol **196**(2): 245-250.*

*Bajpai, V. K., P. Mistriotis, et al. (2012). "Clonal multipotency and effect of long-term in vitro expansion on differentiation potential of human hair follicle derived mesenchymal stem cells." Stem Cell Res **8**(1): 74-84.*

*Barberi, T., L. M. Willis, et al. (2005). "Derivation of multipotent mesenchymal precursors from human embryonic stem cells." PLoS Med **2**(6): e161.*

*Bartsch, G., J. J. Yoo, et al. (2005). "Propagation, expansion, and multilineage differentiation of human somatic stem cells from dermal progenitors." Stem Cells Dev **14**(3): 337-348.*

*Beanes, S. R., F. Y. Hu, et al. (2002). "Confocal microscopic analysis of scarless repair in the fetal rat: defining the transition." Plast Reconstr Surg **109**(1): 160-170.*

*Beaudry, P., Y. Hida, et al. (2007). "Endothelial progenitor cells contribute to accelerated liver regeneration." J Pediatr Surg **42**(7): 1190-1198.*

*Bell, E., B. Ivarsson, et al. (1979). "Production of a tissue-like structure by contraction of collagen lattices by human fibroblasts of different proliferative potential in vitro." Proc Natl Acad Sci U S A **76**(3): 1274-1278.*

*Benjamin, L. E., D. Golijanin, et al. (1999). "Selective ablation of immature blood vessels in established human tumors follows vascular endothelial growth factor withdrawal." J Clin Invest **103**(2): 159-165.*

*Bey, E., M. Prat, et al. (2010). "Emerging therapy for improving wound repair of severe radiation burns using local bone marrow-derived stem cell administrations." Wound Repair Regen **18**(1): 50-58.*

*Black, A. F., F. Berthod, et al. (1998). "In vitro reconstruction of a human capillary-like network in a tissue-engineered skin equivalent." FASEB J **12**(13): 1331-1340.*

*Blanpain, C., W. E. Lowry, et al. (2004). "Self-renewal, multipotency, and the existence of two cell populations within an epithelial stem cell niche." Cell **118**(5): 635-648.*

*Boyd, N. L., S. S. Nunes, et al. (2011). "Microvascular mural cell functionality of human embryonic stem cell-derived mesenchymal cells." Tissue Eng Part A **17**(11-12): 1537-1548.*

*Boyd, N. L., K. R. Robbins, et al. (2009). "Human embryonic stem cell-derived mesoderm-like epithelium transitions to mesenchymal progenitor cells." Tissue Eng Part A **15**(8): 1897-1907.*

*Breau, M. A., T. Pietri, et al. (2008). "A nonneural epithelial domain of embryonic cranial neural folds gives rise to ectomesenchyme." Proc Natl Acad Sci U S A **105**(22): 7750-7755.*

*Breitkreutz, D., N. Mirancea, et al. (2004). "Inhibition of basement membrane formation by a nidogen-binding laminin gamma1-chain fragment in human skin-organotypic cocultures." J Cell Sci **117**(Pt 12): 2611-2622.*

*Brignier, A. C. and A. M. Gewirtz (2010). "Embryonic and adult stem cell therapy." J Allergy Clin Immunol **125**(2 Suppl 2): S336-344.*

*Brittan, M., K. M. Braun, et al. (2005). "Bone marrow cells engraft within the epidermis and proliferate in vivo with no evidence of cell fusion." J Pathol **205**(1): 1-13.*

*Brzoska, M., H. Geiger, et al. (2005). "Epithelial differentiation of human adipose tissue-derived adult stem cells." Biochem Biophys Res Commun **330**(1): 142-150.*

*Caplan, A. I. (2008). "All MSCs are pericytes?" Cell Stem Cell **3**(3): 229-230.*

*Caplan, A. I. and J. E. Dennis (2006). "Mesenchymal stem cells as trophic mediators." J Cell Biochem **98**(5): 1076-1084.*

*Carlson, M., K. Faria, et al. (2011). "Epidermal stem cells are preserved during commercial-scale manufacture of a bilayered, living cellular construct (Apligraf(R))." Tissue Eng Part A **17**(3-4): 487-493.*

*Cass, D. L., K. M. Bullard, et al. (1998). "Epidermal integrin expression is upregulated rapidly in human fetal wound repair." J Pediatr Surg **33**(2): 312-316.*

*Cedar, S. H., J. A. Cooke, et al. (2007). "The therapeutic potential of human embryonic stem cells." Indian J Med Res **125**(1): 17-24.*

*Chang, H. Y., J. T. Chi, et al. (2002). "Diversity, topographic differentiation, and positional memory in human fibroblasts." Proc Natl Acad Sci U S A **99**(20): 12877-12882.*

*Chen, H. F., C. Y. Chuang, et al. (2009). "Novel autogenic feeders derived from human embryonic stem cells (hESCs) support an undifferentiated status of hESCs in xeno-free culture conditions." Hum Reprod **24**(5): 1114-1125.*

*Chen, M., M. Przyborowski, et al. (2009). "Stem cells for skin tissue engineering and wound healing." Crit Rev Biomed Eng **37**(4-5): 399-421.*

*Chmielowiec, J., M. Borowiak, et al. (2007). "c-Met is essential for wound healing in the skin." J Cell Biol **177**(1): 151-162.*

*Chojkier, M., K. Houglum, et al. (1989). "Stimulation of collagen gene expression by ascorbic acid in cultured human fibroblasts. A role for lipid peroxidation?" J Biol Chem **264**(28): 16957-16962.*

*Choo, A., A. S. Ngo, et al. (2008). "Autogeneic feeders for the culture of undifferentiated human embryonic stem cells in feeder and feeder-free conditions." Methods Cell Biol **86**: 15-28.*

*Chun-mao, H., W. Su-yi, et al. (2007). "Human bone marrow-derived mesenchymal stem cells differentiate into epidermal-like cells in vitro." Differentiation **75**(4): 292-298.*

*Chung, Y., I. Klimanskaya, et al. (2008). "Human embryonic stem cell lines generated without embryo destruction." Cell Stem Cell **2**(2): 113-117.*

*Chuong, C. M., G. Cotsarelis, et al. (2007). "Defining hair follicles in the age of stem cell bioengineering." J Invest Dermatol **127**(9): 2098-2100.*

*Chuong, C. M., P. Wu, et al. (2006). "Engineering stem cells into organs: topobiological transformations demonstrated by beak, feather, and other ectodermal organ morphogenesis." Curr Top Dev Biol **72**: 237-274.*

*Clark, R. A., K. Ghosh, et al. (2007). "Tissue engineering for cutaneous wounds." J Invest Dermatol **127**(5): 1018-1029.*

*Collett, G. D. and A. E. Canfield (2005). "Angiogenesis and pericytes in the initiation of ectopic calcification." Circ Res **96**(9): 930-938.*

*Colwell, A. S., M. T. Longaker, et al. (2008). "Identification of differentially regulated genes in fetal wounds during regenerative repair." Wound Repair Regen **16**(3): 450-459.*

*Compton, C. C. (1992). "Current concepts in pediatric burn care: the biology of cultured epithelial autografts: an eight-year study in pediatric burn patients." Eur J Pediatr Surg **2**(4): 216-222.*

*Coraux, C., C. Hilmi, et al. (2003). "Reconstituted skin from murine embryonic stem cells." Curr Biol **13**(10): 849-853.*

*Covas, D. T., R. A. Panepucci, et al. (2008). "Multipotent mesenchymal stromal cells obtained from diverse human tissues share functional properties and gene-expression profile with CD146+ perivascular cells and fibroblasts." Exp Hematol **36**(5): 642-654.*

*Crisan, M., S. Yap, et al. (2008). "A perivascular origin for mesenchymal stem cells in multiple human organs." Cell Stem Cell **3**(3): 301-313.*

*Crosby, J. R., R. A. Seifert, et al. (1998). "Chimaeric analysis reveals role of Pdgf receptors in all muscle lineages." Nat Genet **18**(4): 385-388.*

*Dang, C. M., S. R. Beanes, et al. (2003). "Scarless fetal wounds are associated with an increased matrix metalloproteinase-to-tissue-derived inhibitor of metalloproteinase ratio." Plast Reconstr Surg **111**(7): 2273-2285.*

*Dar, A., H. Domev, et al. (2012). "Multipotent vasculogenic pericytes from human pluripotent stem cells promote recovery of murine ischemic limb." Circulation **125**(1): 87-99.*

*de Jager, M., W. Groenink, et al. (2006). "Preparation and characterization of a stratum corneum substitute for in vitro percutaneous penetration studies." Biochim Biophys Acta **1758**(5): 636-644.*

*Dominici, M., K. Le Blanc, et al. (2006). "Minimal criteria for defining multipotent mesenchymal stromal cells. The International Society for Cellular Therapy position statement." Cytotherapy **8**(4): 315-317.*

*Egles, C., J. A. Garlick, et al. (2010). "Three-dimensional human tissue models of wounded skin." Methods Mol Biol **585**: 345-359.*

*Egles, C., H. A. Huet, et al. (2010). "Integrin-blocking antibodies delay keratinocyte re-epithelialization in a human three-dimensional wound healing model." PLoS One **5**(5): e10528.*

*Egles, C., Y. Shamis, et al. (2008). "Denatured collagen modulates the phenotype of normal and wounded human skin equivalents." J Invest Dermatol **128**(7): 1830-1837.*

*Enge, M., M. Bjarnegard, et al. (2002). "Endothelium-specific platelet-derived growth factor-B ablation mimics diabetic retinopathy." EMBO J **21**(16): 4307-4316.*

*Estes, J. M., J. S. Vande Berg, et al. (1994). "Phenotypic and functional features of myofibroblasts in sheep fetal wounds." Differentiation **56**(3): 173-181.*

*Evensen, L., D. R. Micklem, et al. (2009). "Mural cell associated VEGF is required for organotypic vessel formation." PLoS One **4**(6): e5798.*

*Falanga, V. (2005). "Wound healing and its impairment in the diabetic foot." Lancet **366**(9498): 1736-1743.*

*Feng, J., A. Mantesso, et al. (2011). "Dual origin of mesenchymal stem cells contributing to organ growth and repair." Proc Natl Acad Sci U S A **108**(16): 6503-6508.*

*Feng, Q., S. J. Lu, et al. (2010). "Hemangioblastic derivatives from human induced pluripotent stem cells exhibit limited expansion and early senescence." Stem Cells **28**(4): 704-712.*

*Fentem, J. H. and P. A. Botham (2002). "ECVAM's activities in validating alternative tests for skin corrosion and irritation." Altern Lab Anim **30 Suppl 2**: 61-67.*

*Fernandes, K. J., I. A. McKenzie, et al. (2004). "A dermal niche for multipotent adult skin-derived precursor cells." Nat Cell Biol **6**(11): 1082-1093.*

*Ferreira, L. S., S. Gerecht, et al. (2007). "Vascular progenitor cells isolated from human embryonic stem cells give rise to endothelial and smooth muscle like cells and form vascular networks in vivo." Circ Res **101**(3): 286-294.*

*Frantz, F. W., D. A. Bettinger, et al. (1993). "Biology of fetal repair: the presence of bacteria in fetal wounds induces an adult-like healing response." J Pediatr Surg **28**(3): 428-433; discussion 433-424.*

*Fu, W., S. J. Wang, et al. (2012). "Residual undifferentiated cells during differentiation of induced pluripotent stem cells in vitro and in vivo." Stem Cells Dev **21**(4): 521-529.*

*Gabbanini, S., E. Lucchi, et al. (2009). "In vitro evaluation of the permeation through reconstructed human epidermis of essentials oils from cosmetic formulations." J Pharm Biomed Anal **50**(3): 370-376.*

*Galkowska, H., U. Wojewodzka, et al. (2006). "Chemokines, cytokines, and growth factors in keratinocytes and dermal endothelial cells in the margin of chronic diabetic foot ulcers." Wound Repair Regen **14**(5): 558-565.*

*Gallico, G. G., 3rd, N. E. O'Connor, et al. (1984). "Permanent coverage of large burn wounds with autologous cultured human epithelium." N Engl J Med **311**(7): 448-451.*

*Gambaro, K., E. Aberdam, et al. (2006). "BMP-4 induces a Smad-dependent apoptotic cell death of mouse embryonic stem cell-derived neural precursors." Cell Death Differ **13**(7): 1075-1087.*

*Garlick, J. A., W. C. Parks, et al. (1996). "Re-epithelialization of human oral keratinocytes in vitro." J Dent Res **75**(3): 912-918.*

*Gerecht-Nir, S., J. E. Dazard, et al. (2005). "Vascular gene expression and phenotypic correlation during differentiation of human embryonic stem cells." Dev Dyn **232**(2): 487-497.*

*Gerhardt, H. and C. Betsholtz (2003). "Endothelial-pericyte interactions in angiogenesis." Cell Tissue Res **314**(1): 15-23.*

*Gharzi, A., A. J. Reynolds, et al. (2003). "Plasticity of hair follicle dermal cells in wound healing and induction." Exp Dermatol **12**(2): 126-136.*

*Ghosh, Z., K. D. Wilson, et al. (2010). "Persistent donor cell gene expression among human induced pluripotent stem cells contributes to differences with human embryonic stem cells." PLoS One **5**(2): e8975.*

*Giuliani, M., M. Fleury, et al. (2011). "Long-lasting inhibitory effects of fetal liver mesenchymal stem cells on T-lymphocyte proliferation." PLoS One **6**(5): e19988.*

*Grainger, S. J. and A. J. Putnam (2011). "Assessing the permeability of engineered capillary networks in a 3D culture." PLoS One **6**(7): e22086.*

*Groeber, F., M. Holeiter, et al. (2011). "Skin tissue engineering--in vivo and in vitro applications." Adv Drug Deliv Rev **63**(4-5): 352-366.*

*Guenou, H., X. Nissan, et al. (2009). "Human embryonic stem-cell derivatives for full reconstruction of the pluristratified epidermis: a preclinical study." Lancet **374**(9703): 1745-1753.*

*Guenther, M. G., G. M. Frampton, et al. (2010). "Chromatin structure and gene expression programs of human embryonic and induced pluripotent stem cells." Cell Stem Cell **7**(2): 249-257.*

*Gurkan, U. A., X. Cheng, et al. (2010). "Comparison of morphology, orientation, and migration of tendon derived fibroblasts and bone marrow stromal cells on electrochemically aligned collagen constructs." J Biomed Mater Res A **94**(4): 1070-1079.*

*Gurtner, G. C., S. Werner, et al. (2008). "Wound repair and regeneration." Nature **453**(7193): 314-321.*

*Haniffa, M. A., X. N. Wang, et al. (2007). "Adult human fibroblasts are potent immunoregulatory cells and functionally equivalent to mesenchymal stem cells." J Immunol **179**(3): 1595-1604.*

*Harding, K. G., K. Moore, et al. (2005). "Wound chronicity and fibroblast senescence--implications for treatment." Int Wound J **2**(4): 364-368.*

*Hata, R. and H. Senoo (1989). "L-ascorbic acid 2-phosphate stimulates collagen accumulation, cell proliferation, and formation of a three-dimensional tissuelike substance by skin fibroblasts." J Cell Physiol **138**(1): 8-16.*

*Hausman, M. R. and B. D. Rinker (2004). "Intractable wounds and infections: the role of impaired vascularity and advanced surgical methods for treatment." Am J Surg **187**(5A): 44S-55S.*

*Hellstrom, M., H. Gerhardt, et al. (2001). "Lack of pericytes leads to endothelial hyperplasia and abnormal vascular morphogenesis." J Cell Biol **153**(3): 543-553.*

*Hewitt, K. J., Y. Shamis, et al. (2009). "Three-dimensional epithelial tissues generated from human embryonic stem cells." Tissue Eng Part A **15**(11): 3417-3426.*

*Hewitt, K. J., Y. Shamis, et al. (2011). "Epigenetic and phenotypic profile of fibroblasts derived from induced pluripotent stem cells." PLoS One **6**(2): e17128.*

*Hirschi, K. K., S. A. Rohovsky, et al. (1998). "PDGF, TGF-beta, and heterotypic cell-cell interactions mediate endothelial cell-induced recruitment of 10T1/2 cells and their differentiation to a smooth muscle fate." J Cell Biol **141**(3): 805-814.*

*Hocking, A. M. and N. S. Gibran (2010). "Mesenchymal stem cells: paracrine signaling and differentiation during cutaneous wound repair." Exp Cell Res **316**(14): 2213-2219.*

*Hoogduijn, M. J., M. J. Crop, et al. (2007). "Human heart, spleen, and perirenal fat-derived mesenchymal stem cells have immunomodulatory capacities." Stem Cells Dev **16**(4): 597-604.*

*Hsu, M., Z. M. Peled, et al. (2001). "Ontogeny of expression of transforming growth factor-beta 1 (TGF-beta 1), TGF-beta 3, and TGF-beta receptors I and II in fetal rat fibroblasts and skin." Plast Reconstr Surg **107**(7): 1787-1794; discussion 1795-1786.*

*Huangfu, D., R. Maehr, et al. (2008). "Induction of pluripotent stem cells by defined factors is greatly improved by small-molecule compounds." Nat Biotechnol **26**(7): 795-797.*

*Hunt, D. P., C. Jahoda, et al. (2009). "Multipotent skin-derived precursors: from biology to clinical translation." Curr Opin Biotechnol **20**(5): 522-530.*

*Irion, S., M. C. Nostro, et al. (2008). "Directed differentiation of pluripotent stem cells: from developmental biology to therapeutic applications." Cold Spring Harb Symp Quant Biol **73**: 101-110.*

*Ito, M., Y. Liu, et al. (2005). "Stem cells in the hair follicle bulge contribute to wound repair but not to homeostasis of the epidermis." Nat Med **11**(12): 1351-1354.*

*Ito, M., Z. Yang, et al. (2007). "Wnt-dependent de novo hair follicle regeneration in adult mouse skin after wounding." Nature **447**(7142): 316-320.*

*Itoh, M., M. Kiuru, et al. (2011). "Generation of keratinocytes from normal and recessive dystrophic epidermolysis bullosa-induced pluripotent stem cells." Proc Natl Acad Sci U S A **108**(21): 8797-8802.*

*Jain, R. K. (2003). "Molecular regulation of vessel maturation." Nat Med **9**(6): 685-693.*

*Javazon, E. H., S. G. Keswani, et al. (2007). "Enhanced epithelial gap closure and increased angiogenesis in wounds of diabetic mice treated with adult murine bone marrow stromal progenitor cells." Wound Repair Regen **15**(3): 350-359.*

*Jiang, X., Y. Gwye, et al. (2009). "Isolation and characterization of neural crest stem cells derived from in vitro-differentiated human embryonic stem cells." Stem Cells Dev **18**(7): 1059-1070.*

*Jo, Y. Y., H. J. Lee, et al. (2007). "Isolation and characterization of postnatal stem cells from human dental tissues." Tissue Eng **13**(4): 767-773.*

*Jones, P. H. and F. M. Watt (1993). "Separation of human epidermal stem cells from transit amplifying cells on the basis of differences in integrin function and expression." Cell **73**(4): 713-724.*

*Kandarova, H., M. Liebsch, et al. (2006). "Assessment of the human epidermis model SkinEthic RHE for in vitro skin corrosion testing of chemicals according to new OECD TG 431." Toxicol In Vitro **20**(5): 547-559.*

*Kannan, R. Y., H. J. Salacinski, et al. (2005). "The roles of tissue engineering and vascularisation in the development of micro-vascular networks: a review." Biomaterials **26**(14): 1857-1875.*

*Kaufman, D. S., R. L. Lewis, et al. (2004). "Functional endothelial cells derived from rhesus monkey embryonic stem cells." Blood **103**(4): 1325-1332.*

*Kaur, P. and A. Li (2000). "Adhesive properties of human basal epidermal cells: an analysis of keratinocyte stem cells, transit amplifying cells, and postmitotic differentiating cells." J Invest Dermatol **114**(3): 413-420.*

*Khachemoune, A., Y. M. Bello, et al. (2002). "Factors that influence healing in chronic venous ulcers treated with cryopreserved human epidermal cultures." Dermatol Surg **28**(3): 274-280.*

*Kim, B. C., H. T. Kim, et al. (2003). "Fibroblasts from chronic wounds show altered TGF-beta-signaling and decreased TGF-beta Type II receptor expression." J Cell Physiol **195**(3): 331-336.*

*Kim, D. S., H. J. Cho, et al. (2009). "Insulin-like growth factor-binding protein contributes to the proliferation of less proliferative cells in forming skin equivalents." Tissue Eng Part A **15**(5): 1075-1080.*

*Klimanskaya, I., Y. Chung, et al. (2005). "Human embryonic stem cells derived without feeder cells." Lancet **365**(9471): 1636-1641.*

*Klimanskaya, I., N. Rosenthal, et al. (2008). "Derive and conquer: sourcing and differentiating stem cells for therapeutic applications." Nat Rev Drug Discov **7**(2): 131-142.*

*Kolokol'chikova, E. G., L. I. Budkevich, et al. (2001). "Morphological changes in burn wounds after transplantation of allogenic fibroblasts." Bull Exp Biol Med **131**(1): 89-93.*

*Koumas, L., A. E. King, et al. (2001). "Fibroblast heterogeneity: existence of functionally distinct Thy 1(+) and Thy 1(-) human female reproductive tract fibroblasts." Am J Pathol **159**(3): 925-935.*

*Kretlow, J. D., Y. Q. Jin, et al. (2008). "Donor age and cell passage affects differentiation potential of murine bone marrow-derived stem cells." BMC Cell Biol **9**: 60.*

*Lamme, E. N., R. T. Van Leeuwen, et al. (2000). "Higher numbers of autologous fibroblasts in an artificial dermal substitute improve tissue regeneration and modulate scar tissue formation." J Pathol **190**(5): 595-603.*

*Lammert, E., O. Cleaver, et al. (2001). "Induction of pancreatic differentiation by signals from blood vessels." Science **294**(5542): 564-567.*

*Lapasset, L., O. Milhavet, et al. (2011). "Rejuvenating senescent and centenarian human cells by reprogramming through the pluripotent state." Genes Dev **25**(21): 2248-2253.*

*Larson, B. J., M. T. Longaker, et al. (2010). "Scarless fetal wound healing: a basic science review." Plast Reconstr Surg **126**(4): 1172-1180.*

*Lee, G., H. Kim, et al. (2007). "Isolation and directed differentiation of neural crest stem cells derived from human embryonic stem cells." Nat Biotechnol **25**(12): 1468-1475.*

*Leveen, P., M. Pekny, et al. (1994). "Mice deficient for PDGF B show renal, cardiovascular, and hematological abnormalities." Genes Dev **8**(16): 1875-1887.*

*Levenberg, S., L. S. Ferreira, et al. (2010). "Isolation, differentiation and characterization of vascular cells derived from human embryonic stem cells." Nat Protoc **5**(6): 1115-1126.*

*Levenberg, S., J. S. Golub, et al. (2002). "Endothelial cells derived from human embryonic stem cells." Proc Natl Acad Sci U S A **99**(7): 4391-4396.*

*Levy, V., C. Lindon, et al. (2005). "Distinct stem cell populations regenerate the follicle and interfollicular epidermis." Dev Cell **9**(6): 855-861.*

*Lewis, D. A., J. B. Travers, et al. (2009). "A new paradigm for the role of aging in the development of skin cancer." J Invest Dermatol **129**(3): 787-791.*

*Li, J., C. Miao, et al. (2008). "Enrichment of putative human epidermal stem cells based on cell size and collagen type IV adhesiveness." Cell Res **18**(3): 360-371.*

*Lian, Q., E. Lye, et al. (2007). "Derivation of clinically compliant MSCs from CD105+, CD24- differentiated human ESCs." Stem Cells **25**(2): 425-436.*

*Lian, Q., Y. Zhang, et al. (2010). "Functional mesenchymal stem cells derived from human induced pluripotent stem cells attenuate limb ischemia in mice." Circulation **121**(9): 1113-1123.*

*Liechty, K. W., N. S. Adzick, et al. (2000). "Diminished interleukin 6 (IL-6) production during scarless human fetal wound repair." Cytokine **12**(6): 671-676.*

*Liechty, K. W., T. M. Crombleholme, et al. (1998). "Diminished interleukin-8 (IL-8) production in the fetal wound healing response." J Surg Res **77**(1): 80-84.*

*Lin, T., R. Ambasudhan, et al. (2009). "A chemical platform for improved induction of human iPSCs." Nat Methods **6**(11): 805-808.*

*Lindahl, P., B. R. Johansson, et al. (1997). "Pericyte loss and microaneurysm formation in PDGF-B-deficient mice." Science **277**(5323): 242-245.*

*Lister, R., M. Pelizzola, et al. (2009). "Human DNA methylomes at base resolution show widespread epigenomic differences." Nature **462**(7271): 315-322.*

*Liu, H., Y. Kim, et al. (2011). "In vivo liver regeneration potential of human induced pluripotent stem cells from diverse origins." Sci Transl Med **3**(82): 82ra39.*

*Lokmic, Z. and G. M. Mitchell (2008). "Engineering the microcirculation." Tissue Eng Part B Rev **14**(1): 87-103.*

*Longaker, M. T., D. J. Whitby, et al. (1990). "Studies in fetal wound healing, VI. Second and early third trimester fetal wounds demonstrate rapid collagen deposition without scar formation." J Pediatr Surg **25**(1): 63-68; discussion 68-69.*

*Longaker, M. T., D. J. Whitby, et al. (1994). "Adult skin wounds in the fetal environment heal with scar formation." Ann Surg **219**(1): 65-72.*

*Loot, M. A., S. B. Kenter, et al. (2002). "Fibroblasts derived from chronic diabetic ulcers differ in their response to stimulation with EGF, IGF-I, bFGF and PDGF-AB compared to controls." Eur J Cell Biol **81**(3): 153-160.*

*Lorenz, H. P., M. T. Longaker, et al. (1992). "Scarless wound repair: a human fetal skin model." Development **114**(1): 253-259.*

*Lorenz, K., M. Sicker, et al. (2008). "Multilineage differentiation potential of human dermal skin-derived fibroblasts." Exp Dermatol **17**(11): 925-932.*

*Maherali, N., T. Ahfeldt, et al. (2008). "A high-efficiency system for the generation and study of human induced pluripotent stem cells." Cell Stem Cell **3**(3): 340-345.*

*Maherali, N. and K. Hochedlinger (2008). "Guidelines and techniques for the generation of induced pluripotent stem cells." Cell Stem Cell **3**(6): 595-605.*

*Mansilla, E., G. H. Marin, et al. (2005). "Human mesenchymal stem cells are tolerized by mice and improve skin and spinal cord injuries." Transplant Proc **37**(1): 292-294.*

*Marion, R. M. and M. A. Blasco (2010). "Telomeres and telomerase in adult stem cells and pluripotent embryonic stem cells." Adv Exp Med Biol **695**: 118-131.*

*Martin, M. J., A. Muotri, et al. (2005). "Human embryonic stem cells express an immunogenic nonhuman sialic acid." Nat Med **11**(2): 228-232.*

*Martin, P. and S. J. Leibovich (2005). "Inflammatory cells during wound repair: the good, the bad and the ugly." Trends Cell Biol **15**(11): 599-607.*

*Matsumoto, K. and T. Nakamura (1997). "Hepatocyte growth factor (HGF) as a tissue organizer for organogenesis and regeneration." Biochem Biophys Res Commun **239**(3): 639-644.*

*McCluskey, J. and P. Martin (1995). "Analysis of the tissue movements of embryonic wound healing--DiI studies in the limb bud stage mouse embryo." Dev Biol **170**(1): 102-114.*

*Meirelles Lda, S., A. M. Fontes, et al. (2009). "Mechanisms involved in the therapeutic properties of mesenchymal stem cells." Cytokine Growth Factor Rev **20**(5-6): 419-427.*

*Metallo, C. M., L. Ji, et al. (2008). "Retinoic acid and bone morphogenetic protein signaling synergize to efficiently direct epithelial differentiation of human embryonic stem cells." Stem Cells **26**(2): 372-380.*

*Metcalfe, A. D. and M. W. Ferguson (2007). "Tissue engineering of replacement skin: the crossroads of biomaterials, wound healing, embryonic development, stem cells and regeneration." J R Soc Interface **4**(14): 413-437.*

*Mine, S., N. O. Fortunel, et al. (2008). "Aging alters functionally human dermal papillary fibroblasts but not reticular fibroblasts: a new view of skin morphogenesis and aging." PLoS One **3**(12): e4066.*

*Murad, S., D. Grove, et al. (1981). "Regulation of collagen synthesis by ascorbic acid." Proc Natl Acad Sci U S A **78**(5): 2879-2882.*

*Murry, C. E. and G. Keller (2008). "Differentiation of embryonic stem cells to clinically relevant populations: lessons from embryonic development." Cell **132**(4): 661-680.*

*Nakahara, M., N. Nakamura, et al. (2009). "High-efficiency production of subculturable vascular endothelial cells from feeder-free human embryonic stem cells without cell-sorting technique." Cloning Stem Cells **11**(4): 509-522.*

*Namazi, M. R., M. K. Fallahzadeh, et al. (2011). "Strategies for prevention of scars: what can we learn from fetal skin?" Int J Dermatol **50**(1): 85-93.*

*Nolte, S. V., W. Xu, et al. (2008). "Diversity of fibroblasts--a review on implications for skin tissue engineering." Cells Tissues Organs **187**(3): 165-176.*

*O'Ceallaigh, S., S. E. Herrick, et al. (2006). "Quantification of total and perfused blood vessels in murine skin autografts using a fluorescent double-labeling technique." Plast Reconstr Surg **117**(1): 140-151.*

*Olivier, E. N., A. C. Rybicki, et al. (2006). "Differentiation of human embryonic stem cells into bipotent mesenchymal stem cells." Stem Cells **24**(8): 1914-1922.*

*Ongenae, K. C., T. J. Phillips, et al. (2000). "Level of fibronectin mRNA is markedly increased in human chronic wounds." Dermatol Surg **26**(5): 447-451.*

*Pan, Q., S. M. Fouraschen, et al. (2011). "Mobilization of hepatic mesenchymal stem cells from human liver grafts." Liver Transpl **17**(5): 596-609.*

*Paunescu, V., E. Deak, et al. (2007). "In vitro differentiation of human mesenchymal stem cells to epithelial lineage." J Cell Mol Med **11**(3): 502-508.*

*Peterkofsky, B. (1972). "The effect of ascorbic acid on collagen polypeptide synthesis and proline hydroxylation during the growth of cultured fibroblasts." Arch Biochem Biophys **152**(1): 318-328.*

*Phan, S. H. (2008). "Biology of fibroblasts and myofibroblasts." Proc Am Thorac Soc **5**(3): 334-337.*

*Phinney, D. G. and D. J. Prockop (2007). "Concise review: mesenchymal stem/multipotent stromal cells: the state of transdifferentiation and modes of tissue repair--current views." Stem Cells **25**(11): 2896-2902.*

*Ponec, M., A. Weerheim, et al. (1997). "The formation of competent barrier lipids in reconstructed human epidermis requires the presence of vitamin C." J Invest Dermatol **109**(3): 348-355.*

*Pouyani, T., V. Ronfard, et al. (2009). "De novo synthesis of human dermis in vitro in the absence of a three-dimensional scaffold." In Vitro Cell Dev Biol Anim **45**(8): 430-441.*

*Proulx, S., J. d'Arc Uwamaliya, et al. (2010). "Reconstruction of a human cornea by the self-assembly approach of tissue engineering using the three native cell types." Mol Vis **16**: 2192-2201.*

*Revazova, E. S., N. A. Turovets, et al. (2007). "Patient-specific stem cell lines derived from human parthenogenetic blastocysts." Cloning Stem Cells **9**(3): 432-449.*

*Rheinwald, J. G. and H. Green (1975). "Serial cultivation of strains of human epidermal keratinocytes: the formation of keratinizing colonies from single cells." Cell **6**(3): 331-343.*

*Riekstina, U., I. Cakstina, et al. (2009). "Embryonic stem cell marker expression pattern in human mesenchymal stem cells derived from bone marrow, adipose tissue, heart and dermis." Stem Cell Rev **5**(4): 378-386.*

*Roobrouck, V. D., F. Ulloa-Montoya, et al. (2008). "Self-renewal and differentiation capacity of young and aged stem cells." Exp Cell Res **314**(9): 1937-1944.*

*Rosova, I., D. Link, et al. (2010). "shRNA-mediated decreases in c-Met levels affect the differentiation potential of human mesenchymal stem cells and reduce their capacity for tissue repair." Tissue Eng Part A **16**(8): 2627-2639.*

*Sarrazy, V., F. Billet, et al. (2011). "Mechanisms of pathological scarring: role of myofibroblasts and current developments." Wound Repair Regen **19 Suppl 1**: s10-15.*

*Schechner, J. S., A. K. Nath, et al. (2000). "In vivo formation of complex microvessels lined by human endothelial cells in an immunodeficient mouse." Proc Natl Acad Sci U S A **97**(16): 9191-9196.*

*Schmidt, D. and S. P. Hoerstrup (2006). "Tissue engineered heart valves based on human cells." Swiss Med Wkly **136**(39-40): 618-623.*

*Schnickmann, S., D. Camacho-Trullio, et al. (2009). "AP-1-controlled hepatocyte growth factor activation promotes keratinocyte migration via CEACAM1 and urokinase plasminogen activator/urokinase plasminogen receptor." J Invest Dermatol **129**(5): 1140-1148.*

*Schultz, G. S. and A. Wysocki (2009). "Interactions between extracellular matrix and growth factors in wound healing." Wound Repair Regen **17**(2): 153-162.*

*Seda Tigli, R., S. Ghosh, et al. (2009). "Comparative chondrogenesis of human cell sources in 3D scaffolds." J Tissue Eng Regen Med **3**(5): 348-360.*

*Segal, N., F. Andriani, et al. (2008). "The basement membrane microenvironment directs the normalization and survival of bioengineered human skin equivalents." Matrix Biol **27**(3): 163-170.*

*Sen, C. K., G. M. Gordillo, et al. (2009). "Human skin wounds: a major and snowballing threat to public health and the economy." Wound Repair Regen **17**(6): 763-771.*

*Shamis, Y., K. J. Hewitt, et al. (2012). "iPSC-derived fibroblasts demonstrate augmented production and assembly of extracellular matrix proteins." In Vitro Cell Dev Biol Anim **48**(2): 112-122.*

*Shamis, Y., K. J. Hewitt, et al. (2011). "Fibroblasts derived from human embryonic stem cells direct development and repair of 3D human skin equivalents." Stem Cell Res Ther **2**(1): 10.*

*Shepherd, B. R., D. R. Enis, et al. (2006). "Vascularization and engraftment of a human skin substitute using circulating progenitor cell-derived endothelial cells." FASEB J **20**(10): 1739-1741.*

*Sheridan, S. D., K. M. Theriault, et al. (2011). "Epigenetic characterization of the FMR1 gene and aberrant neurodevelopment in human induced pluripotent stem cell models of fragile X syndrome." PLoS One **6**(10): e26203.*

*Siddappa, R., R. Licht, et al. (2007). "Donor variation and loss of multipotency during in vitro expansion of human mesenchymal stem cells for bone tissue engineering." J Orthop Res **25**(8): 1029-1041.*

*Silva, E. A., E. S. Kim, et al. (2008). "Material-based deployment enhances efficacy of endothelial progenitor cells." Proc Natl Acad Sci U S A **105**(38): 14347-14352.*

*Sinha, S., M. H. Hoofnagle, et al. (2004). "Transforming growth factor-beta1 signaling contributes to development of smooth muscle cells from embryonic stem cells." Am J Physiol Cell Physiol **287**(6): C1560-1568.*

*Smith, A. N., E. Willis, et al. (2010). "Mesenchymal stem cells induce dermal fibroblast responses to injury." Exp Cell Res **316**(1): 48-54.*

*Smola, H., G. Thiekotter, et al. (1993). "Mutual induction of growth factor gene expression by epidermal-dermal cell interaction." J Cell Biol **122**(2): 417-429.*

*Soriano, P. (1994). "Abnormal kidney development and hematological disorders in PDGF beta-receptor mutant mice." Genes Dev **8**(16): 1888-1896.*

*Sorrell, J. M., M. A. Baber, et al. (2007). "Clonal characterization of fibroblasts in the superficial layer of the adult human dermis." Cell Tissue Res **327**(3): 499-510.*

*Sorrell, J. M., M. A. Baber, et al. (2008). "Human dermal fibroblast subpopulations; differential interactions with vascular endothelial cells in coculture: nonsoluble factors in the extracellular matrix influence interactions." Wound Repair Regen **16**(2): 300-309.*

*Sorrell, J. M. and A. I. Caplan (2004). "Fibroblast heterogeneity: more than skin deep." J Cell Sci **117**(Pt 5): 667-675.*

*Sottile, J., F. Shi, et al. (2007). "Fibronectin-dependent collagen I deposition modulates the cell response to fibronectin." Am J Physiol Cell Physiol **293**(6): C1934-1946.*

*Stappenbeck, T. S. and H. Miyoshi (2009). "The role of stromal stem cells in tissue regeneration and wound repair." Science **324**(5935): 1666-1669.*

*Strande, L. F., S. T. Foley, et al. (1997). "In vitro bioartificial skin culture model of tissue rejection and inflammatory/immune mechanisms." Transplant Proc **29**(4): 2118-2119.*

*Sudo, K., M. Kanno, et al. (2007). "Mesenchymal progenitors able to differentiate into osteogenic, chondrogenic, and/or adipogenic cells in vitro are present in most primary fibroblast-like cell populations." Stem Cells **25**(7): 1610-1617.*

*Suga, H., H. Eto, et al. (2009). "IFATS collection: Fibroblast growth factor-2-induced hepatocyte growth factor secretion by adipose-derived stromal cells inhibits postinjury fibrogenesis through a c-Jun N-terminal kinase-dependent mechanism." Stem Cells **27**(1): 238-249.*

*Suhr, S. T., E. A. Chang, et al. (2009). "Telomere dynamics in human cells reprogrammed to pluripotency." PLoS One **4**(12): e8124.*

*Suhr, S. T., E. A. Chang, et al. (2010). "Mitochondrial rejuvenation after induced pluripotency." PLoS One **5**(11): e14095.*

*Summer, R. and A. Fine (2008). "Mesenchymal progenitor cell research: limitations and recommendations." Proc Am Thorac Soc **5**(6): 707-710.*

*Supp, D. M. and S. T. Boyce (2005). "Engineered skin substitutes: practices and potentials." Clin Dermatol **23**(4): 403-412.*

*Swistowski, A., J. Peng, et al. (2010). "Efficient generation of functional dopaminergic neurons from human induced pluripotent stem cells under defined conditions." Stem Cells **28**(10): 1893-1904.*

*Szabowski, A., N. Maas-Szabowski, et al. (2000). "c-Jun and JunB antagonistically control cytokine-regulated mesenchymal-epidermal interaction in skin." Cell **103**(5): 745-755.*

*Takahashi, K., K. Tanabe, et al. (2007). "Induction of pluripotent stem cells from adult human fibroblasts by defined factors." Cell **131**(5): 861-872.*

*Takahashi, K. and S. Yamanaka (2006). "Induction of pluripotent stem cells from mouse embryonic and adult fibroblast cultures by defined factors." Cell **126**(4): 663-676.*

*Taylor, G., M. S. Lehrer, et al. (2000). "Involvement of follicular stem cells in forming not only the follicle but also the epidermis." Cell **102**(4): 451-461.*

*Telgenhoff, D. and B. Shroot (2005). "Cellular senescence mechanisms in chronic wound healing." Cell Death Differ **12**(7): 695-698.*

*Thomson, J. A., J. Itskovitz-Eldor, et al. (1998). "Embryonic stem cell lines derived from human blastocysts." Science **282**(5391): 1145-1147.*

*Throm, A. M., W. C. Liu, et al. (2010). "Development of a cell-derived matrix: effects of epidermal growth factor in chemically defined culture." J Biomed Mater Res A **92**(2): 533-541.*

*Toma, J. G., I. A. McKenzie, et al. (2005). "Isolation and characterization of multipotent skin-derived precursors from human skin." Stem Cells **23**(6): 727-737.*

*Tremblay, P. L., V. Hudon, et al. (2005). "Inosculation of tissue-engineered capillaries with the host's vasculature in a reconstructed skin transplanted on mice." Am J Transplant **5**(5): 1002-1010.*

*Vacharathit, V., E. A. Silva, et al. (2011). "Viability and functionality of cells delivered from peptide conjugated scaffolds." Biomaterials **32**(15): 3721-3728.*

*Vailhe, B., D. Vittet, et al. (2001). "In vitro models of vasculogenesis and angiogenesis." Lab Invest **81**(4): 439-452.*

*Vallier, L. (2011). "Serum-free and feeder-free culture conditions for human embryonic stem cells." Methods Mol Biol **690**: 57-66.*

*Vo, E., D. Hanjaya-Putra, et al. (2010). "Smooth-muscle-like cells derived from human embryonic stem cells support and augment cord-like structures in vitro." Stem Cell Rev **6**(2): 237-247.*

*Vojtassak, J., L. Danisovic, et al. (2006). "Autologous biograft and mesenchymal stem cells in treatment of the diabetic foot." Neuro Endocrinol Lett **27 Suppl 2**: 134-137.*

*Wagner, W., S. Bork, et al. (2009). "Aging and replicative senescence have related effects on human stem and progenitor cells." PLoS One **4**(6): e5846.*

*Wang, L., L. Li, et al. (2004). "Endothelial and hematopoietic cell fate of human embryonic stem cells originates from primitive endothelium with hemangioblastic properties." Immunity **21**(1): 31-41.*

*Wang, Z. Z., P. Au, et al. (2007). "Endothelial cells derived from human embryonic stem cells form durable blood vessels in vivo." Nat Biotechnol **25**(3): 317-318.*

*Watt, F. M. (1998). "Epidermal stem cells: markers, patterning and the control of stem cell fate." Philos Trans R Soc Lond B Biol Sci **353**(1370): 831-837.*

*Watt, F. M., C. Lo Celso, et al. (2006). "Epidermal stem cells: an update." Curr Opin Genet Dev **16**(5): 518-524.*

*Werner, S. and R. Grose (2003). "Regulation of wound healing by growth factors and cytokines." Physiol Rev **83**(3): 835-870.*

*Whitby, D. J., M. T. Longaker, et al. (1991). "Rapid epithelialisation of fetal wounds is associated with the early deposition of tenascin." J Cell Sci **99 (Pt 3)**: 583-586.*

*Widgerow, A. D. (2011). "Current concepts in scar evolution and control." Aesthetic Plast Surg **35**(4): 628-635.*

*Woll, P. S., J. K. Morris, et al. (2008). "Wnt signaling promotes hematoendothelial cell development from human embryonic stem cells." Blood **111**(1): 122-131.*

*Wong, C. E., C. Paratore, et al. (2006). "Neural crest-derived cells with stem cell features can be traced back to multiple lineages in the adult skin." J Cell Biol **175**(6): 1005-1015.*

*Wong, T., J. A. McGrath, et al. (2007). "The role of fibroblasts in tissue engineering and regeneration." Br J Dermatol **156**(6): 1149-1155.*

*Woodley, D. T., H. D. Peterson, et al. (1988). "Burn wounds resurfaced by cultured epidermal autografts show abnormal reconstitution of anchoring fibrils." JAMA **259**(17): 2566-2571.*

Wu, R., B. Gu, et al. (2011). "Derivation of multipotent nestin(+)/CD271 (-)/STRO-1 (-) mesenchymal-like precursors from human embryonic stem cells in chemically defined conditions." Hum Cell.

*Wu, Y., L. Chen, et al. (2007). "Mesenchymal stem cells enhance wound healing through differentiation and angiogenesis." Stem Cells **25**(10): 2648-2659.*

*Xu, C., M. S. Inokuma, et al. (2001). "Feeder-free growth of undifferentiated human embryonic stem cells." Nat Biotechnol **19**(10): 971-974.*

*Xu, C., J. Jiang, et al. (2004). "Immortalized fibroblast-like cells derived from human embryonic stem cells support undifferentiated cell growth." Stem Cells **22**(6): 972-980.*

*Yamaguchi, Y., S. Itami, et al. (1999). "Regulation of keratin 9 in nonpalmoplantar keratinocytes by palmoplantar fibroblasts through epithelial-mesenchymal interactions." J Invest Dermatol **112**(4): 483-488.*

*Yang, L., P. G. Scott, et al. (2005). "Identification of fibrocytes in postburn hypertrophic scar." Wound Repair Regen **13**(4): 398-404.*

*Yannas, I. V. and J. F. Burke (1980). "Design of an artificial skin. I. Basic design principles." J Biomed Mater Res **14**(1): 65-81.*

*Yoo, S. J., B. S. Yoon, et al. (2005). "Efficient culture system for human embryonic stem cells using autologous human embryonic stem cell-derived feeder cells." Exp Mol Med **37**(5): 399-407.*

*Yoshikawa, T., H. Mitsuno, et al. (2008). "Wound therapy by marrow mesenchymal cell transplantation." Plast Reconstr Surg **121**(3): 860-877.*

*Yu, J., M. A. Vodyanik, et al. (2007). "Induced pluripotent stem cell lines derived from human somatic cells." Science **318**(5858): 1917-1920.*

*Zhao, X. Y., W. Li, et al. (2009). "iPS cells produce viable mice through tetraploid complementation." Nature **461**(7260): 86-90.*

*Zhao, X. Y., W. Li, et al. (2010). "Viable fertile mice generated from fully pluripotent iPS cells derived from adult somatic cells." Stem Cell Rev **6**(3): 390-397.*

*Zhukareva, V., M. Obrocka, et al. (2010). "Secretion profile of human bone marrow stromal cells: donor variability and response to inflammatory stimuli." Cytokine **50**(3): 317-321.*